Université de Montréal

Exploration of the Cerebral Dysfunctions Induced by Arterial Rigidity and/or the Overexpression of TGFβ in a Mouse Model

par Sherri Bloch

Département de Pharmacologie et Physiologie
Faculté de Médecine

Mémoire présenté
en vue de l'obtention du grade de Maîtrise
en Pharmacologie

Juin 2017

Résumé

Exploration des dysfonctions cérébrales induites par la rigidité artérielle et / ou la surexpression de TGFβ chez la souris

Introduction: Les déficits cérébrovasculaires au cours de la maladie d'Alzheimer (MA) et la démence vasculaire (DV) sont multiples et ne se limitent pas à la pathologie amyloïde-β (Aß). Les modifications comprennent des modifications de structure des vaisseaux sanguins telles que reproduites dans les souris transgéniques qui surexpriment le facteur TGF-β1, une cytokine accrue dans le cerveau avec démence vasculaire et les patients avec la MA. Une circulation cérébrale compromise de façon chronique comme on le voit chez les souris surexprimant la TGF-β1 peut ainsi précipiter les troubles cognitifs lorsqu'elle est combinée avec des facteurs de risque pour les démences, telle que la rigidité artérielle. **Objectif:** Déterminer si la rigidité artérielle induite par calcification va aggraver les dysfonctions vasculaires cérébrales chez les souris surexprimant la TGF-β1 et déclencher des troubles cognitifs. **Méthodologie:** Nous avons testé si la rigidité artérielle induite par une chirurgie servant à calcifier des artères carotides pourrait induire les troubles de la mémoire et d'apprentissage chez les souris de type sauvage ou souris surexprimant la TGF-β1. L'apprentissage, la mémoire spatiale et la consolidation de la mémoire ont été étudiées avec la Piscine de Morris et le test de reconnaissance des objets nouveaux (RON) à un, deux et quatre mois après la chirurgie. **Résultats:** Aucune différence significative n'a été observée entre tous les groupes dans le test de RON spatiales (1, 2 et 4 mois post-chirurgie). Cependant, à 4 mois post-opératoire, les souris de type TGFβ dont la carotide a été calcifiée ont montré une mauvaise consolidation de la mémoire par rapport à des souris de type TGFbeta dont la carotide n'a pas été calcifiée (p <0,05). **Conclusion:** Ces résultats suggèrent que la calcification artérielle et la surexpression de TGF-β1 peuvent agir en synergie pour aggraver les troubles de la mémoire. Par conséquent, ces deux voies pourraient constituer des cibles thérapeutiques pour prévenir les démences.

Mots-clés : TGFβ, rigidité artérielle, démence, Alzheimer, démence vasculaire, piscine de Morris, calcification, dysfunction cérébrale, unité neurovasculaire

Abstract

Exploration of the Cerebral Dysfunctions Induced by Arterial Rigidity and/or the Overexpression of TGFβ in a Mouse Model

Introduction: Alzhemer's disease (AD) and vascular dementia (VaD) is multifaceted with multiple cerebrovascular deficits and not limited to the amyloidβ (Aβ) pathology. Cerebral modifications include changes to vascular structure, which can be reproduced in transgenic mice overexpressing transforming growth factor β1 (TGFβ1), a cytokine found in increased quantities in brains of AD and VaD patients. The mouse model overexpressing TGFβ demonstrates a chronically compromised cerebral circulation, which may precipitate cognitive deficits if combined with other risk factors of cognitive decline, such as arterial rigidity. **Objective:** To determine whether arterial rigidity induced by calcification will provoke cerebrovascular dysfunctions in the TGFβ mouse and trigger cogitive deficits. **Methodology:** We tested whether arterial rigidity induced by calcification of the right carotid artery trigger deficits in memory and learning in mice overexpressing TGFβ1 and their wild type litermates in a set of young and a set of aged mice. Spatial memory and memory consolidation were studied via the Morris water maze (MWM) and novel object recognition (NOR) at 1-, 2- and 4-months followin surgery to induce arterial calcification. **Results:** No significant difference was observed between all groups in the NOR test or the spatial learning of MWM (1-, 2- and 4-months post-surgery). For the memory consolidation tests of the MWM, young TGF mice with calcification showed significance at 4-months post-surgery (p <0,05) while TGF mice without calcification failed to demonstrate cognitive deficits. **Conclusion:** These results suggest that arterial calcification and overexpression of TGFβ1 may act in a synergistic manner to trigger cognitive deficits. Therefore, these two pathways may constitute possible therapeutic targets for prevention of dementia.

Keywords : TGFβ, arterial rigidity, dementia, Alzheimer, vascular dementia, Morris water maze, calcification, cerebral dysfunction, neurovascular unit

Table of Contents

RESUME ..... **I**

TABLE OF CONTENTS ..... **III**

LIST OF TABLES ..... **VI**

LIST OF FIGURES ..... **VII**

LIST OF ABBREVIATIONS ..... **VIII**

ACKNOWLEDGEMENTS ..... **XII**

INTRODUCTION **1**

LITERATURE REVIEW **3**

1. DEMENTIA 3

1.2 Vascular Dementia *4*

1.2.1 Neuropathological features of VaD 5

1.2.2 Brain-related structures of VaD 6

1.3 AD and VaD Comorbidity *7*

1.3.1 Current hypotheses linking AD and VaD 9

1.3.2 Mouse model 10

2. NEUROVASCULAR COUPLING 11

2.1 Vasculature of the CNS, Aging and Dementia *11*

2.1.1 Macrovasculature 12

2.1.2 Microvasculature 14

2.1.3 Pericytes 17

2.2 The Neurovascular Unit, Aging and Dementia *19*

2.2.1 Neurons 21

2.2.2 Glial Cells 22

2.2.2.1 Astrocytes 22

2.2.2.2 Microglia 24

2.2.2.3 Oligodendrocytes 25

2.3 TGFβ-associated pathologies *25*

2.3.1 Physiological use of TGFβ in Brain 26

2.3.2 Impact of TGFβ-associated vascular pathologies on NVC 27

2.3.3 Linking TGFβ mouse and AD patients 28

3. ARTERIAL RIGIDITY 28
3.1 Layers of the vasculature *29*
3.1.2 Vascular Compliance and distensibility 32
3.2 Arterial Rigidity, Aging and Dementia *32*
3.2.1 Arterial Stiffness model 34
3.2.1.1 Vascular significance in the mouse model 34
3.2.1.2 Neurological significance in the mouse model 36
4. NEUROLOGICAL INSULTS 37
4.1 Oxidative stress *37*
4.1.1 Free Radicals: Formation and Biological Uses 38
4.1.2 Markers of Oxidative stress 39
4.2 Gliosis *40*
4.2.1 Microglia: Activation and labeling 41
4.2.2 Astrocytes: astrogliosis and labeling 42
5. BEHAVIORAL TESTING 43
5.1 Morris Water Maze *43*
5.1.1 Brain-related areas 44
5.1.2 Limitations 45
5.1.3 MWM and TGF mice 45
5.2 Novel Object Recognition *46*
5.2.1 Brain-related areas 46
5.2.2 Limitations 47
5.2.3 NOR and TGF mice 47
HYPOTHESIS AND OBJECTIVES 48
METHODS 50
RESULTS 59
DISCUSSION 87
PART I – BAHAVIORAL TESTING 87
Morris Water Maze *87*
Novel Object Recognition *89*
PART II – VASCULAR ASSESSMENTS 91
Circumferential Strain *91*
Cerebral Blood Flow *91*
PART III – GLIOSIS AND OXIDATIVE STRESS 93

Gliosis *93*
Oxidative Stress *95*
PART IV – LIMITATIONS 97
CONCLUSION **97**
BIBLIOGRAPHIE **100**

List of Tables

TABLE I VAD RISK FACTORS [MODIFIED FROM (12)] 5
TABLE II COMMON PATHOLOGICAL LESIONS IN AD AND VAD [DATA FROM (41)] 9

List of figures

FIGURE 1 **VASCULAR DEMENTIA BRAIN TARGETS AND EFFECTS (MODIFIED FROM(13))** 7
FIGURE 2 **MACROVASCULATURE AND MICROVASCULATURE** 14
FIGURE 3 **COMPONENTS OF THE NEUROVASCULAR UNIT** 20
FIGURE 4 **LAYERS OF THE VASCULATURE** 30
FIGURE 5 **MWM ESCAPE LATENCIES OF YOUNG AND OLDER MICE THROUGH TIME.** 59
FIGURE 6 **MWM PROBES OF YOUNG AND OLD MICE CONDUCTED 1 MONTH POST-SURGERY.** 61
FIGURE 7 **MWM PROBES OF YOUNG AND MIDDLE-AGED MICE CONDUCTED 2 MONTHS POST-SURGERY.** 63
FIGURE 8 **MWM PROBES OF YOUNG AND MIDDLE AGE MICE CONDUCTED 4 MONTHS POST-SURGERY.** 65
FIGURE 9 **NOVEL OBJECT RECOGNITION OF YOUNG AND OLDER MICE.** 67
FIGURE 10 **CIRCUMFERENTIAL STRAIN DETECTED IN OLDER MICE.** 69
FIGURE 11 **CEREBRAL BLOOD FLOW OF OLDER MICE 5 MONTHS POST-SURGERY.** 71
FIGURE 12 **PERCENTAGE OF AREA STAINED FOR GFAP OR IBA1 IN THE CORTEX OF YOUNG MICE.** 73
FIGURE 13 **CORTEX OF MIDDLE AGE MICE, COMPARING DAB AND FLUORESCENT STAINING.** 75
FIGURE 14 **HIPPOCAMPAL CA1 REGION OF AGED MICE, COMPARING DAB AND FLUORESCENT STAINING.** 77
FIGURE 15 **HIPPOCAMPAL CA3 REGION OF AGED MICE, COMPARING DAB AND FLUORESCENT STAINING.** 79
FIGURE 16 **HIPPOCAMPAL DG REGION OF AGED MICE, COMPARING DAB AND FLUORESCENT STAINING.** 81
FIGURE 17 **4-HYDROXYNONENAL (HNE) ELISA ASSESSING OXIDATIVE STRESS IN THE CORTEX AND HIPPOCAMPUS OF YOUNG AND AGED MICE.** 83

List of abbreviations

3-NT	3-Nitrotyrosine
AD	Alzheimer's Disease
Aβ	Amyloid β
APP	Amyloid precursor protein
ATP	Adenosine triphosphate
BBB	Blood brain barrier
Ca^{2+}	Calcium ion
CA1	Cornus Ammonis 1 of the hippocampus
CA3	Cornus Ammonis 3 of the hippocampus
CAA	Cerebral amyloid angiopathy
$CaCl_2$	Calcium chloride
CBF	Cerebral bloof flow
COX-1	Cyclooxygenase-1
CNS	Central nervous system
DG	Dentate gyrus of the hippocampus
DHE	Dihydroethidium
E	East
EC	Endothelial cell
ECM	Extracellular matrix
EDHF	Endothelium derived hyperpolarizing factor
eNOS	Endothelial nitric oxide synthase
GFAP	Glial fibrillary acidic protein
HNE	4-Hydroxynonenal
H_2O_2	Hydrogen peroxide
HOO•	Hydroperoxy radical
Iba1	Ionized calcium-binding adapter protein molecule 1
IFN-γ	Interferon γ
ILβ1	Interleukin β1
IL-6	Interleukin 6

iNOS	Inducible nitric oxide synthase
L•	Lipid radical
LO•	Lipid hydroxyl radical
LOO•	Lipid peroxyl radical
LOOH	Lipid hydroperoxide
LPS	Lipopolysaccharide
MWM	Morris Water Maze
N	North
nNOS	Neuronal nitric oxide synthase
NADPH	Nicotinamide adenine dinucleotide phosphate
NMDA	N-methyl-D-aspartate
NO	Nitric Oxide
NO2	Nitrogen dioxide
NO2•	Nitrogen dioxide radical
NOR	Novel object recognition test
NVC	Neurovascular coupling
NVU	Neurovascular unit
O^{2}•-	Superoxide anion
•OH	Hydroxyl radical
ONOO-	Peroxynitrite
OPC	Oligodendrite precursor cell
PFA	Paraformaldehyde
PUFA	Poly-unsaturated fatty acids
PWV	Pulse wave velocity
RNS	Reactive nitrogen species
ROH	Peroxyl radical
ROS	Reactive oxygen species
α-SMA	α Smooth muscle actin
S	South
SMC	Smooth muscle cell

SOD	Superoxide dismutase
SVD	Small vessel disease
TGFβ1	Transforming growth factor β1
TNFα	Tumor necrosis factor α
VaD	Vascular dementia
W	West

This memoir is dedicated to my family. Thank you for making me smile everyday.

Acknowledgements

First I would like to thank my principal investigator, Dr. Girouard, for believing in me and offering her continuous support. No matter how stressed I was, she always managed to put a smile on my face. Next I would like to thank Dr. Hamel who allowed me the use of her lab, her ever-helpful consultations and always inspiring me to work harder.

From the Girouard laboratory, I would like to thank Diane for her assistance in my experiments as well as easy-going advice and guidance. Furthermore, I would like to thank Kelly Xuewei Wang for always letting me know when I was headed in the wrong direction and making me laugh, Dima Obari for her awesome companionship and Gervais Muhire for his guidance and wisdom, and Florencia Iulita for imparting her vast knowledge. I also would like to thank all other members of the Girouard Lab for their friendship and support: Lin Li, Maryam Tabatabaei, Stéphane Lique, Adrian Noriega, Steven Kammi and Atef Badji.

From the Hamel laboratory, I would like to thank Clotilde Lecrux, Lianne Trigani, Maria La Calle Aurioles and Diego Fernandes for all their help, guidance and companionship during my time at their lab. I would like to especially thank Jessika Royea and Xinkang Tong for their guidance and help.

Finally, I would like to thank my family for their continued support throughout my life, which contributed to who I am today. Thanks to my parents, Tamar and Yoram Bloch; my grandparents, Violet and David Bensamuel and Roza and Leon Bloch; my brother, Jonathan Bernard Bloch; my aunts Dalia and Nora and their beautiful families. I would also like to extend my thanks to Jonathan K. Lai who always tells me to finish what I start and believe in myself and to Alia Yousif who gave me the strength to apply for a master's degree.

Introduction

One of the major growing health issues is dementia affecting approximately 47.5 million worldwide with an expected increase of 7.7million every year. Of these numbers, Alzheimer's disease is the cause of 60 to 80% while vascular dementia comes in next with approximately 10% of cases. Other causes of dementia include dementia with lewy bodies, Parkinson's disease, frontotemporal dementia, Creutzfeldt Jakob disease, normal pressure hydrocephalus, Huntington's disease and Wernicke-Korsakoff syndrome. Interestingly, in the Memory and Aging project study, 94% of patients demonstrating dementia were diagnosed with AD, and of those, 54% displayed a coexisting pathology (1). The AD exhibits multiple pathophysiological characteristics outside of the well defined Aβ pathology. Overexpression of TGFβ cytokine has been identified as an etiology of the cerebrovascular pathology of AD. TGFβ is central to fibrotic responses and is elevated in brain tissue, cerebrospinal fluid, blood and cerebral blood vessels of AD patients. Vascular fibrosis, thickened vessel walls, degenerating capillaries (also known as string vessel pathology) and hypoperfusion are all pathological events found in AD and mimicked in transgenic mice overexpressing the TGFβ1 cytokine.

Another suggested predictor of cognitive decline in AD patients is the increase in pulse-wave velocity caused by arterial stiffness. Recent studies have shown a significant correlation between increasing pulse-wave velocity and cognitive decline from normal cognitive function to impaired cognition to AD to vascular dementia. Whether the relationship between arterial stiffness and cognitive degeneration is causal, additive or synergistic has yet to be classified.

This memoir aims to elucidate the relationship between dementia, arterial stiffness and the cerebrovascular pathology found in AD and VaD. To achieve this objective, we combine a surgically altered mouse model of arterial stiffness and the TGFβ mouse model of AD. Following surgery, mice undergo behavioural testing via the Morris Water Maze and Novel Object Recognition. Cerebral blood flow is observed and brain slices are immunostained to

reveal astrocytic and microglial gliosis. Finally, lipid peroxidation is quantified by ELISA assay to reveal reactive oxygen species in the cortex and hippocampus.

Literature Review

1. Dementia

Dementia is an overall term for a decline in mental ability severe enough to affect daily activities. Symptoms may include impairment of memory, communication and language, focus and attention, reasoning and visual perception. Alzheimer's Disease accounts for 60 to 80% of cases while Vascular dementia is the second principal type of dementia attributing to approximately 10% of cases(1, 2). To elucidate the defining characteristics of the two leading causes of dementia, significant behavioral and post mortem data have been accumulated regarding neuropathological features and changes in brain-related structures of the diseases. These findings have brought a greater awareness of overlapping AD and VaD characteristics in up to 50% of demented elder patients (3, 4). Following AD and VaD, dementia with Lewy bodies has been found to account for 10 to 25% of dementia cases, while other causes of dementia such as Creutzfeldt-Jakob disease, frontotemporal dementia, huntington's disease and others are rare (1).

1.1 Alzheimer's Disease

Alzheimer's disease is a progressive neurodegenerative disorder with classic clinical characteristics such as language deterioration, visuospatial deficits and amnestic-type memory impairment (5, 6). As the leading cause of dementia world wide, much investigation has been conducted on AD forecasting future social and economical issues. In 2015, the International

Alzheimer's Disease Report estimated 47 million people around the world to be living with AD and an anticipated increase of 131 million people by 2050 (4). To determine targets for treatment, multiple features in the AD brain have been examined.

Typical neuropathological features of AD include amyloid beta deposits into senile plaques (6, 7), hyperphosphorylated tau proteins forming neurofibrillary tangles, neuronal degeneration, loss of synapses and gliosis (4, 6). Furthermore, AD is associated with a cerebrovascular pathology where Aβ deposits are observed within the cerebrovasculature, described as cerebral amyloid angiopathy, and an increase in transforming growth factor β1 (TGFβ1) brain levels (8).

These characteristics of AD are accompanied by alterations in brain structure and functions. Indeed, cognitive and behavioral deficits observed in AD patients have been correlated with neuronal loss and atrophy detected mainly in the hippocampus and neocortex (6). The hippocampus, which is critical for the encoding and storage of information in memory (9), is of particular interest. Experiments using MRI in AD patients have shown severe and progressive hippocampal atrophy throughout the advancement of AD as well as a decrease in the volume of the hippocampus (10, 11).

1.2 Vascular Dementia

Known as the second leading cause for dementia in the elder with 17-20% of cases worldwide, VaD is defined as reduced blood flow to the brain causing a progressive degeneration of

cognitive abilities. Patients are prone to suffer from delayed thinking, forgetfulness, depression and anxiety, disorientation, loss of executive functions such as problem solving, working memory, thinking, reasoning, judgment, planning and execution of tasks, and task performance declining with increased complexity (4, 12, 13). Vascular risk factors such as hypertension, hyperlipidemia, diabetes, smoking and aging have been tied to the alteration of vessels in end organs, including the brain (14) (**Table I**). Depending on the neuropathological features displayed, VaD has been broken into multiple subtypes and different brain-related structures may be affected.

Table I VaD Risk Factors [modified from (12)]

RISK FACTOR	REFERENCE
Adiponectin	(15, 16)
Apolipoprotein E4	(17, 18)
Atherosclerosis	(19, 20)
Blood-brain barrier deficiency	(21, 22)
Diabetes	(4, 23)
Metabolic syndrome	(14, 24, 25)
Hypertension	(26, 27)
Aging	(4, 14, 28)
Late-life depression	(29, 30)
Caspase-cleaved Tau protein	(31)
Stroke	(32, 33)

1.2.1 Neuropathological Features of VaD

There are multiple subtypes of VaD that may or may not be due to stroke. A common neuropathological characteristic among VaD patients is cerebrovascular alterations due to vascular remodeling and disrupted blood vessel integrity caused by disturbances of the macro-

and microvasculature (3, 12). Hemodynamic abnormalities caused by vascular risk factors lead to a variety of possible lesions. The most common subtypes are multi-infarct dementia resulting from multiple small strokes, single-infarct dementia caused by a single stroke inciting hippocampal damage, small vessel disease (SVD) and mixed dementia which is based on a combination of AD and VaD pathologies (12, 13, 34).

1.2.2 Brain-Related Structures of VaD

While in the case of AD specific brain-related structures have been identified, those of VaD are highly variable and dependent upon the size and location of brain injury (35, 36). However, a popular hypothesis in the field of VaD research claims that the prefrontal cortical-basal ganglia networks, periventricular white matter and the hippocampus are the locations of initial hemodynamic-based insult resulting in various pathological consequences (12). Experimental data with VaD patients show that neurodegeneration in prefrontal and frontal-subcortical circuits may be responsible for the impairment of elaboration and undertaking of memory retrieval strategies (9). A summary of possible locations of damage and the resulting behavioral features is shown in figure 1.

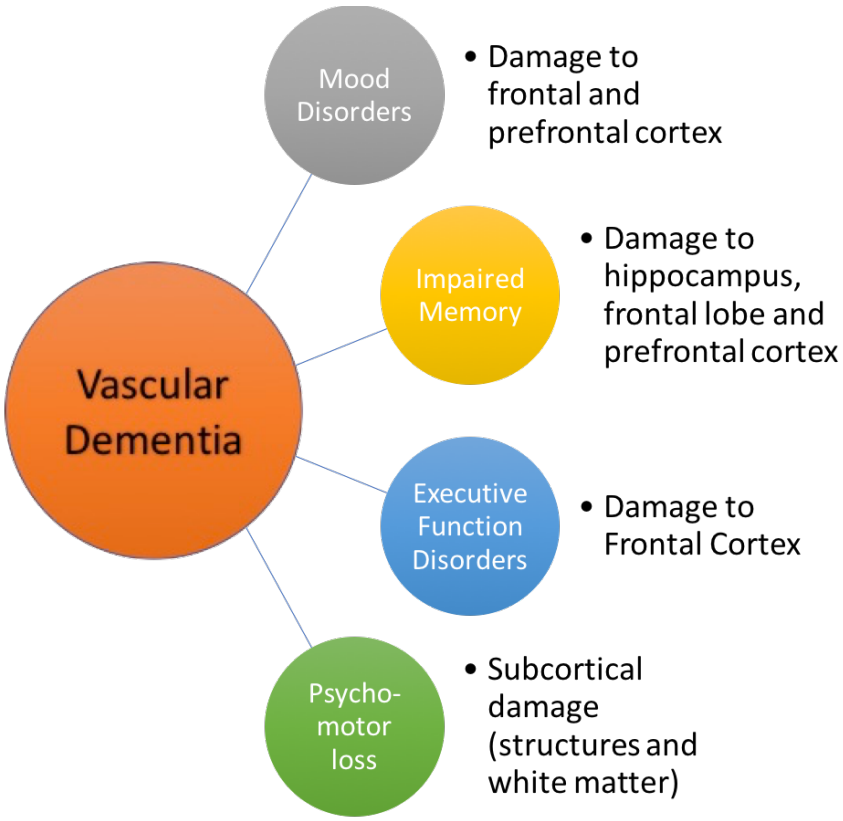

Figure 1 **Vascular Dementia brain targets and effects (Modified from(13))**

1.3 AD and VaD Comorbidity

Brain autopsies of elder patients who displayed AD dementia exhibited a spectrum of conditions, suggesting AD dementia in aged patients to be multifactorial (4). Interestingly, several studies have shown that of all mixed brain pathologies, the type most commonly demonstrated in aging community-based populations is AD and VaD (37-39). In fact, the mixed AD VaD pathology has been displayed in up to 50% of dementia cases (14). Given this information, it is important to note that though these two diseases are distinct, they can share clinically similar symptoms [see table II], which leads to confusion (12, 13). Therefore,

following the question of overlaps, another question that arises is the relationship these two diseases might share.

In the case of AD, one of the primary targets of mainstream research is misfolded amyloid-β for prevention and treatment (35). In AD patients, Aβ accumulates to form senile plaques, attach to blood vessels, which causes cerebral amyloid angiopathy (CAA), and free-float in its soluble form (4, 6, 8); however, Aβ abnormalities are also present in VaD. In fact, multiple sources in the literature define CAA as a vascular pathology of VaD (4, 40, 41). Furthermore, recent research comparing CAA found in autopsied AD, VaD and mixed dementia patients showed that the mixed dementia patients showed a higher severity of CAA and were older than the other patients (42). Additionally, multi-infarct VaD patients show an increase in amyloid precursor protein and Aβ1-42 in brain (12) as well as amyloid precursor protein mRNA increase in the periphery following stroke (12, 40).

Multiple vascular pathologies have been associated with aged AD patients, such as tortuous vessels, venous collagenosis, SVD, decreased microvascular density and microembolic brain injury (43). Again, SVD is a subtype of VaD (12, 13) and can be found in demented patients without signs of AD, such as patients with degenerative dementia like Parkinson's Disease (44, 45).

All these similarities have lead researchers to speculate about the connection these two separate but coinciding diseases might share.

Table II Common pathological lesions in AD and VaD [data from (41)]

PATHOLOGICAL CHARACTERISTIC	AD (%)	VAD (%)
Cardiovascular disease	77	60
Microvascular degeneration	100	30
Cerebral Amyloid Angiopathy	98	30
Total Infarcts	36	100
Micro-infarcts	31	65
Intracerebral hemorrhage	7	15
Loss of cholinergic neurons	70	40
White matter lesions	35	70

1.3.1 Current Hypotheses Linking AD and VaD

Two main hypothesis relating AD and VaD exist in the literature: 1) the two diseases are independent but additive; 2) one disease gives rise to the other, also known as the two-hit theory. Chui et al explored the relationship between the two diseases using cognitive data from autopsied patients. According to their investigation, the cognitive deficits caused by microinfarcts were not exacerbated by the presence of AD, leading them to conclude that the two pathologies were independent but additive (35). It is interesting to note however that another author declared that microinfarcts in the cortex could give rise to the acceleration of AD (36). In the case of the two-hit theory, there are multiple models being studied in the literature. One model posits vascular damage to cause deficits in Aβ clearance and thus causing Aβ accumulation and aggregation in brain (46). Another model suggests that the chronic cerebral hypoperfusion due to vascular lesions triggers cascades leading to Aβ overproduction and tau hyperphosphorylation (47).

Due to the confusion caused by these coinciding diseases, the elucidation of the effects of the vascular pathologies seen in AD is of utmost importance. Furthermore, an important question that arises is how the vascular pathologies of AD might make the brain more vulnerable to the defects of the vasculature of the periphery.

1.3.2 Mouse Model

An important mouse model investigating the vascular pathologies displayed in AD is the TGFβ mouse. The TGFβ mouse is a transgenic mouse overexpressing a constitutively active form of TGFβ1, driven by GFAP promoter (8, 48). Pathological features present in this mouse model are vascular fibrosis, SVD, cerebral microhemorrages, thickened vessel walls, chronic hypoperfusion as well as compromised vascular dilation and contraction (8). Most of these pathologies are seen in AD patients (43). For further detail concerning the TGFβ mouse model, please refer to *section 2.2*.

2. Neurovascular Coupling

Though the brain only makes up 2% of total body mass, it requires up to 20% of total cardiac output to conduct all its required activities, thus making it one of the most highly perfused organs in the body (49, 50). A delicately balanced homeostasis is required in brain environment through functional hyperaemia, also known as neurovascular coupling (51) in which the communicating mechanisms among neurons, astrocytes and vessels of the neurovascular unit function together to spatially and temporally adjust cerebral blood flow (CBF) probably to ensure a continuous supply of essential nutrients needed by activated neurons (52). In fact, any kind of imbalance in homeostasis arising from the inability of cerebral blood vessels to respond to neurons, also known as neurovascular uncoupling, is associated with several cerebral diseases leading to neurodegeneration and dementia (51, 53). To be precise, neuron protein synthesis is inhibited at only 80% of the normal CBF flow rate, followed by modified glucose uptake, energy and neurotransmitter production and anoxic depolarization at 20% of normal CBF (54). Given these facts, one can only imagine the delicate nature of the neuron and the importance of a reliable homeostatic environment.

2.1 Vasculature of the CNS, Aging and Dementia

Compared to other organs, the brain has a particularly high metabolic demand for nutrients delivered by the microvasculature of the CNS (55). The vascular network of the CNS responds to the high metabolic demands of activated neurons. It is responsible for the homeostatic maintenance of essential nutrients, careful pressure conservation as well as clearance of

metabolic waste (14, 52). The vascular network of the CNS is divided into the macrovasculature comprised of the larger proximal vessels, and the microvasculature defined by the small penetrating capillaries (55, 56).

2.1.1 Macrovasculature

Blood is delivered to the brain by the two carotid arteries (each contributing roughly 40% of total brain perfusion) and the two vertebral arteries that combine to form the basilar artery. Finally, the carotid arteries and the basilar artery are linked to form the circle of Willis (CW) (57). The CW's primary role is believed to be the control of pressure reaching the capillaries (58). Interestingly, the vascular system of the brain branches out into smaller and smaller vessels that are progressively more vulnerable to blood pressure; however, these bifurcations cause an increase in resistance, which dampens pressure (58). To protect the most distal vessels from the high blood pressure, the large proximal cerebral arteries are responsible for up to 40% of complete cerebrovascular resistance (55, 58). The intrinsic myogenic response of smooth muscle cells (SMC) to changes in blood pressure is fundamental to CBF autoregulation (55). The importance of the resistance created by arterioles penetrating the parenchyma is a point of debate among authors. Capillaries provide minimal damping of the pulsatile pressure and flow, therefore, intact function of the large proximal vessels as well as the CW is necessary for maintenance of physiologic pressure (59). Other studies have observed that the large proximal arteries together with the intracranial pial arteries and arterioles contribute ~50% of cerebrovascular resistance (60, 61).

While age-related dysfunction in the myogenic responses to pressure have been found in rodents (62), different research groups exploring dynamic myogenic responses yielded mixed results when comparing aged and young control patients (55). Regardless, diminished dilatation of aged proximal cerebral arteries responsible for resistance might increase the risk of ischemia during hypotensive conditions (55).

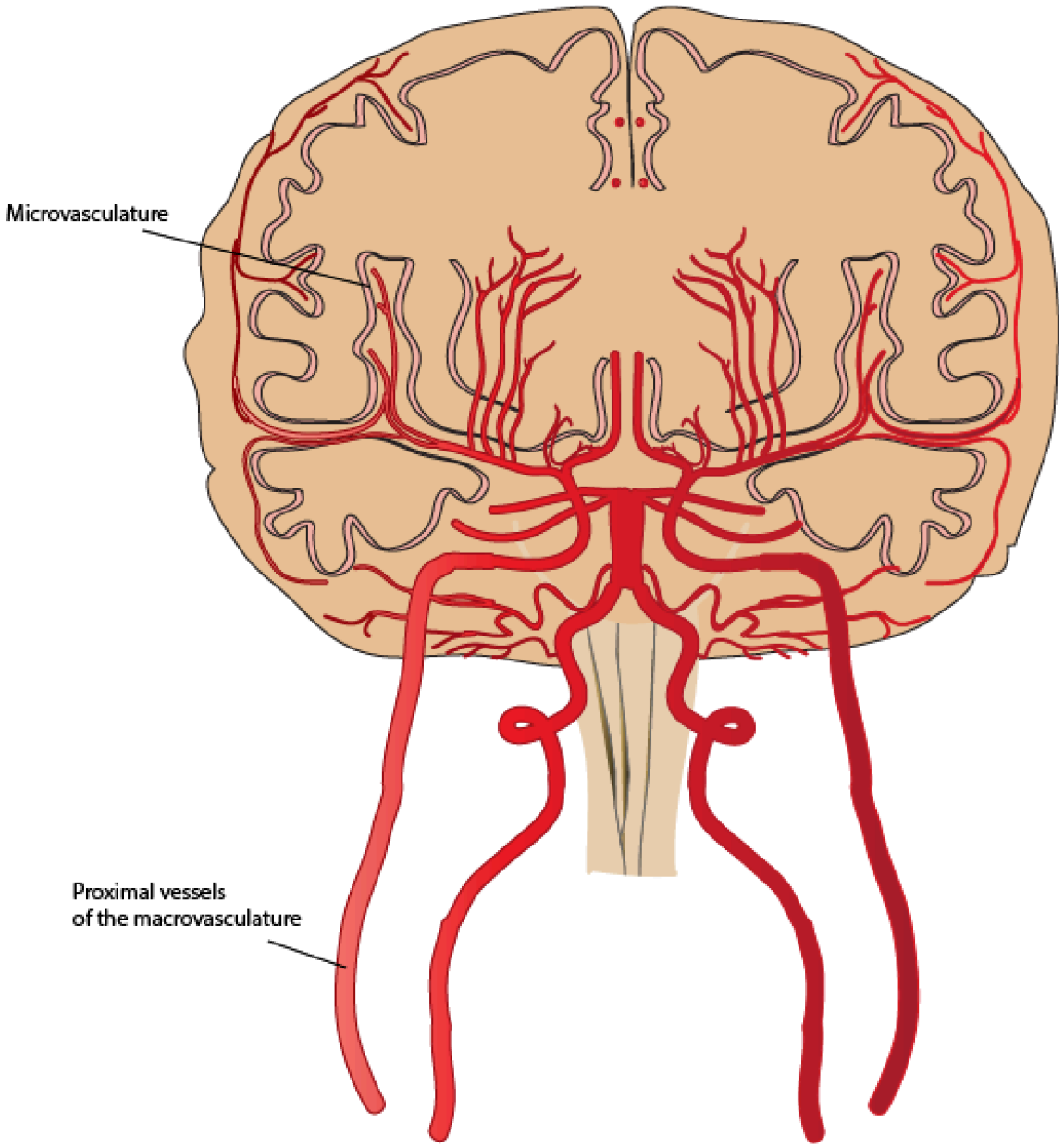

Figure 2 **Macrovasculature and microvasculature**

2.1.2 Microvasculature

At the distal end of cerebral circulation, delicate regulation of tissue perfusion must be maintained through finely tuned signals released by neurons and communicated through

astrocytes to the nearby vessels. This regulation may be done through metabolic, myogenic and neurogenic mechanisms (58, 63). Approximately 90% of the arteriolar surface penetrating the brain parenchyma is covered with astrocytic endfeet, which emit signals for CBF maintenance. It has been shown that impairing astrocytic signaling of arterioles (*in* vivo) can cause approximately a 50% decrease of CBF(64). The capillaries within brain parenchyma are abundant in inter-endothelial tight junctions formed through interactions between endothelial cells (EC), pericytes and astrocytes. Therefore, the tight junctions, which are a fundamental component of microvascular permeability regulation, are dependent upon the integrity of the neurovascular unit (NVU) (63). Another interesting point about the pericytes and the ECs of capillaries is that they both secrete extracellular matrix which forms the basal lamina of capillaries (65).

Altogether, the tight junctions, basal lamina, ECs, pericytes and astrocyte endfeet function together form the blood brain barrier (BBB) (63). The BBB is responsible for metabolic homeostasis of the CNS and the passage of essential nutrients into the CNS environment; BBB disruption is linked with pathogenesis of multiple CNS diseases (66). The main component of the BBB is ECs, therefore, proper function of the BBB is highly dependent on EC integrity.

EC are also highly involved in CBF through multiple pathways. A first proposed way is through cyclo-oxygenase-1 (COX-1), a rate limiting enzyme produced in most cells responsible for the production of prostanoids by arachidonic acid (67). Experimental evidence demonstrates that COX-1 is capable of influencing resting CBF as well as vasodilation induced by certain endothelium-dependent vasodilators or hypercapnea (67). However, COX-

1 has no impact on CBF increase induced by vibrissal stimulation to the whisker-barrel cortex (67). A second recent model posits that pulse pressure plays a central role in the optimal function of cerebrovascular endothelium and eNOS coupling (68). When eNOS coupling is engaged, eNOS produces nitric oxide, a vasodilator; however, when eNOS uncoupling is engaged, eNOS instead produces reactive oxygen species (ROS) such as H_2O_2 which functions to signal dilation of the vessel as well as the free radial O_2^- (68, 69). Experimentation with mouse cerebral arteries demonstrated that physiological pulse pressure enhanced sensitization of EC to shear stress as well as myogenic contractions and prompted the production of NO by supporting eNOS coupling. Furthermore, experimental evidence suggested that mechanical flow signal was transferred via NOX2 as it was necessary for stimulating both the coupled and uncoupled eNOS pathways (68). NOX2 is a superoxide generating enzyme and one of the isoforms of the catalytic subunit of NADPH oxidase (70).

Modifications in functions of pericytes (2.1.3) and astrocytes (2.2.2.1) due to aging will be discussed later in this memoir; here we will focus on the age-related endothelial dysfunction. A proposed theory is that accumulation of ROS in brain due to aging is responsible for decreased production of NO by ECs (55). Superoxide, in particular, readily reacts with NO to form peroxynitrite and decrease bioavailability of NO (71). It has been proposed that decreased NO production is a universal effect of aging due to an increase in arginase production leading to decreases in L-arginine necessary for production of NO (72). Therefore, since endothelium-derived NO is involved in vascular tone, it is likely that the decreased production of the dilator NO will cause chronic hypoperfusion giving rise to cerebral dysfunction and dementia (55). It is important to note that NO is also involved in platelet

aggregation inhibition, SMC proliferation and exerts anti-inflammatory, anti-apoptotic and pro-angiogenic effects. Altogether, this information suggests that age-related decrease in NO influences neuronal, astrocytic, microglial and cerebrovascular functions. Therefore, mounting evidence points to the association of dysfunctional production of NO by ECs with augmented amyloid precursor protein and Aβ, as well as increased microglial activation leading to degeneration of cognitive function (73). Interestingly, it has been proposed that changes in cerebrovascular reactivity provoked by APP and Aβ which result in increased vasoconstriction may be mediated by ROS. Experimental evidence has demonstrated that exogenous free radical scavenger superoxide dismutase (SOD) as well as the overexpression of SOD1 rescued endothelial dysfunction in APP mice (74). Overall, ROS may play an important role in mediating age-related changes in the vasculature as well as APP and Aβ-related changes seen in AD.

2.1.3 Pericytes

In the CNS, pericytes are a type of contractile cell found embedded within the basal lamina, that may participate in the regulation of CBF (66). In fact, smooth muscle cells responsible for contraction of blood vessels are not present in capillaries, leaving pericytes and EC responsible for fine regulation of blood supply through their capacity for contractility (66). The main contracting protein in pericytes is α-SMA, which can be upregulated by TGFβ (75). Interestingly, different levels of α-SMA have been observed depending on the location of pericytes, with the highest concentration of α-SMA in the arteriolar side of capillaries (66). As

mentioned before, arterioles are an important contributor of vascular resistance in the CNS and have a strong impact on CBF (64). In NVC, pericytes receive signaling information from astrocytes, which are also capable of secreting TGFβ (63, 76).

In the aging brain, the number of pericytes as well as the secretion of TGFβ by astrocytes decreases, although α-SMA within pericytes increase (63, 77). Experiments conducted in pericyte-deficient mice demonstrated that a reduction in pericytes induces increased permeability of the microvasculature (78). Furthermore, it is suggested that the accumulation of toxic blood-derived proteins around the vessels may take advantage of the resulting permeability to cross the BBB with consequential neurodegeneration (77-79). Although TGFβ production by astrocytes decreases with age, the increased production of TGFβ seen in AD patients is capable of inducing high levels of α-SMC in pericytes (66, 80). Other alterations seen in senescent pericytes include vacuoles and inclusions, which have been suspected to contribute to the inability of pericytes to deposit the contents back through capillaries; possible pericyte sclerosis which may lower the ability of pericytes to control CBF. Furthermore, the increased oxidative stress seen in older patients leads to the heightened intensity of pericyte constriction and subsequent significant hypoperfusion. Due to these pathological changes, it has been suggested that age-dependent modifications to pericytes may contribute to vascular changes that have been shown to foreshadow the neurodegeneration and neuroinflammation. Finally, these age related changes may make the brain more vulnerable to vascular lesions such as ischemic and reperfusion injury (66).

2.2 The Neurovascular Unit, Aging and Dementia

The acting players in NVC are the neurons, glial cells and vascular cells, which make up the NVU (63, 81). Working together as a finely tuned orchestra to maintain optimal conditions for neurons, the smallest discord or dysfunction can lead to pathogenic circumstances. Furthermore, the natural process of aging is capable of manifesting senile alterations to the components of the NVU (56, 63). Here, we will discuss the instruments of the NVU within the context of age-related impairments leading to cognitive impairments and dementia.

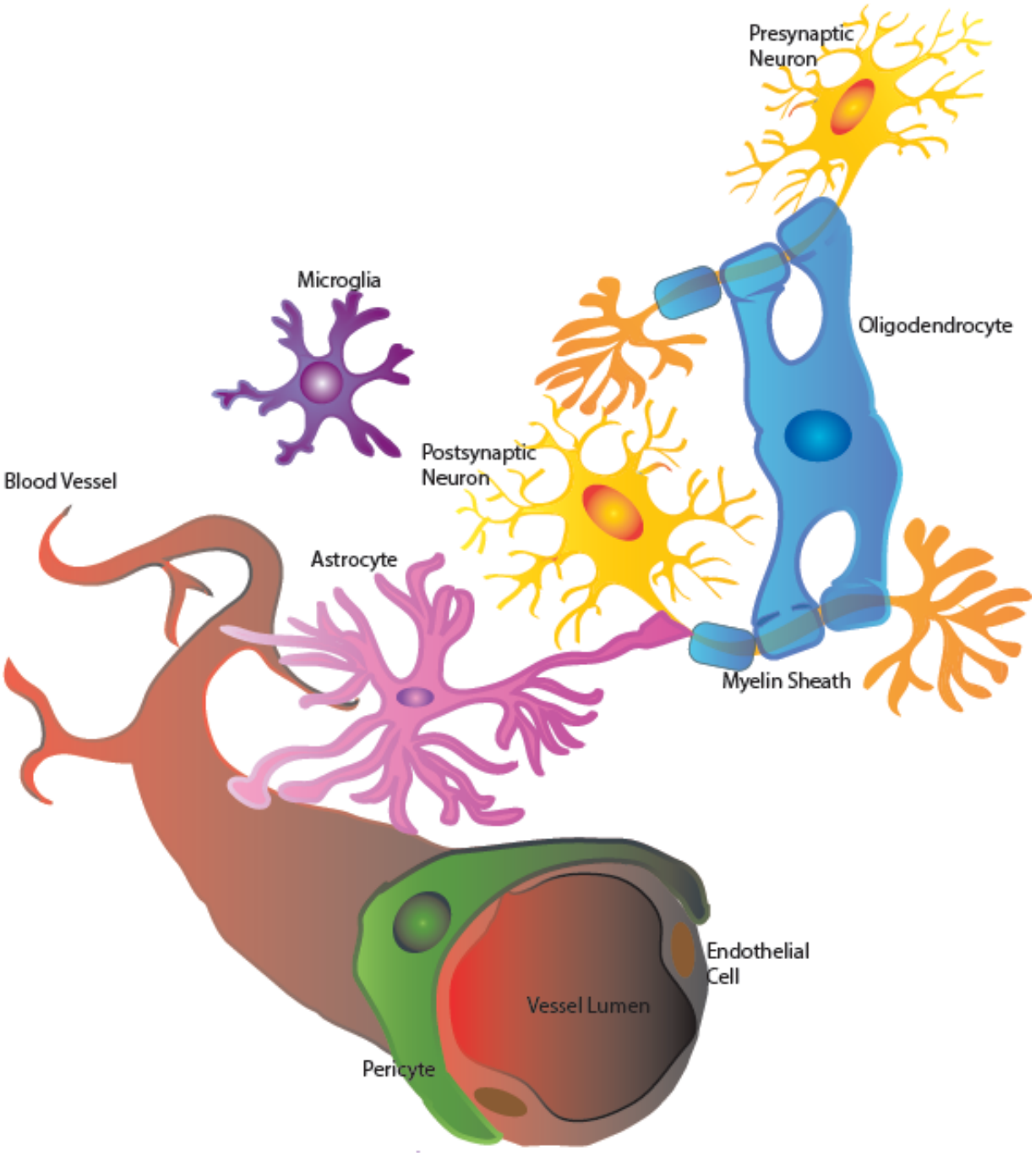

Figure 3 **Components of the neurovascular unit**

2.2.1 Neurons

Neurons make up the basic unit of the central nervous system, their cells composed of two parts, the cell body (or soma) and the processes. The soma contains the genetic material and machinery required for protein synthesis while the processes are long extensions connecting neurons to other cells (82). Neurons are constantly at work and have a very high metabolic demand. However, they are not capable of storing large amounts of energy and are constantly releasing large amounts of metabolic products (52, 63). Due to these conditions, it is up to the proper function of the local microvasculature and other cells of the NVU to maintain homeostasis.

Among the different populations of cells in brain, neurons are among the most vulnerable to age-related dysfunction. Neurons are highly active and therefore require large amounts of energy, which are generated by mitochondria. Another thing the mitochondria are responsible for is the production of large amounts of toxic ROS and oxidative stress in the cell. ROS attach to and cause the disruption of nucleic acids (the building blocks of DNA), proteins and lipoproteins. As time goes by, the endogenous DNA repair and ROS clearance functions decrease, allowing an accumulation of damaged DNA, modified proteins and peroxidated lipoproteins. It is to be noted that the mitochondria is itself severely affected over time due to its unprotected DNA's proximity to the electron transport chain leading to mitochondrial dysfunction. Overall, the accumulation of toxic conditions in the neuron due to aging make the cell even more dependent on other members of the NVU. For this reason, the system of an

aged NVU is vulnerable to brain injuries leading to cognitive impairments which progress to dementia. (63)

2.2.2 Glial Cells

There exist three types of glial cells in brain: astrocytes, microglia and oligodendrocytes, all of which are vulnerable to the aging process. There is mounting evidence indicating that impaired function of any of the glial cells leads to neurovascular uncoupling. (63)

2.2.2.1 Astrocytes

As the most abundant cell type in brain, astrocytes have been found to be responsible for numerous roles (80). In the human brain, astrocytes form highly complex networks: a single astrocyte contacts thousands of neuronal synapses while the astrocytic endfeet cover approximately 99% of blood vessel surface (83). The astrocyte maintains ion and metabolic homeostasis for the neuronal cells as well as control of glutamate signaling in the synapse through Ca^{2+} oscillations (63, 80). In fact, increasing evidence suggests astrocytes are used for modulation of microglial response (84) and inter-astrocytic tight gap junctions have an active role in information processing (83, 85) and long-distance synaptic homeostasis (63); however, for the purpose of this memoir, we will focus on the role of astrocytes in NVC. As members of the NVU, astrocytes serve to communicate with neurons and conduct cross talk between the neuroglial segment and cerebral vessels in proximity to the astrocytic endfeet (63). Depending

on the level of neuronal activity, the astrocyte is responsible for modulation of cerebral blood flow and capillary permeability to adjust the supply of glucose and oxygen (63, 86, 87).

As the number of astrocytes does not change much with the aging of the organism, astrocytes are thought to be the type of glial cell least affected by aging; however, senescent astrocytes do display a decrease in their supportive functions (63, 80). To begin, the abnormal protein accumulation in senescent astrocytes affects their capacity for neuronal metabolic support (88). Another change is the reduction of inter-astrocytic gap junctions, leading to impairment of inter-astrocytic cross-talk and synaptic function (63). Next, chronic stress during aging causes the secretory profile of astrocytes to become inflammatory by the release of soluble mediators such as ROS, leading to inflammation in the senile brain (63, 80). Finally, the increase TGFβ production seen in the elder, especially aged AD patients (8), causes an increase in glial fibrillary acidic protein (GFAP) expression in astrocytes (80). Not only is the increased GFAP associated with senescent morphology (80), but also the repression of the supportive capacity of astrocytes (89), one being glutamate clearance leading to neuronal cytotoxicity and another the reduction in neurotransmitter-induced Ca^{2+} signaling (63). Finally, it has been proposed that these age-related alterations to astrocytes may be a contributing factor to cognitive degeneration as a result of loss of function and neuroinflammation (90).

2.2.2.2 Microglia

Microglia are mobile glial cells that patrol the CNS environment, responsible for CNS pathologies as well as homeostasis maintenance (91). As the innate immune cells of the CNS, microglia are the first line of defense against invading microbes leading to microglial activation and release of protective substances (92). Except for micro-organisms, microglia sense the neural environment to detect neuronal health. Mounting evidence shows microglia function in synaptic pruning (92, 93), pruning of axonal collaterals (92, 94), phagocytosis of apoptotic neurons (92, 95), facilitation of axonal sprouting (92, 96), and remyelination of central axons (92, 97). Therefore, microglial function is necessary for neuronal health and brain homeostasis.

Interestingly, although microglia increase in numbers in the aged brain, there is accumulating evidence suggesting the decline of microglial function due to decreased mobility and efficiency (63). Impaired capacity of senescent microglia also extends to their ability to respond to regulatory signals such as TGFβ (98) capable of inhibiting microglial activation. The senile microglia have impaired mobility (99), loss of microbial elimination (100) and metabolite elimination (101) such as Aβ. However, though senescent microglia have a decrease in functions, they tend to shift to the M1 phenotype, which has elevated production of pro-inflammatory molecules (63). Interestingly, there is mounting evidence suggesting that TGFβ signaling in the brain is in part responsible for the development into adult microglia (102, 103). Mounting evidence links age-related changes in microglial function to neurodegenerative disorders (92).

2.2.2.3 Oligodendrocytes

Neural axons are sheathed with lipid-enriched myelin produced by proximal oligodendrocytes, which speed up signal conduction and allow higher velocity (63, 82, 104). Not all oligodendrocytes in the CNS act as supporting cells: some remain free-floating and act as oligodendrocyte precursor cells (OPC). Under normal conditions, degenerated myelin and exposed axons stimulate the proliferation of OPCs and remyelination of axons (63).

As seen in other glial cells, the aging process impairs oligodendrocyte function. In the aged brain, recruitment of OPCs and remyelination is compromised potentially leading to broad and irreversible demyelination in the event of myelin injury (63, 105). Furthermore, myelin sheaths formed by senile oligodendrocytes are thin with short inter-nodal lengths resulting in lower conduction velocity and brain dysfunction (14, 106).

2.3 TGFβ-Associated Pathologies

As previously mentioned, vascular pathologies displayed in AD patients with increased of all TGFβ isoforms comprise vascular fibrosis, SVD, cerebral microhemorrages, thickened vessel walls, chronic hypoperfusion as well as compromised vascular dilation and contraction: abnormalities mirrored in TGFβ mice (8). Because, of the very similar cerebrovascular pathology compared with AD, transgenic mice overexpressing the TGFβ1 isoform are

instrumental in the elucidation of the effects of increased this cytokine in AD patients. However, it is important to note that the TGFβ mouse is not a model of AD neuropathology per se although they display multiple abnormalities found in AD (52). For instance, TGFβ mice show no signs of Aβ or tau accumulations, though it has been shown that an increase in TGFβ1 aids in the microglial clearance of Aβ (107). To be specific, the TGFβ mouse is a model of cerebrovascular dysfunction associated with AD. However, it has to be noted that a decrease in neuronal TGFβ signaling has also been associated with neurodegeneration (108).

2.3.1 Physiological use of TGFβ in Brain

To understand the abnormalities provoked by pathological over-production of TGFβ1, it is necessary to comprehend the physiological function of TGFβ1 in the healthy brain. Under normal conditions, TGFβ1 is a cytokine central to injury response in the CNS and is responsible for the initiation of fibrotic response and wound healing (48, 109, 110). Upon injury, TGFβ is released by a multitude of cells including platelets, microglia and astrocytes (111, 112). Through experimental data with mice, we know that TGFβ causes overexpression of ECM proteins for wound closure and scarring as well as contraction of the ECM (109, 110). Under pathological conditions, upregulation of TGFβ levels in transgenic mice induces thickened ECM and contracted vasculature. This evidence leads researchers to believe that TGFβ upregulation is responsible for the vascular pathogenesis in AD patients.

2.3.2 Impact of TGFβ-associated vascular pathologies on NVC

Through use of transgenic TGFβ mouse, researchers could unravel the mystery surrounding the effects of TGFβ upregulation on NVC. *In vitro* experiments showed impaired responses to dilatory substances and inability to contract in response to contractile agents (52, 113, 114). These dysfunctional responses to signaling lead to hypoperfusion at baseline in limbic brain regions such as the hippocampus (8) of TGFβ mice with up to 33% decrease when compared to wild type (WT) controls (52, 115). There was a 23% reduction in CBF response to neuronal activation (52, 116). Another important impairment is resting glucose uptake by brain structures, which showed a 15 to 20% decrease in transgenic mice (52, 117). Furthermore, postmortem tissues from AD patients as well as TGFβ mice display astrogliosis (116), which has been associated with demyelination, degeneration of neuronal axons and white matter dysfunction (34). Overall, TGFβ transgenic mice present both neurovascular and neurometabolic deficits mirroring effects seen in AD patients. With age, the increased deposition of profibrotic proteins, namely fibronectin, perlecans, connective tissue growth factor and collagen I and IV which lead to fibrosis cause stiffening and damage to the cerebral blood vessels, as well as capillary degeneration (SVD) (8). However, it is important to note that despite these changes, there is no marked cognitive deficits in young TGFβ mice, while senescent TGFβ transgenic mice showed only insignificant cognitive impairment (52).

2.3.3 Linking TGFβ Mouse and AD Patients

The involvement of TGFβ1 in pathological situations such as AD, Parkinson's disease, stroke, brain tumors, ischemia and abscess is marked by an increase in cerebrospinal fluid TGFβ1 levels (48). Tremendous amounts of research have been conducted targeting multiple facets of AD. However, drugs that were found to be successful on transgenic TGF mice failed when tried on humans (8). To this extent, double mutants combining the Aβ pathology with TGF vascular pathology (APP/TGF mice) were used to emulate neuronal, cerebrovascular and cognitive impairments seen in AD patients (8). However, treatments that were successful on an isolated mutation had no effect on the double mutant suggesting different patterns between cerebrovascular dysfunctions induced by these two parameters (118, 119). Given these facts, it is clear that other factors involved in AD must be traced and treated. A possible culprit for the vascular contribution to dementia in the elder is arterial stiffness.

3. Arterial Rigidity

Arterial rigidity has long been shown to be an independent predictor of cognitive decline in the elderly (27, 120-123). Multiple studies have been conducted in seniors measuring pulse wave velocity, that is the rate at which pressure waves move down the vessel, between the femoral and carotid arteries (cfPWV). The results of these studies pointed to a positive correlation between the increase in cfPWV and deterioration of cognitive abilities in the elder

(27, 124, 125). To fully appreciate the effects of arterial rigidity, we must first appreciate the peripheral vasculature and its mechanics.

3.1 Layers of the Vasculature

The network of tubes responsible for the transportation of essential nutrients throughout the body is composed of three layers: the abluminal layer known as the adventitia, the medial layer known as the media and the luminal layer named the intima (82, 126). Each layer is responsible for supplying proper amounts of nutrients in the case of active hyperemia where an organ has increased metabolic demands.

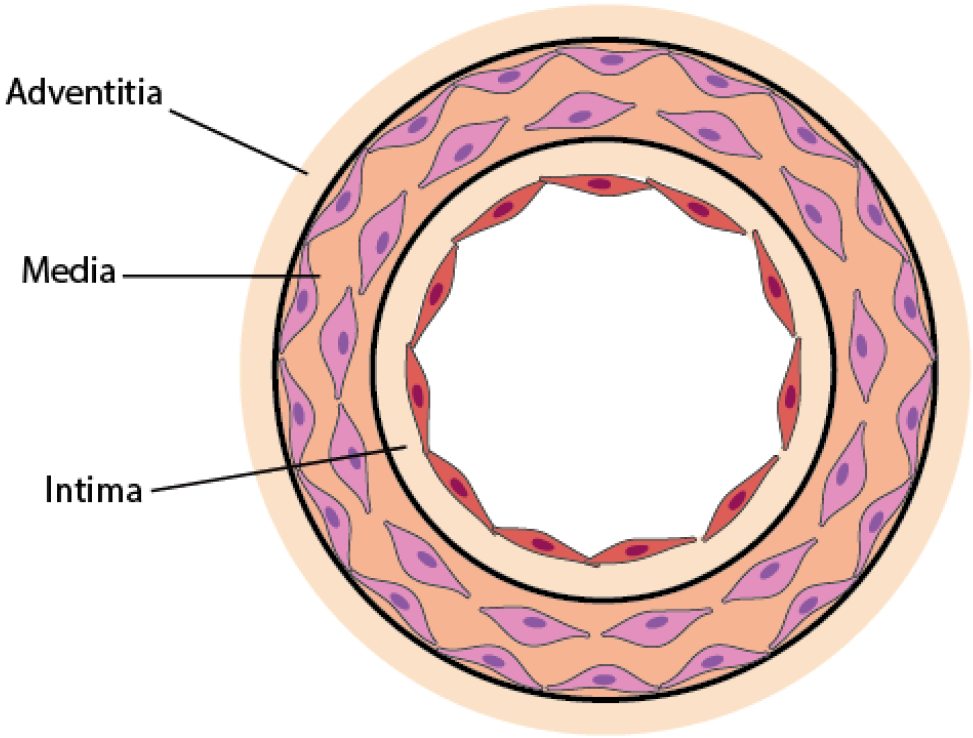

Figure 4 **Layers of the Vasculature**

Beginning with the outermost layer in contact with peripheral tissue, the adventitia functions in the transfer of nutrients and waste substances between the blood and the environment. This layer is looser and thinner than the media from which it is separated by a thin layer of elastin called the external elastic lamina. It is composed of collagen fibres and fibroblasts that produce collagen as well as nets of elastic fibre (126, 127).

Next, the media is the thickest layer and is composed of vascular smooth muscle cells, elastin and collagen as connective tissue, and polysaccharides. The smooth muscle cells relax and contract in response to chemical (NO) and mechanical (blood flow) stimuli to regulate the diameter of the arteries and blood flow. The large arteries closest to the heart, such as the

carotid artery have much higher levels of elastin, and therefore are more compliant. On the other hand, arteries further away from the heart (arterioles) around the muscular tissue have a lower amount of elastin compared to collagen. Collagen protein found in connective tissue is very stiff (126).

Finally, The intima layer of the artery is described as a thin monolayer of ECs attached to a layer of elastin called the internal elastic lamina, spanning approximately 10μm in thickness (126). The endothelial layer presents a large interface ($350m^2$) with the passing blood of the lumen and creates an excellent location for the exchange of substances. In addition to nutrient exchange, ECs serve a multitude of purposes such as being a barrier for large molecules, secreting antithrombotic and anticoagulant molecules, modulating vascular tone, inflammation and angiogenesis.

The adhesive structures between ECs control vascular permeability and are regulated in coordination with the organ through which the vessel passes. This is important in connection with vessels that pass through brain tissue. In physiopathological conditions, permeability is compromised. Another function of ECs is the secretion of antithrombotic and anticoagulant molecules to maintain blood fluidity. The ECs also regulate vascular tone through the secretion of the free radical gas NO, generated by NOS isoforms (eNOS and iNOS) found in the cellular cytoplasm which respond to forces on the cell wall as well as prostaglandins and the endothelium derived hyperpolarizing factor (EDHF). The ECs of the intima are also involved in inflammatory reactions through their response to cytokines and signalling to

leukocytes during leukocyte extravasation (128). Finally, the ECs are responsible for neoangiogenesis, the formation of new blood vessels (128).

3.1.2 Vascular Compliance and Distensibility

One of the important functions of the vascular wall is the compliance, or distensibility, of the elastic arteries, which depends on the ratio of elastin fibres in proportion to collagen fibres. This gives the vessel the ability to dampen the pulsatile intensity of the heart. If the intensity were too high, downstream capillaries in end organs, such as the brain, would undergo micro haemorrhaging. It is the elastin together with the smooth muscle cells in the vascular wall that account for the flexibility and resilience of the vessel wall. It is the larger vessels closest to the heart, such as the aorta and carotid arteries, which have relatively higher amounts of elastin, compared to the smaller downstream vessels (58, 129). It has been shown that stiffening of the vessel is inversely related to pulse wave velocity; that is, an increase of PWV is associated with decreased distensibility (27, 130). Therefore, measurement of propagation of the pulse wave or cfPWV allows for a robust and reproducible method to measure arterial stiffness (27, 131).

3.2 Arterial Rigidity, Aging and Dementia

Aging is the cause of various changes in the physiology of large arteries in the periphery responsible for stiffness. To begin, the principal structural change in arteries is due to the

fatigue and fracture of the media layer of vessels. Given that media is accountable for mechanical properties of the vessel, the fragmentation of elastin and fracture of muscle attachment due to age leads to arterial stiffening (132). Next, there are increases in factors of the arterial ECM including collagen, fibronectin, proteoglycans and vascular smooth muscle cells (27, 132). A decrease in the elastin to collagen ratio in the media decreases distensibility of large arteries such as the aorta and the carotid artery (125, 133). An important change to the arterial wall due to aging is the increase in calcium deposits after the 5^{th} decade (27, 134). While aging induces the production of matrix metaloproteinases (MMPs), which degrade elastin, vessel calcification has also been associated with concomitant elastin degradation (134, 135). Further changes due to aging are impaired vascular EC function, which has been previously discussed in *section 2.1.4.2*. EC dysfunction affects vascular smooth muscle response, which is suggested to modify vascular tone (27).

Hardening of the vessel wall leads to numerous mechanical changes that have multifactorial effects on the body. Impaired function to diminish the pulse wave emanating from the heart is associated with microvascular remodeling and dysfunctional autoregulation, which ultimately leads to end organ injury (124, 133). Furthermore, stiffness of the aorta is the cause for increased workload on the heart via increased reflected waves, which result in decreased stroke volume and coronary artery perfusion (133). Interestingly, various studies have linked increased pulse wave reflection and cardiovascular disease (136). Indeed, arterial stiffness has been associated with multiple risk factors of cardiovascular disease such as hypertension (137), atherosclerosis (138), kidney disease (139) and metabolic syndrome (123, 140). Experimental data studying the effects of cfPWV on brain using magnetic resonance imaging

noted an increased risk of silent subcortical infarcts, higher white matter hyperintensity volume and a decline in grey matter, white matter and whole brain volumes (141). It is important to note that due to the multifactorial influences of arterial stiffness on the body, isolating the effects of arterial stiffness on brain is very difficult. Therefore, we will continue to elucidate the effects of arterial stiffness on brain using a mouse model of arterial stiffness developed by Girouard's Lab (124).

3.2.1 Arterial Stiffness Model

Here we will discuss the published data of the arterial stiffness model developed by Sadekova *et al.* (124). The carotid calcification model has a significant advantage over past models of arterial stiffness: the ability to isolate the effects of arterial stiffness on brain without affecting any other organs or systems in the body, which may then affect the CNS. As the blood journeying from the carotid artery goes directly toward the circle of Willis and the brain, this model ensures that only the brain will be affected by surgical calcification of the right carotid artery.

3.2.1.1 Vascular Significance in the Mouse Model

The effects of periarterial application of calcium chloride coincide with the literature describing the effects of calcium deposits on arteries. However, it is important to note that all arterial changes occurring due to the periarterial application of $CaCl_2$ remain localized.

Two weeks post-surgery, the artery displays fragmentation of elastin, an increase in collagen and media thickness with accompanying decrease in distensibility of the carotid artery and the resulting increase in cerebral blood flow pulsatility. Furthermore, all of these changes manifested without altering systemic blood pressure or vessel radius. Therefore, the model is capable of examining the effect of arterial stiffness on brain and dementia without affecting the systemic networks. Reporting on the short-term effects of carotid calcification, Sadekova noted the cerebral blood flow pulsatility increased from 17.2±5.2% to 23.1±5.1% and 15.1±0.8% to 18.7±1.0% in mice with a calcified carotid in medium-sized arteries (diameter of 50 to 95 μm) and large arteries (>95μm), respectively. Importantly, the treated right side of the brain had significantly higher blood velocity, changing from 16.9±4.3% in the sham group to 23.5±5.7% in the group with the calcified carotid, while the blood speed of the left brain depicted only a non significant increase. These changes in cerebral blood flow pulsatility and blood speed seen in the mouse model give indices of the effects of arterial stiffness on the vasculature and hemodynamics in humans.

Previously, we described the distal microvasculature of the brain to be characterized by the inability to dampen increased pulsatile load. It has been proposed that a protective measure in the brain to intercept the increased load is hypertrophic remodeling (142). Although this response would initially function to limit penetration of the pulsatile load, it will eventually lead to impaired vasoreactivity, hypoperfusion and chronic ischemia: symptoms present in vascular dementia (125).

Given the effects of the model on the vascular bed, Sadekova proceeded with the exploration of the factors most vulnerable to fluctuations in vascular integrity: neurodegeneration and oxidative stress.

3.2.1.2 Neurological Significance in the Mouse Model

As mentioned before, neuronal maintenance is dependent upon the ability of local capillaries to provide proper amounts of nutrients and oxygen. A lack of proper oxygenation would lead to hypoxia and the resulting toxic oxidative stress, which would cause neurodegeneration.

To investigate the possibility of oxidative stress, Sadekova performed dihydroethidium staining which allowed for the revelation as well as the localization of the production of superoxide anion, a reactive oxygen species. Staining revealed a 1.2-fold increase of the superoxide anion in the cornu ammonis 1 and 3 (CA1 and CA3 respectively) of the hippocampus as well as the dentate gyrus (DG). Interestingly, although only the right carotid artery was calcified, no inter-hemispheric difference in superoxide anion production was observed.

For the purpose of examining the manifestation of neurodegeneration, Sadekova used Fluorojade B staining, which also had the added benefit of localizing neurodegeneration in the brain. Realization of the experiment lead to the discovery that the area of neurodegeneration was specific to the lacunosum moleculare in the CA1 region of the hippocampus with a percentage of area shift from 0.4±0.2% in the control group to 13.7±1.0% in the calcium-

treated group. The lacunosum moleculare is the layer of the hippocampus that serves as the connection between the entorhinal cortex and the CA1 of the hippocampus(143). The fact that this specific layer is targeted is an important finding to the field of AD: the first sign of neurodegeneration in AD is the group of neurons in the entorhinal cortex that project into the CA1 (144). Therefore, due to Sadekova's model of arterial stiffness, a clear liaison has been mapped between arterial rigidity, VaD, AD and ultimately dementia.

4. Neurological Insults

Until now, this memoir has discussed several perturbations of the neuronal environment, which have been linked with dementia. Here, we will discuss these symptoms in greater detail.

4.1 Oxidative Stress

Oxidative stress has been widely defined as an imbalance between the production of reactive oxygen species and the ability to counteract through antioxidants defenses (145). The hypoxic conditions that arise from the VaD facet of mixed AD/VaD dementia as well as aging are responsible for the injurious increase in ROS (12, 63). Mitochondrial respiration through the electron transport chain (ETC) is responsible for 90% of both cellular oxygen consumption and ROS production (12, 63); also, mitochondria are very susceptible to age-related impairments (63, 146).

4.1.1 Free Radicals: Formation and Biological Uses

Physiological as well as pathological systems yield free radicals. Free radicals have been defined as molecules with a single unpaired electron in search of its pair (147). It is the unpaired electron in the outer orbit that causes the molecule to be unstable and highly reactive, attaching itself to proteins, lipids and DNA, thus altering their normal structure and function (148, 149). Among these reactive species, there are also non-radical molecules such as H_2O_2 and $ONOO^-$ and which do not have an unpaired electron (147). There exist three types of reactive species: ROS, reactive nitrogen species (RNS) and reactive chlorine species, although during brain injury, ROS and RNS are the major sources of oxidative stress (149, 150). ROS include peroxyl radicals ROH, hydroxyl radicals $^{\bullet}OH$, superoxide $O_2^{\bullet-}$ and H_2O_2 while RNS contain $ONOO^-$, nitrogen dioxide radical $^{\bullet}NO_2$ and nitric oxide $^{\bullet}NO$.

The superoxide $O_2^{\bullet-}$ is very reactive and is involved in the formation of other highly reactive ROS. Its production accounted for the development of many pathologies. Enzymes responsible for the generation of $O_2^{\bullet-}$ are the electron transport chain of mitochondria, NADPH oxidase (NOX family subunits), xanthine oxidase as well as NOS in the case of its uncoupling (68, 147).

Multiple significant members of RNS exist. To begin, $^{\bullet}NO$ is an important signaling molecule involved in inflammation, nerve transmission, vasodilation and perfusion, as seen earlier (147). It is formed by members of the NOS family, which include iNOS (inducible NOS), nNOS (neuronal NOS) and eNOS (endothelial NOS), all of which require L-arginine,

molecular oxygen and NADPH. eNOS and nNOs are constitutively actives whereas iNOS is inducible. An important cofactor also involved in NOS activity is BH_4: when the source of BH_4 is exhausted, NOS becomes uncoupled and produces $O_2^{\bullet -}$ and H_2O_2 (147). A second important RNS is the non-radical $ONOO^-$, produced when superoxide reacts with $^{\bullet}NO$. $ONOO^-$ has been proposed to have anti-microbial features, although it is mainly known to be deleterious to biomolecules (147, 149). A third RNS is generated when $ONOO^-$ undergoes homolytic cleavage to compose $^{\bullet}OH$ and $^{\bullet}NO_2$ (147).

Therefore, although free radicals have been shown to be an important component of physiological functions through signal transduction, regulation of enzymatic activity and gene transduction, they are injurious to cells at pathologic concentrations (149).

4.1.2 Markers of Oxidative Stress

In an attempt to pair their unpaired electrons, free radicals attach to proteins, lipids and DNA, thus altering their structures and functions. The resulting modifications can be used to trace the level of oxidative stress. As oxidative stress has been linked to aging, protein nitration and lipid peroxidation products have been recognized as age-related modifications (63, 151).

A possible protein marker is 3-NT, which is generated when $ONOO^-$ undergoes homolytic cleavage to compose $^{\bullet}OH$ and $^{\bullet}NO_2$, leaving the $^{\bullet}NO_2$ to attach to a nearby tyrosine molecule (152). Concentrations of 3-NT above physiological levels denote an environment with elevated quantities of RNS. Interestingly, if RNS imbalance occurs under neurodegenerative

circumstances, it may result in altered metabolism, enzymatic reactions and activities necessary for cell maintenance. All these changes may ultimately result in cell death (147).

The brain is rich in poly-unsaturated fatty acids (PUFAs), which compose the neuronal membranes as well as other features. PUFAs have nucleophilic unsaturated double bonds, which are a target for oxidation. Lipid peroxidation occurs in three stages: initiation, propagation and termination (147). The first stage occurs when a reactive species, such as $^{\bullet}OH$, $ONOO^{-}$ or $HOO^{\bullet}$ attack the hydrogen double bond on the PUFA to extract the hydrogen, leaving behind a carbon-centered lipid radical $L^{\bullet}$. In the next phase, oxygen is added to produce a lipid peroxyl radical $LOO^{\bullet}$ which will then snatch a hydrogen from another nearby PUFA. These reactions yield a highly unstable lipid hydroperoxide LOOH that soon decays into a lipid hydroxyl radical $LO^{\bullet}$, while the second PUFA reacts with oxygen to begin its own chain of events. These reactions continue to propagate unless termination occurs through one of two methods to ultimately form non radical end-products. The first method is when two $L^{\bullet}$ or two $LOO^{\bullet}$ conjugate, the second method is through the aid of an antioxidant (147, 149). Multiple markers of oxidative stress arise from lipid peroxidation, one of them being 4-hydroxynonenal, which is a cytotoxic unsaturated aldehyde as well as a main lipid peroxidation endproduct (63, 147).

4.2 Gliosis

In reaction to perturbations of different severities within the CNS, such as lesions and diseases of varying nature, glial cells activate to potentially remove the perturbation and reestablish

homeostasis (92, 153). In the case of neuroinflammation in age-related dementias, the major contributors are microglia and astrocytes (34).

4.2.1 Microglia: Activation and Labeling

Microglia makeup the first line of defense against injury and disease (91). Upon activation, they are capable of mobilizing to the desired site and transforming into the M1 phenotype, which releases pro-inflammatory signals such as TNFα, IL-6, ILβ1, interferon-γ (IFN-γ) and iNOS (63). Microglia may also transform into the M2 phenotype, which releases anti-inflammatory signals. The phenotype the microglia will choose depends on the signals it receives from neurons and astrocytes in the vicinity, as well as the environment itself (92). Another feature that happens during activation is microglial proliferation. Once tissue integrity has been reestablished, excess microglia undergo activation-induced cell death (98). Therefore, microglia must be tightly regulated to prohibit pathological conditions incited by continuous microglial activation. Uncontrolled microglial activation can potentially lead to further development of brain damage around the original injury, and possible cognitive deterioration. Furthermore, microglia have the ability to undermine oligodendrogenesis, neurogenesis as well as axon regeneration (91).

Microglial activation can be labeled through Iba-1, the ionized calcium binding adaptor molecule1, with a suggested role in calcium homeostasis (95, 154). Iba-1 has been shown to be specifically expressed in the cytoplasm of activated microglia (155, 156).

4.2.2 Astrocytes: Astrogliosis and Labeling

Astrogliosis is activated in response to multiple triggers and signaling molecules. Such events include cell damage and death, ischemia, neuronal hyperactivity and neurodegenerative diseases such as AD and VaD. Signals arising from these events include adenosine triphosphate (ATP), ROS, NO, Aβ and LPS. Astrocytes also receive signals from neurons, oligodendrocytes, pericytes, EC and microglia as well as other astrocytes. These regulatory indicators comprise IFNγ, TGFβ, TNFα, IL-1β and IL-6, all of which were previously mentioned to be released by the M1 pro-inflammatory activated microglia (63, 157). Depending on the severity of the perturbation, astrocytes will react with different levels of reactive astrogliosis. At levels of mild astrogliosis, there is little to no proliferation of astrocytes while in the cases of severe diffuse reactive astrogliosis and severe astrogliosis with glial scar formation, there is astrocytic proliferation (153, 157). Glial scars are composed of collagenous ECM containing signals that bar cellular and axonal passage, thus acting as neuroprotective barriers (158). Reactive astrogliosis offers many benefits such as protection of oxidative stress through the production of scavenger glutathione, degradation of Aβ, reducing vasogenic edema after trauma and limiting the spread of inflammatory cells through glial scar formation. However, astrogliosis also has many detrimental effects. Experimental evidence has demonstrated reactive astrogliosis as the cause of chronic pain, BBB impairment through release of VEGF, the production of glutamate, which may potentially cause excitotoxicity, inducing secondary inflammation through cytokine signaling, potential involvement in seizures as well as the production of ROS at levels toxic to neurons (153, 157).

A label sensitive to reactive astrocytes is GFAP, which not only becomes upregulated when astrogliosis takes place, but is in fact necessary for glial scar development and astrogliosis. Astrocytes produce small concentrations of GFAP in healthy tissue and so it is important to note that not all astrocytes produce detectable levels of GFAP. Experimental evidence has shown that GFAP upregulation may occur in the absence of proliferation and astrocyte population increase, such as in the case of mild astrogliosis. Therefore, at both mild and severe levels of reactive astrogliosis, there is an increase in GFAP production and most astrocytes are detectable through immunochemistry (153). Another astrocyte marker is S100β, a calcium-binding protein produced principally by astrocytes in the brain of vertebrates. S100β has been used as a marker for brain activity and injury and the results are often compared to GFAP staining (159).

5. Behavioral Testing

5.1 Morris Water Maze

The Morris Water Maze (MWM) is a widely used behavioral test of the water escape variety (160). The protocol of this test requires the mouse to be deposited into a circular pool of opaque water with hidden platform. The pool is divided into four based on the four poles of the pool (North (N), South (S), East (E) and West (W)) connecting to form four quadrants. To escape from the water, the mouse must first find the platform located in the center of one of the pool's quadrants. Every day the mouse will perform three trials to find the hidden platform, entering the pool from three different poles. Each day, the time necessary for the

mouse to locate the hidden platform becomes shorter: this portion of the MWM protocol is linked to memory acquisition. On the final day, 24 hours after the last trial, the mouse performs a probe trial with an absent platform, recording the amount of time spent in the quadrant as well as counting the entries into the location where the platforms was previously located: this final part of the MWM protocol is connected to memory consolidation (161, 162).

5.1.1 Brain-Related Areas

This test is based upon the concept of place cells, neurons located in the hippocampus responsible for spatial learning (162, 163). NMDA receptor function and long-term potentiation have been connected to mouse performance in the MWM, thus making the MWM a fundamental test of hippocampal circuitry (161). Specifically, experimental evidence has shown that the CA3 subfield of the hippocampus is important for memory acquisition and specifically consolidation in the MWM (164). However, experimental evidence has demonstrated that other areas of the brain are also responsible for proper navigation of the task. Other brain areas involved include the insular, cingulate and prefrontal cortex as well as the cerebellum to a lesser degree (161, 165). Interestingly, experimental evidence in rats demonstrated that the inactivation of the insular cortex was responsible for impaired performance in the probe trial(165). Furthermore, NMDA receptor blockade in the insular cortex caused compromised performance in both the hidden platform trial and probe trial(165).

5.1.2 Limitations

Although the MWM is a widely used procedure, there are certain limitations. When experimenting with mice, there are often subjects who choose not to swim, termed 'non-performers'. These mice float on the surface of the water and appear to lack the necessary motivation to escape. Mice are capable of floating due to the oil on their coats lending them a buoyant quality. Interventions by the experimenter may cause bias in the data (161). A second concern is the water temperature: if the water is warm, there may be a lack of motivation, if too cold, the stress may inhibit learning (161, 162). Another limitation is that not all poles are equidistant from the hidden platform, causing one path to be much shorter and quicker than the others although this is circumvented by alternating poles (161). Finally, it has been noted that performance in the MWM is affected by multiple parameters so that the tasks deliver a vague analysis which has to be supported by other behavioural tests and biological analysis (162).

5.1.3 MWM and TGF Mice

The MWM is often used to reveal learning and memory deficits in animal models for AD or other types of dementia. Indeed, APP mice show significant and reproducible cognitive impairment compared to control mice (165). However, TGF mice have displayed nonsignificant impairments in the MWM tasks. Limited cognitive impairment was displayed in senescent mice, with hippocampal differences at 12 months (8).

5.2 Novel Object Recognition

Since its conception in 1988, the one trial novel object recognition test (NOR) has become popular due in part to its ability to be modified to assess working memory, anxiety, attention and preference for novelty. Moreover, no punishment, reward or external motivation is necessary. Simply, this test assesses the subject's ability to distinguish a novel object from a familiar one. A concept fundamental to human amnesia is inability to identify a familiar stimulus. NOR is divided into three phases: habituation, familiarization and test phase. During habituation, the subject becomes familiar with the environment, usually a tall white box with an open ceiling. In the second phase, two identical objects are placed at opposite corners of the box, and the mouse is given time to familiarize itself with the object. In the final test phase, after a designated amount of time has passed, the mouse is returned to the box with two objects: one familiar, the second novel. This test is evaluated through measurement of the time spent with the novel object in ratio with the time spent with the familiar object. Therefore, the results of this test is sensitive to multiple variables such as the time spent in habituation and familiarization, as well as the time spent in between phases. (166, 167)

5.2.1 Brain-Related Areas

The NOR test identifies impairments in both the cortex and the hippocampus (168, 169). Interestingly, cortex regions surrounding the hippocampus such as the entorhinal cortex have been identified as responsible for visual memory, the medial temporal lobe of the cortex are necessary to determine an object as familiar and the perirhinal area is responsible for memory relating to recognition (166). In the case of the hippocampus, its integrity is crucial for proper function of recognition memory (169).

5.2.2 Limitations

Though widely used, the NOR has limitations. A first limitation is the effect of the environment on the subject. The material, height and area of the box all affect the level of exploration to the point where distinction between objects may become non significant. A second limitation is the delay between phases: if the interval is too long, the subject may favor the familiar object or a null preference may be observed. Finally, it is important to note that this test is limited to the recognition of an object, its context and location. The strength of the memory may not be determined from analysis of this test. (166)

5.2.3 NOR and TGF Mice

Mice displaying AD and various forms of dementia have been successfully tested by NOR to display significance in comparison to control mice (166, 170). Interestingly, though irrelevant significance was obtained by TGF mice in the MWM, the NOR test showed significantly poor performance by senescent TGF mice (aged 16 months).

Hypothesis and objectives

The AD pathology is known to be multifactorial and not limited to the Aβ profile. A pattern detected among AD patients is an increase in transforming growth factor β (TGFβ) cytokine in cerebrospinal fluid. Interestingly, transgenic mice with an overexpression of TGFβ display multiple vascular pathologies mirrored in AD patients such as small vessel disease (SVD), vascular fibrosis and microhemorrhages. Furthermore, these mice display increased astrogliosis and microglial activation. A chronically compromised cerebral circulation as seen in TGF mice may thus precipitate cognitive failure when combined with risk factors for VaD or AD, such as arterial calcification.

A novel murine model of surgically induced arterial stiffness has successfully demonstrated effects such as increased astrogliosis and microglial activation as well as increased reactive oxidative species and neuronal death in hippocampus. Therefore, we posit here that a combined model of TGFβ overexpression and arterial rigidity may display an additive effect on cognition attributed to AD/VaD as well as on gliosis, cerebral blood flow and oxidative stress in both young and aged mice, respectively. We thus aim to test: i) whether arterial calcification will worsen cerebrovascular dysfunction and trigger cognitive decline in TGF mice; and ii) whether these effects are accompanied by increased gliosis an oxidative stress.

To successfully demonstrate cognitive and behavioral deficits over time, subjects will undergo the Morris Water Maze and Novel Object Recognition at 1, 2 and 4 months post-surgery. Changes in cerebral blood flow will be detected through Laser Doppler and verification of arterial stiffness will be done through measurement of changes in circumferential strain.

Gliosis will be measured by immunohistochemistry of GFAP and Iba1 for astrogliosis and microglial activation, respectively. Finally, oxidative stress will we revealed through ELISA assay of 4-Hydroxynonenal produced as a result of lipid peroxidation.

Methods

Animals. Heterozygous transgenic mice overexpressing TGF-β1 under the control of the constitutively active GFAP promoter on a C57BL/6J background and their wild type littermates were bred in the Animal Care Facility of the Montreal Neurological Institute and used for experiments. Transgene expression was pre-verified through touchdown PCR using DNA extracted from tail tissue. Mice were individually housed in a controlled environment with circadian light-dark cycles and access to food and water *ad libitum*. The first group of mice was submitted to periarterial carotid calcification at 3 months of age, while the second group received the surgery at 6 months of age. The literature does not indicate significant differences in pathophysiology between the two age groups. However, differences in hippocampal structure were observed at 12 months, and subtle nonsignificant effects were observed in memory and spatial learning at 18-20 months (8). Experiments were approved by the Animal Ethics Committee of the Montreal Neurological Institute as well as the Animal Care and Use Committee of Université de Montréal, and respected guidelines of the Canadian Council for Animal Care.

Periarterial Carotid Artery Calcification The protocol for arterial stiffness by periarterial application of $CaCl_2$ was done as previously described (124). Briefly, in 3- to 6-month-old mice, anesthesia was induced using a 0.025% xylazine (Rompun, 20mg/mL, Bayer) in PBS solution, to which 0.1ml ketamine (Narketan, 100mg/mL, Vetoquinol) was added per mL. Mice receive ketamine/xylazine (80 mg/Kg and 8 mg/Kg respectively). Level of anaethesia was supervised throughout the surgery by tail-pinch motor responses. The workbench was sterilized prior to manipulations using. Once anaesthetized, mice were placed on a pre-heated

heating pad under a dissection microscope. The surgical site was sterilized using a povidone-iodine and 70% isopropyl alcohol and an incision above the trachea was made. The mandibular glands were moved aside with foreceps to expose the trachea and right carotid artery. The exposed area was kept hydrated using a pre-sterilized physiological saline solution. A narrow paraffin tape was inserted under the right common carotid artery and a patch pre-soaked in 0.3 M $CaCl_2$ solution (or sterile 0.9 % NaCl solution for control mice) was applied on top of artery and left for 20 minutes. The patch was then removed and the incision was sutured using 6-0 silk stitches with 1-2 drops of Vetbond tissue glue on top. Mice were pre-treated with a subcutaneous injection of numbing solution Bupivacaine hydrochloride (Marcaine, 4 mg/kg, CDMV, Canada) as well as Carprofen (Rimadyl, 5 mg/kg, CDMV, Canada), an anti-inflammatory drug, directly post-surgery. In addition, Carprofen was dispensed for the two following days at 24-hour intervals. To prevent infection, Trimethoprim Sulfadiazine (Tribrissen, 30mg/kg, CDMV, Canada) was administered directly post-surgery as well as 3 days following surgery at 24-hour intervals. Animals are then sacrificed 6 to 7 months later.

Morris Water Maze. A circular white tank (1.4m diameter) located in a room with four visual cues was filled with water and brought to 17±1°C by depositing ice into the pool as per the protocol of the Hamel's Laboratory (171). Acrylic white powder is mixed into the water to make it an opaque white color. A platform was placed into one of the four quadrants with two possible platform locations: the first visible, 1cm above water, for a three-day training session; the second invisible, 1cm below water, for a 5-day training session. Placements of the visual cues were changed randomly between visible and invisible training sessions. Mice underwent

three trials from different starting locations every day, each trial with a maximum duration of 90 seconds for the visible platform session, and 60 seconds for the invisible trials. On the first day of each session (visible and invisible), mice that were unable to discover the platform were guided and allowed to remain on it for 10 seconds. Memory consolidation was observed during the probe trial, occurring 24 hours after the last trial. There is only one trial for the probe lasting 60 seconds with the platform removed. Water 2020 software (Ganz FC62D video camera; HVS Image, Buckingham, UK) was used to trace trial measurements. Speed and latency were observed during the learning period. Learning curves were analysed using IBM SPSS statistical software (version 24, IBM, New York, US). During the probe trial, percent of time spent in the target quadrant and percent of distance traveled in the target quadrant as well as number of crossings into the platform area were recorded. For both young and aged mice, we performed MWM three times (at 1-, 2-, and 4-months post- surgery) to determine whether calcification of the carotid artery might cause a progression of cognitive deficiencies over time.

Novel Object Recognition. An elevated white plastic box was used as the environment for the NOR test, with two orange, rhombus-shaped wooden blocks as familiar objects and a clear tube with a yellow tape along the sides and a white plastic cap as the novel object. The box was divided into four quadrants with the north-east corner as quadrant 1, going in a clockwise direction. Mice were observed using a small camera lodged on top of the southern wall with iSpy camera security software. On day 1, mice underwent habituation with the empty box and

camera for 7 minutes. On day 2, mice experienced (1) familiarization (5 minutes) with familiar objects placed in quadrants 2 and 4, followed by (2) a 2 hours delay until the test phase (5 minutes) where the familiar object in quadrant 4 was switched for the novel object. The environment was cleaned with 70% alcohol solution between mice. Observation data of time spent with each object was measured using ODlog (created by Macropod Softwar). Exploration time was measured according to the time the mouse spent observing an object.

Laser Doppler. Mice were anesthetized using a ketamine-xylazine mixture (85 mg/kg and 3 mg/kg respectively) administered intramuscularly, placed on a heating pad and fixed in a stereotaxic frame. A drill was used to thin the skull above the left and right barrel cortex. Probes monitored by laser Doppler flowmetry (Transonic Systems Inc. Ithica, NY) were fixed above the left and right barrel cortices to measure variation in CBF due to whisker stimulation. Whiskers were stimulated 4-5 times using an electric toothbrush producing 8-10 Hz for 20 seconds with one-minute intervals: the data of each side was averaged for each mouse. Results were determined as a percent change from baseline.

Mouse Transcardial Perfusion and Carotid Artery Extraction. Mice were anesthetized with an intraperitoneal injection of 0.01469 ml pentobarbital per gram of mouse. Under dissection microscope, a vertical incision from the base of the chin to the top of the chest, is done and the right carotid artery is isolated. To later identify the carotid artery, silk 6.0 thread is passed underneath the top of the carotid and another near the breast bone. Loose knots were tied using foreceps to avoid blocking circulation. Transcardial perfusion was then performed

using a pump machine which ran a solution of 4% Paraformaldehyde (PFA). Butterfly needles were used to inject the solution through the heart and into the circulatory system. Finally, the mouse was moved back under the microscope and the knots around the carotid artery were tightened. The artery was cut using microscissors and the carotid artery was extracted and placed in 4% PFA solution at 4 °C overnight to be transported to Histology Core facility at the Institute for Research in Immunology and Cancer (IRIC, UdM) for histological assessment. The mouse was then decapitated and the brain was extracted and placed in 4% PFA at 4°C for 48 hours and then moved to 30% sucrose solution for 24 hours, 4°C. Brains were removed from sucrose solution and dried briefly on paper towel. Brains are placed in -20°C to -30°C isopentane solution for flash freeze. Brains are then removed using a paddle and quickly placed in aluminum foil to be stored at -80°C.

Brain Sections. Frozen PFA-perfused brains were cut into 25μm-thick sections using Licor microtome. Funnel paper and 1X PBS was applied to the microtome base and glue was used to fixate the brain. Crushed dry ice was intermittently applied to the frozen brain to keep it in optimal frozen condition. The Sections were then placed in 1X PBS for 24 hours and kept at 4°C before being transferred to Antifreeze solution (200 mL of 0.1 M PB, 120 mL of glycerol, 120 mL of ethylglycol; -20°C) until further analysis.

Carotid Compliance. Right Carotid arteries were mounted onto a pressure myograph (Living System Instrumentation, Burlington, Vermont) while submerged in Ca^{2+} free physiological salt solution (PSS, pH 7.4 mmol/L) containing 1 mmol/L EGTA to remove myogenic tone and measure the mechanical properties of the arteries (124). Measurements were taken by video

microscopy at pressures beginning from 60 mmHg and increasing by increments of 20 mmHg to 180 mmHg. Diameter measurement at 60 mmHg was the initial diameter (D_i) and the circumferential strain (%) was determined by the equation $\frac{D-D_i}{D_i}$ where D is the diameter at a set pressure.

ELISA Lysate. For protein carbonyl ELISA, detergents such as Triton X-100 or NP-40 were not used due to their negative effect on protein carbonyl. Instead, isolated cortex and hippocampal samples were resuspended in 1X PBS mixed with a EDTA-free protease inhibitor cocktail tablet produced by Roche (Diagnostic, Canada) at 100µL and 400µL respectively. Samples were homogenized and centrifuged at 12000xg for 15 minutes (4°C). The supernatant was harvested for the protein content and ELISA assays and placed at -80°C.

Protein Content Assay. Colorimetric detection and quantification of total protein in samples was done by BSA protein assay. BSA stock solution was made using Albumin Fraction V salt-free from Bio Basic Canada Inc. 2mg/mL. Standard curve was made using final BSA concentrations of 0 to 2000 µg/mL. Samples were diluted using PBS to 1:20 to obtain the OD value in the middle of the standard curve. 25µL of sample and 200µL of working solution were placed in the 96-well microplate. The plate was then shaken and placed at 37°C for 30 minutes. Next, the plate was cooled to room temperature and absorbance measured at 530nm using Wallac Victor^2 1420 Multilabel counter and the Wallac 1420 Manager software. The standard curve was then extracted using Microsoft Excel. Protein concentration of samples was calculated.

HNE Adduct Competitive ELISA. To evaluate lipid peroxidation caused by reactive oxygen species (ROS), OxiSelect^{TM} HNE Adduct Competitive ELISA Kit produced by Cell BioLabs, Inc. (catalog number STA-310 96 assays) was used. The HNE Conjugate coated plate was prepared the day before and used within 24 hours after coating. 50μL of homogenate and standard curves were added to the plate and left for 10 minutes on the orbital shaker. Next another 50μL of 1:1000 anti-HNE antibody are added to each well to be incubated at room temperature for 1 hour on an orbital shaker. A multichannel pipette was used to wash the plate 3 times with 1X Wash buffer. Next, 100μL of diluted secondary antibody was loaded into each well to be incubated for 1 hour at room temperature on an orbital shaker, followed by a wash (3 times). Finally, 100μL of substrate solution was added to the wells and after approximately 15 minutes, stop solution was added to stop the enzymatic reaction. The plate was then taken for a reading at 450nm on the plate reader Wallac Victor^2 1420 Multilabel counter using the Wallac 1420 Manager software. The trend line of the standard curve was then extracted using Microsoft Excel and the HNE concentrations were calculated using wolframAlpha widget.

Immunohistochemistry

Fluorescence Immunostain was performed over a two-day period. A 24-well plate was used for staining. On **Day 1**, selected sections were removed from antifreeze solution and were grouped according to genotype (TGF or WT) and treatment ($CaCl_2$ or NaCl sham) into the

PBS-filled wells of 24-well plates. The sections are then washed 3 times in PBS (5mins) followed by 4 times in 0.1M PBS-GT (Phosphate buffer saline-gelatine triton, 10 mins). Sections are then placed in diluted Polyclonal Rabbit antibody (GFAP 1:1000, DAKO, Mississauga, ON, Canada; Iba-1 1:300, Wako Pure Chemical Industries, Richmond, VT, USA) in PBS-GT overnight, 4°C. On **Day 2**, the sections are first washed 4 times in PBS-GT (10 mins) and then placed in diluted secondary antibody, Anti-Rabbit Cy2 (1:300 for GFAP and Iba1) for 30 minutes at room temperature to be washed in PBS, mount on slide and examine under the Leitz Aristoplan microscope equipped with epifluorescence (FITC filter). Images were analyzed using ImageJ version d 1.47 (NIH, Bethesda, MD, USA) and 2-way ANOVA was performed using Prism 7 (GraphPad, San Diego, CA, USA).

DAB Immunostain was performed over a two-day period. A 24-well plate was used for staining. On **Day 1**, selected sections were removed from antifreeze solution and were grouped according to genotype (TGF or WT) and treatment ($CaCl_2$ or NaCl sham) into the PBS-filled wells of 24-well plates. The sections are then washed 3 times in PBS (5mins) followed by 4 times in PBS-GT (10 mins). Sections are then placed in diluted Polyclonal Rabbit IgG antibody (GFAP 1:1000, DAKO, Mississauga, ON, Canada; Iba-1 1:300, Wako Pure Chemical Industries, Richmond, VT, USA) in PBS-GT overnight, at room temperature. On **Day 2**, the section are first washed 4 times in PBS-GT (10 minutes) and then placed in diluted Biotynilated IgG Goat Anti-rabbit antibody (1:200 Vector Lab, Burlingame, CA, USA) for 1.5 h at room temperature. The sections are then washed 4 timed with PBS-GT (10 minutes) and placed in AB complex for 1 h at room temperature (ABC kit, Vector Lab). The

sections are washed 1 time in PBS-GT (5 minutes) and then twice in PBS (5 minutes). Sections are submerged in DAB (3, 3'-diaminobenzidine-nickel (DAB-Ni) solution (Vector Lab) kit for approximately 30 seconds before being placed on slides to dry overnight. Sections are then dehydrated in increasing ethanol concentrations and citrus solutions and coverslipped using permount solution (Fisher Scientific, Ottawa, ON, Canada). Images were analyzed using ImageJ version d 1.47 (NIH, Bethesda, MD, USA) and 2-way ANOVA was performed using Prism 7 (GraphPad, San Diego, CA, USA).

Statistical Approach

Data are expressed as means ± SEM. Multiple group comparisons were performed by analysis of variance. Two way ANOVA and Tuckey's test as post-hoc multiple comparison procedures was performed on Prism 7 (GraphPad, San Diego, CA, USA). Three way ANOVA with Mauchly's sphericity test and Greenhouse-Geisser as correction was performed on IBM SPSS statistical software (version 24, IBM, New York, US). Differences will be considered statistically significant when $p<0.05$. The TGFβ-$CaCl_2$ target group was often compared to the WT-NaCl group to infer whether the combined genetic and treatment fators may have a synergistic effect, while showing no significance when apart. In cases where a single factor expressed significance against WT-NaCl but none against TGFβ-NaCl, observing significance of the target group against WT-NaCl allows comparison of the power of significance. When small increases are observed, comparing significance serves as a useful tool.

Results

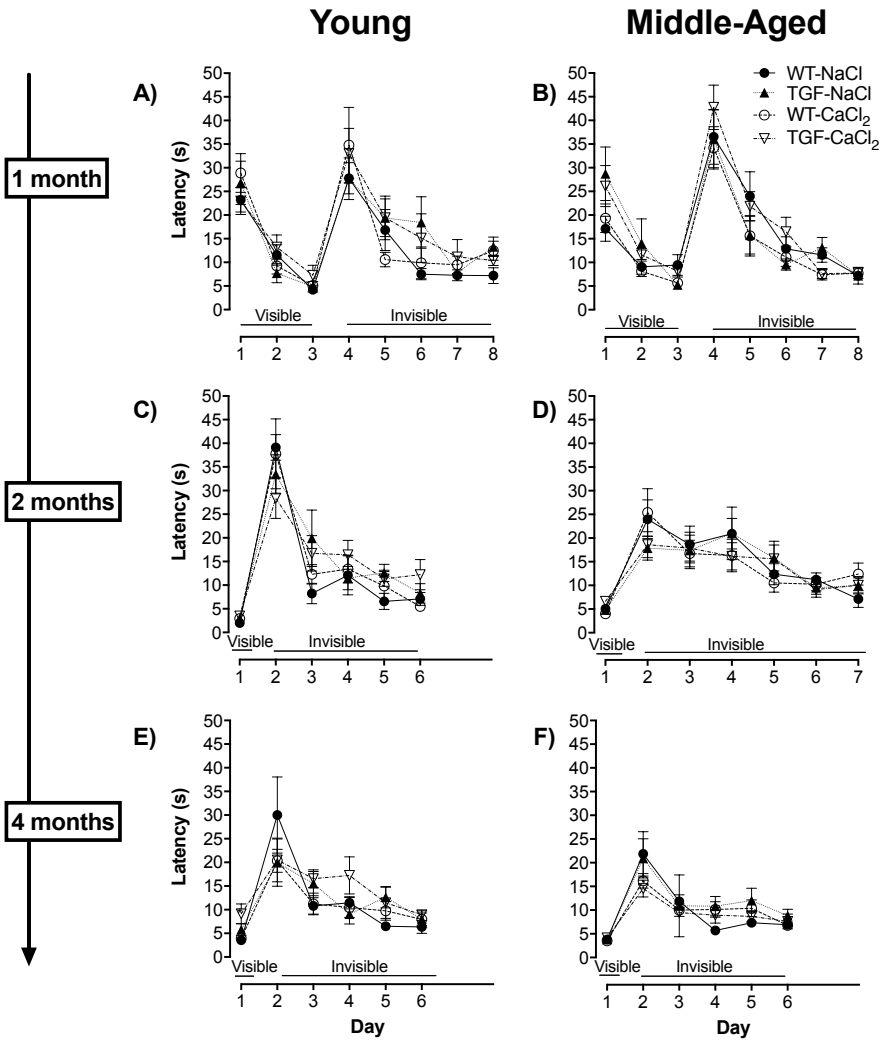

Figure 5 **MWM escape latencies of young and older mice through time.**

Averaged measurements of latency (secs) of the four groups with SEM: WT-NaCl, TGF-NaCl, WT-$CaCl_2$ and TGF-$CaCl_2$. Latencies of young mice from 4 months old (A, C and E) and older mice from 7 months (B, D, and F), taken 1 month, 2 months and four months post-surgery respectively (n=8 to 10 for young mice and n=8 to 13 for older mice). Statistical information was derived using 2-way ANOVA and use of Tuckey's method for multiple comparisons and 3-way ANOVA and use of Mauchly's sphericity test (Greenhouse-Geisser correction).

MWM test shows no effect of the TGF-beta transgene or carotid artery calcification on learning curve, but shows affected performances at the probe test in young and older mice. To assess hippocampal functions of spatial memory and memory consolidation over time in the presence of carotid calcification, mice underwent Morris Water Maze testing 1, 2 and 4 months post-surgery. All learning curves of young and older mice show no significant differences using two-way ANOVA (Fig. 5).

Using three-way ANOVA for factors of genetics, carotid calcification and training days, and mauchly's sphericity test with Greenhouse-Geisser correction, significance was observed for young mice at 5 months (2 months post-surgery) for intra-subject tests of training days and genetics ($F(2.7, 86.7)$ 3.28, $P=0.029$).

However, trends and significances were detected in probe test as described in Fig. 6.

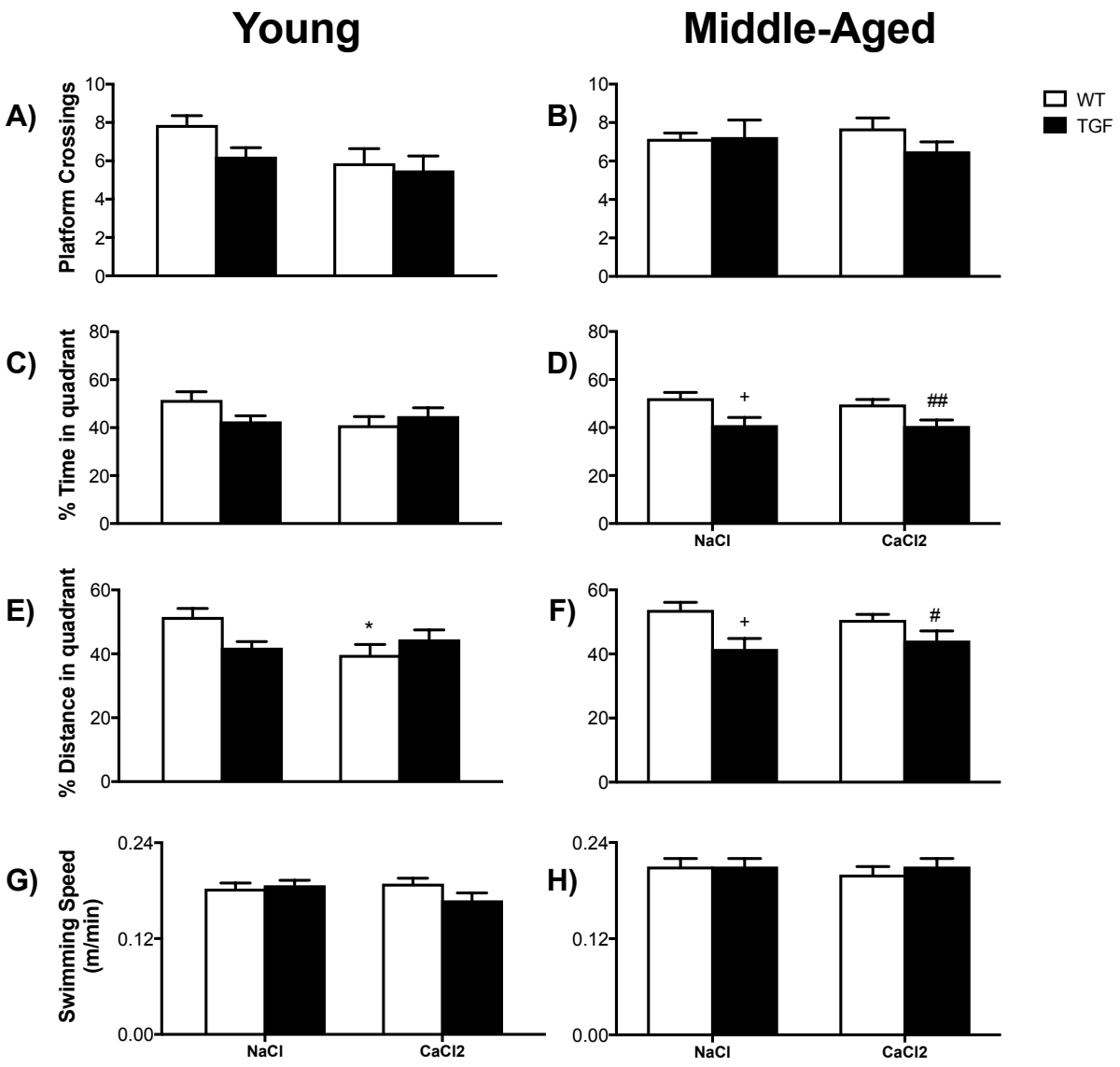

Figure 6 **MWM Probes of young and old mice conducted 1 month post-surgery.**

For young mice aged 4 months (A, C, E, G) and older mice aged 7 months (B, D, F, H) the number of platform crossings, percent of time spent in the target quadrant, percent of distance traveled in the target quadrant, and the swimming speed (meters/minute) were evaluated respectively (n=8 to 10 for young mice and n=8 to 13 for old mice; + $P<0.05$ compared with WT, * $P<0.05$ compared with NaCl, # $P<0.05$, ## $P<0.01$ compared with WT-NaCl). Statistical information was derived using 2-way ANOVA of Tuckey's method for multiple comparison.

Probes of MWM test of TGF mice with calcified carotid arteries show significance at 1 month post-surgery in both young and older mice. At 1 month post-surgery (Fig. 6), platform crossings in young mice (Fig. 6 A) showed a decreasing tendency between WT-NaCl and TGF-$CaCl_2$ (30.1%) with P=0.059. Moreover, calcification as a source of variation showed significance with P=0.0429. However, no significance or tendencies were detected in the number of platform crossings of older mice (Fig. 6 B). Analysis of the percent of overall time spent in the target quadrant by young mice (Fig. 6 C) carried no significance between all groups. In older mice (Fig. 6 D), there was a significance decrease between WT-NaCl and TGF-NaCl (21.6%; P=0.019), as well as WT-NaCl and TGF-$CaCl_2$ (22.2%; P=0.0087). Furthermore, significance in genotype as a source of variation was detected P=0.0002. The next measurement assessed was the percent of distance travelled in the target quadrant. In young mice (Fig. 6 E), significance was detected between WT-NaCl and WT-$CaCl_2$ (23.0%; P=0.0314). In older mice (Fig. 6 F), a significance decrease of percent of distance travelled in target quadrant was revealed between WT-NaCl and TGF-NaCl (22.6%; P=0.0111) as well as between WT-NaCl and TGF- $CaCl_2$ (17.8%; P=0.0415). Again, as seen in percent time spent in the target quadrant by older mice, a high significance for genotype as a source of variation was observed P=0.0007. For the probe trials of middle-age mice, it is possible that no significance was detected in platform crossings due to the limitation that the target is a small area while the pool is large. Furthermore, it is possible that crossover undercounting may have occurred in the software. Comparatively, percent of time and distance spent in target quadrant provide more robust measurements (161). To alleviate the possibility that swimming speeds might have affected the learning curves and probe measurements, a probe assessing speeds was read (Fig. 6 G and H for young and old mice respectively): no trend or significant difference was detected between all groups at 1 month post-surgery.

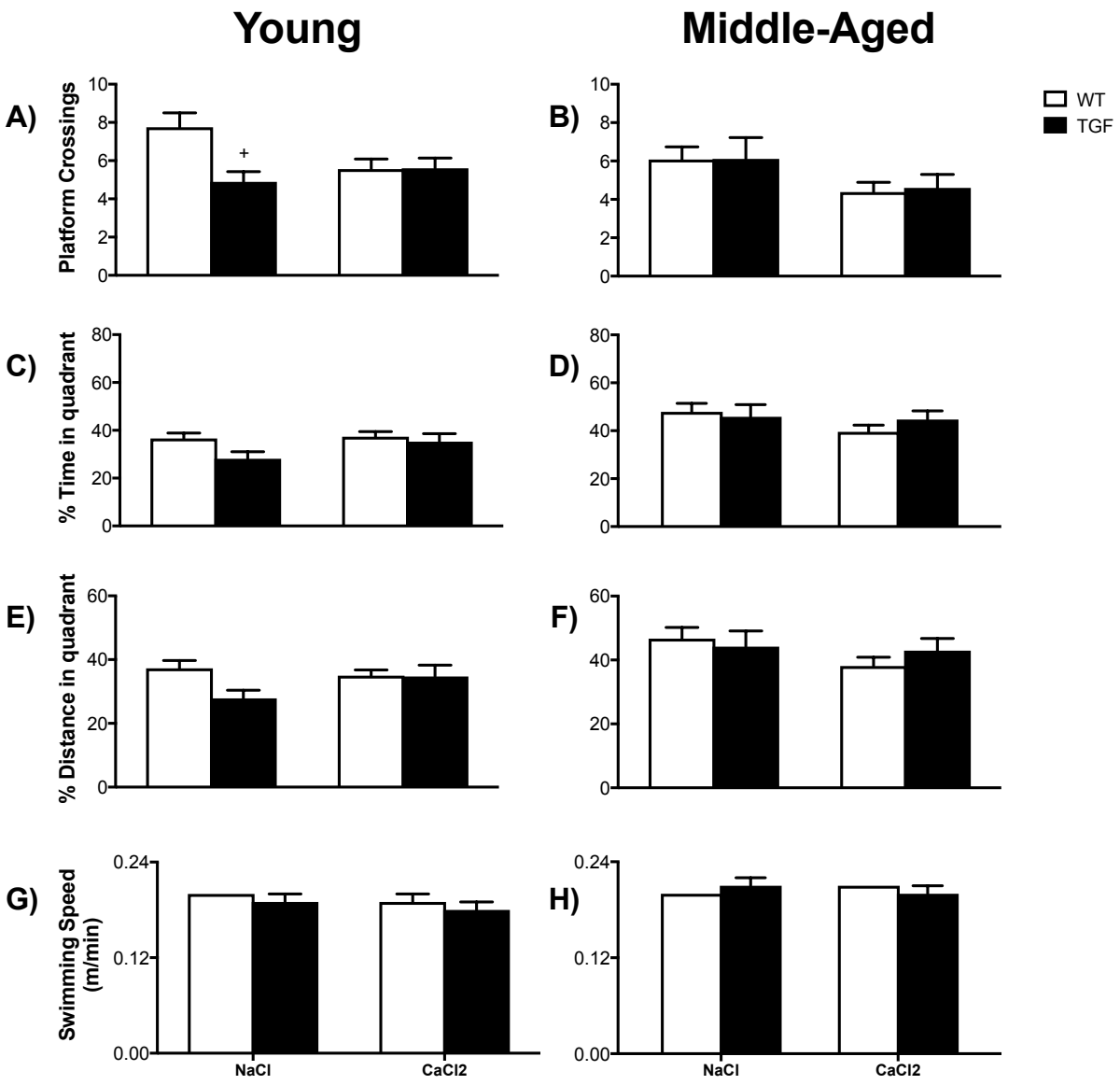

Figure 7 **MWM Probes of young and middle-aged mice conducted 2 months post-surgery.**

Follow-up testing of young mice now aged 5 months (A, C, E, G) and older mice now aged 8 months (B, D, F, H) the number of platform crossings, percent of time spent in the target quadrant, percent of distance traveled in the target quadrant, and the swimming speed (meters/minute) were evaluated respectively (n=8 to 10 for young mice and n=8 to 13 for old mice; + $P<0.05$ compared with WT). Statistical information was derived using 2-way ANOVA and Tuckey's method for multiple comparisons.

Probes of MWM test of TGF mice with calcified carotid arteries show significance at 2 months post-surgery in both young and older mice. At 2 months post-surgery, platform crossings in young mice (Fig. 7A) showed a significant decrease between WT-NaCl and TGF-NaCl (≈37% decrease; P= 0.011). Furthermore, genotype was also detected as a significant source of variation P= 0.023. In older mice (Fig. 7B), no significance was detected between all groups, though calcification of the carotid artery was observed to be a significant source of variation P=0.0343. Analysis of the percent of overall time spent in the target quadrant by young mice (Fig. 7C) carried no significance between all groups. In older mice (Fig. 7D), no significance or trend was detected between all groups or in sources of variation. The percent of distance travelled in the target quadrant by young mice (Fig. 7E) showed a decreasing tendency between WT-NaCl and TGF-NaCl (25.2%; P=0.109). In older mice (Fig. 7F), no significance or tendency was detected between groups or for a source of variation. To alleviate the possibility that swimming speed (Fig. 7G and H) might have affected the learning curves and probe measurements, a probe assessing speeds was read: no trend or significant difference was detected between all groups at 2 months post-surgery.

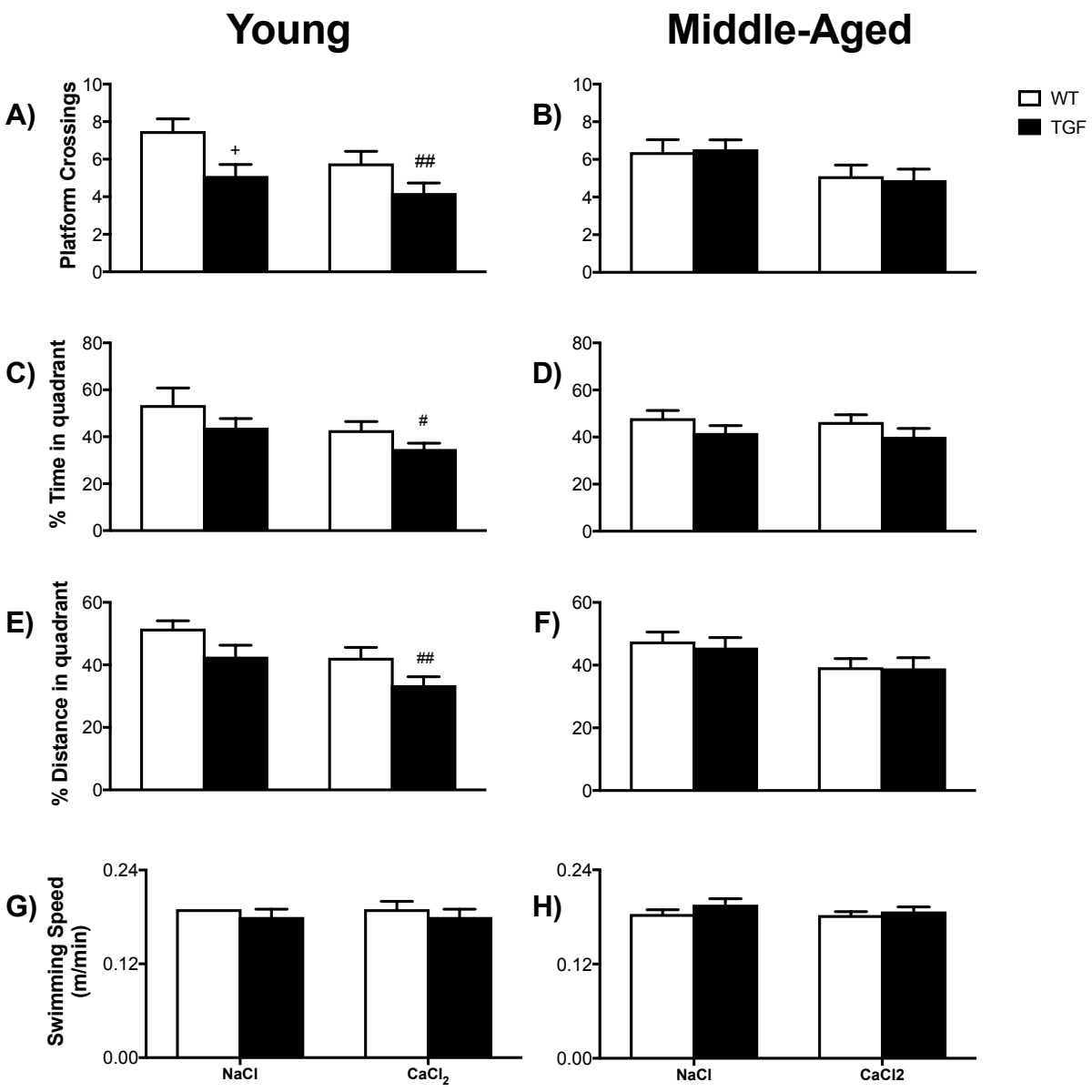

Figure 8 **MWM Probes of young and middle age mice conducted 4 months post-surgery.**

Follow-up testing of young mice now aged 7 months (A, C, E, G) and older mice now aged 10 months (B, D, F, H) the number of platform crossings, percent of time spent in the target quadrant, percent of distance traveled in the target quadrant, and the swimming speed (meters/minute) were evaluated respectively (n=8 to 10 for young mice and n=8 to 13 for middle age mice; + $P<0.05$ compared with WT, # $P<0.05$, ## $P<0.01$ compared with WT-NaCl). Statistical information was derived using 2-way ANOVA and Tuckey's method for multiple comparisons.

Probes of MWM test of TGF mice with calcified carotid arteries show significance at 4 months post-surgery in both young and older mice. At 4 months post-surgery (Fig. 8), the number of platform crossings in young mice (Fig. 8A) showed a significant decrease between WT-NaCl and TGF-NaCl (31.9% decrease; P= 0.0497) as well as between WT-NaCl and TGF- $CaCl_2$ (44% decrease; P=0.003). Furthermore, significance in source of variation was observed for carotid calcification (P=0.038) and genotype (P=0.0026). In older mice (Fig. 8B), no significance was detected in the count of platform crossings between groups; however, calcification displayed significance as a source of variation P=0.021. Analysis of the percent of overall time spent in the target quadrant by young mice (Fig. 8C), shows significant lower time between WT-NaCl and TGF- $CaCl_2$ (34.9%) P=0.0261, as well as carotid calcification as a significant source of variation P=0.0322. In older mice (Fig. 8D), the probe for percent of time spent in the target quadrant demonstrated no significant differences between groups. The percent of distance travelled in the target quadrant by young mice (Fig. 8E) showed a decreasing tendency between WT-NaCl and TGF- $CaCl_2$ (35.0%; P=0.0014). Moreover, both calcification of the carotid artery (P=0.0056) and genotype (P=0.0074) showed significance as sources of variation. In older mice (Fig. 8 F), no significance was detected between all groups, though calcification of the carotid artery showed significance as a source of variation (P=0.0255). To alleviate the possibility that swimming speeds might have affected the learning curves and probe measurements, a probe assessing speeds was read: no trend or significant difference was detected between all groups at 4 months post-surgery.

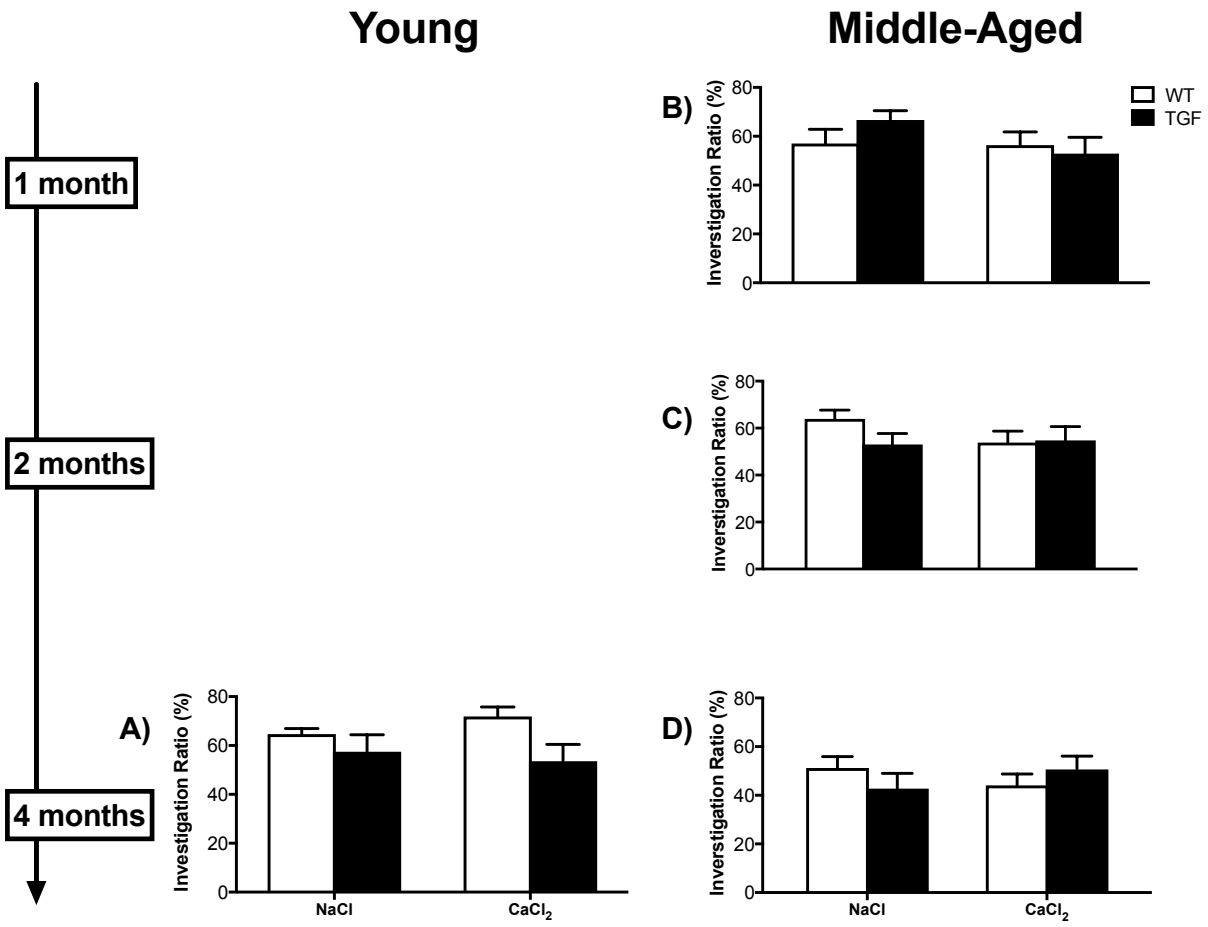

Figure 9 **Novel Object Recognition of young and older mice.**

Averages of percent investigative ratios with SEM of all groups: WT-NaCl, WT-$CaCl_2$, TGF-NaCl and TGF-$CaCl_2$. NOR was conducted on young mice 4 months post-surgery (aged 7 months; n=8 to 10). Older mice underwent NOR 1-, 2- and 4-months post-surgery (aged 7, 8 and 10 months respectively; n=8 to 13). Statistical information was derived using 2-way ANOVA and Tuckey's method for multiple comparisons.

NOR test of young and older TGF mice with calcified carotid arteries shows no significance. To evaluate the effect of calcified carotid arteries on recognition capabilities of TGF mice over time, we performed the Novel Object Recognition test (Fig. 9). For young mice evaluated at 4 months post-surgery (Fig. 9A), no significance was determined between groups (n=8-10). However, there appears to be a trend in the ≈18% decrease between WT-$CaCl_2$ and TGF- $CaCl_2$ P=0.0947. Interestingly, genotype was determined to be a significant source of variation (P=0.0295). Older mice evaluated at 1-month post-surgery (Fig. 9B) did not demonstrate any significant differences between all groups n=8-13). Similarly, no significance was determined between all groups or as sources of variation for older mice at 2-months post-surgery (Fig. 9C: n=8-13) and 4-months post-surgery (Fig. 9D: n=8-13).

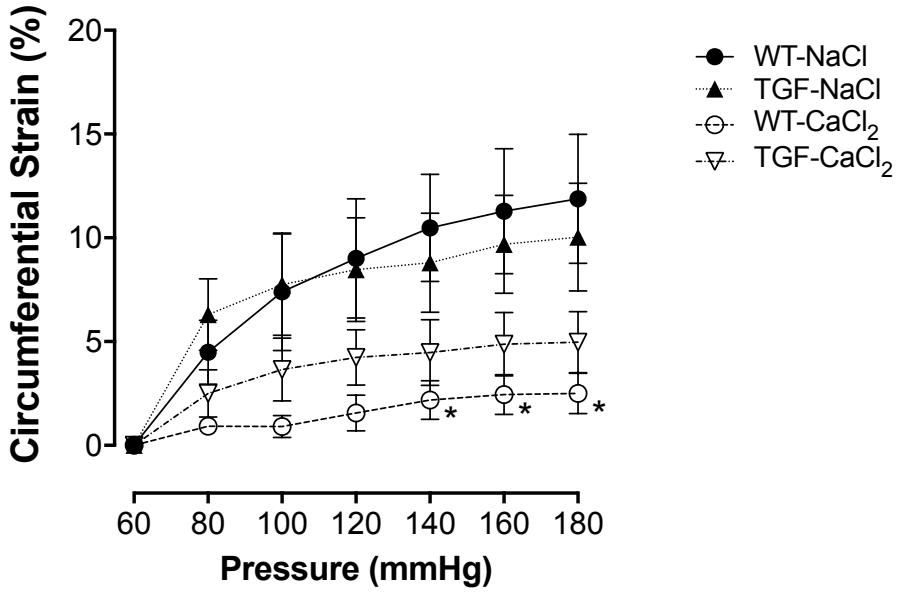

Figure 10 **Circumferential strain detected in older mice**.

Mean percent increase of circumferential strain as a function of pressure (mmHg) between groups WT-NaCl, WT-$CaCl_2$, TGF-NaCl and TGF-$CaCl_2$ (n=5 for all groups, * $P<0.05$ WT-NaCl compared with WT-$CaCl_2$). Statistical information was derived using 2-way ANOVA and Tuckey's method for multiple comparisons.

Carotid Calcification induced a change in circumferential strain. (Fig. 10) To verify the lasting effects of carotid calcification, extracted carotid arteries from all groups were tested for differences in circumferential strain at pressures between 60mmHg and 180mmHg, with 60mmHg acting as the baseline strain. Significance was observed between WT-NaCl and WT- $CaCl_2$ at 140 (P=0.042), 160 (P=0.042) and 180 mm Hg (P=0.038). At all pressure measurements, carotid calcification was determined as a significant source of variation (at 80mmHg P=0.0123, at 100mmHg P=0.0195, at 120mmHg P=0.0122, at 140mmHg P=0.0058, at 160mmHg P=0.0053, and at 180mmHg P=0.0048), indicating that the modifications to the structure of the arterial wall induced by carotid calcification lasts at least 6 months.

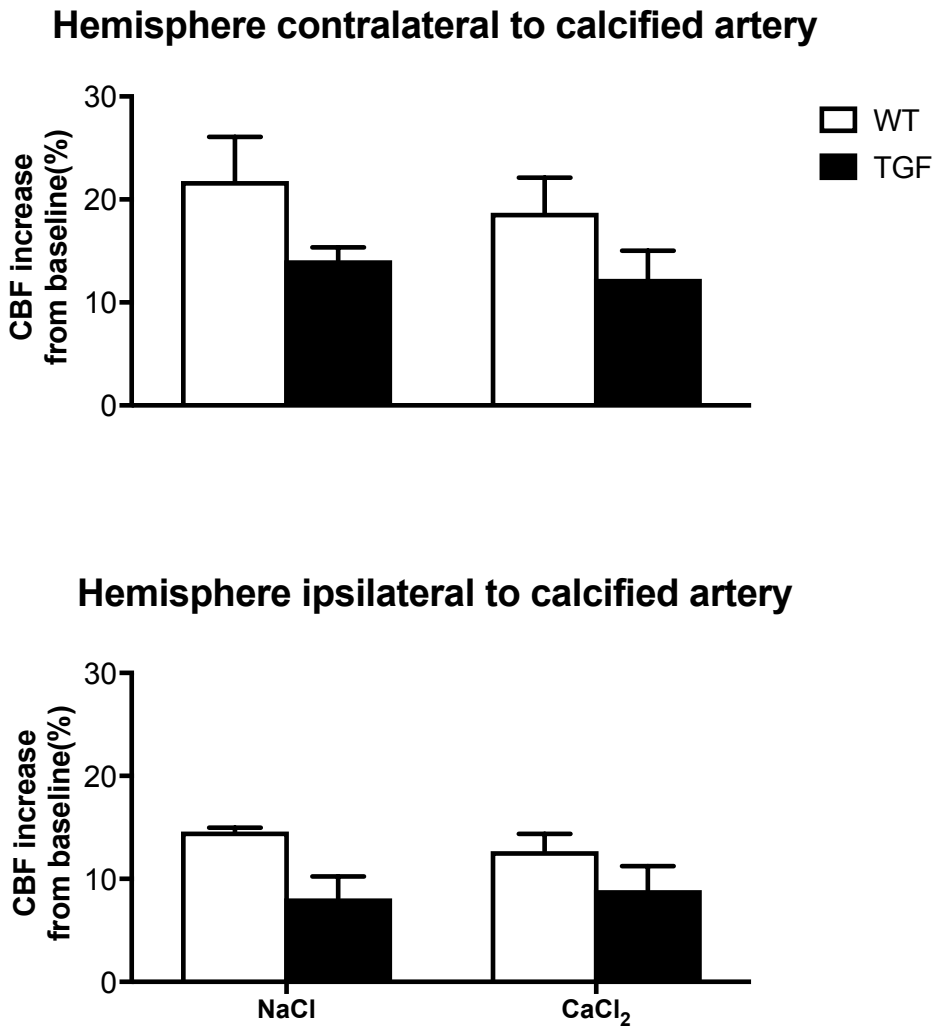

Figure 11 **Cerebral Blood Flow of older mice 5 months post-surgery.**

Averages of percent cerebral blood flow (CBF) increases (%) from baseline with SEM for all groups: WT-NaCl, WT- $CaCl_2$, TGF-NaCl and TGF- $CaCl_2$. Both brain hemispheres were investigated. (n=4 for all groups). Statistical information was derived using 2-way ANOVA and Tuckey's method for multiple comparison.

Calcification did not induce a significant change in cerebral blood flow in older mice. (Fig. 11) At 5 months post-surgery, no significant change in blood flow was observed due to calcification within the ipsilateral hemisphere (n=4). The hemisphere contralateral to the calcified artery did not display a change in CBF percent increase due to calcification (n=4) and no significance was detected between all groups. However, both the ipsilateral and contralateral side showed genotype as a significant source of variation (P=0.0144 and P=0.0432 respectively).

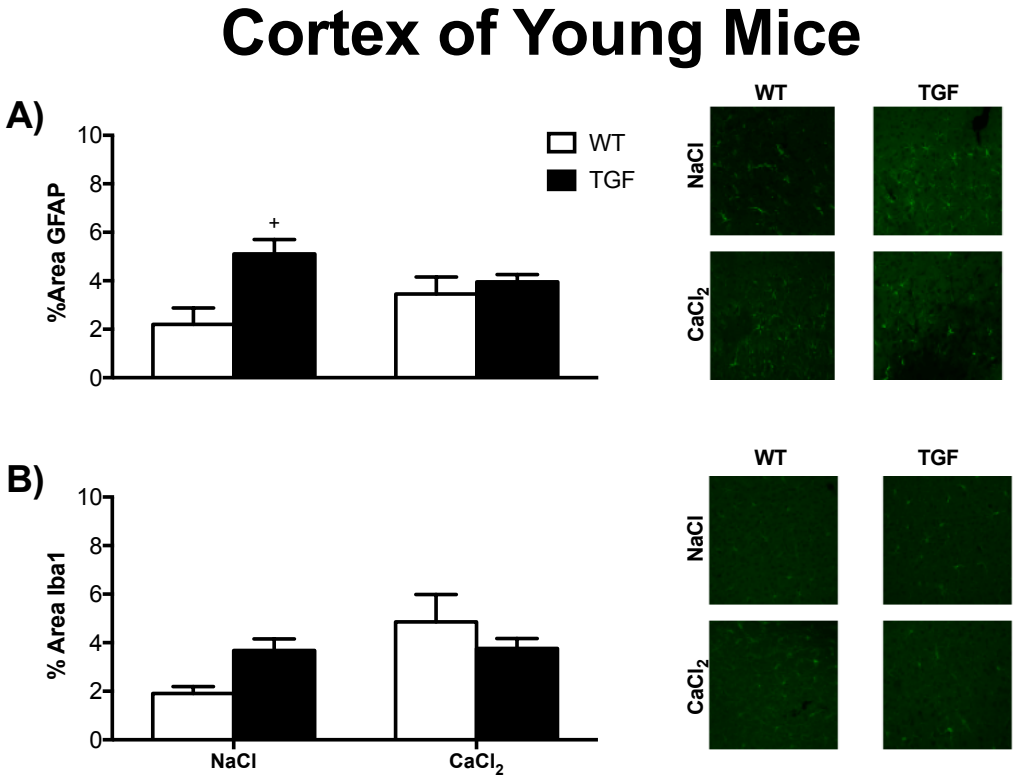

Figure 12 **Percentage of area stained for GFAP or Iba1 in the cortex of young mice.**

For young mice (n=3 to 4), the mean percent (±SEM) of fluorescent area covered due to A) GFAP and B) Iba1 immunoreactivity was evaluated for all groups: WT-NaCl, TGF-NaCl, WT- $CaCl_2$ and TGF- $CaCl_2$ (+ $P<0.05$ compared with WT). Statistical information was derived using 2-way ANOVA and Tuckey's method for multiple comparisons.

No significant increase in GFAP or Iba1 was detected in the cortex of young TGF mice as a result of carotid artery calcification. (Fig. 12) To determine whether the addition of carotid calcification to TGF mice caused an increase in astrogliosis or microglial activation, 25μm sections were stained with fluorescence indicating GFAP and Iba1. In the case of astrogliosis, percent area of fluorescent GFAP showed a significant increase from WT-NaCl to TGF-NaCl (55.9% increase, n=3-4, P=0.0272). Furthermore, the TGF genotype was detected as a source of variation for astrogliosis in the cortex (P=0.0142). However, calcification of the carotid artery did not reveal any significance or trend between all groups, nor as a source or variation for astrogliosis. Microglial activation, indicated by Iba1, did not reveal any significance between all groups; however, there appears to be a tendency between WT-NaCl (1.91%±0.28%, n=3) and WT-$CaCl_2$ (4,86%±1.12%, n=4, P=0.067). Furthermore, calcification of the carotid artery appears to contribute as a source of variation for microglial activation in the cortex (P=0.0563).

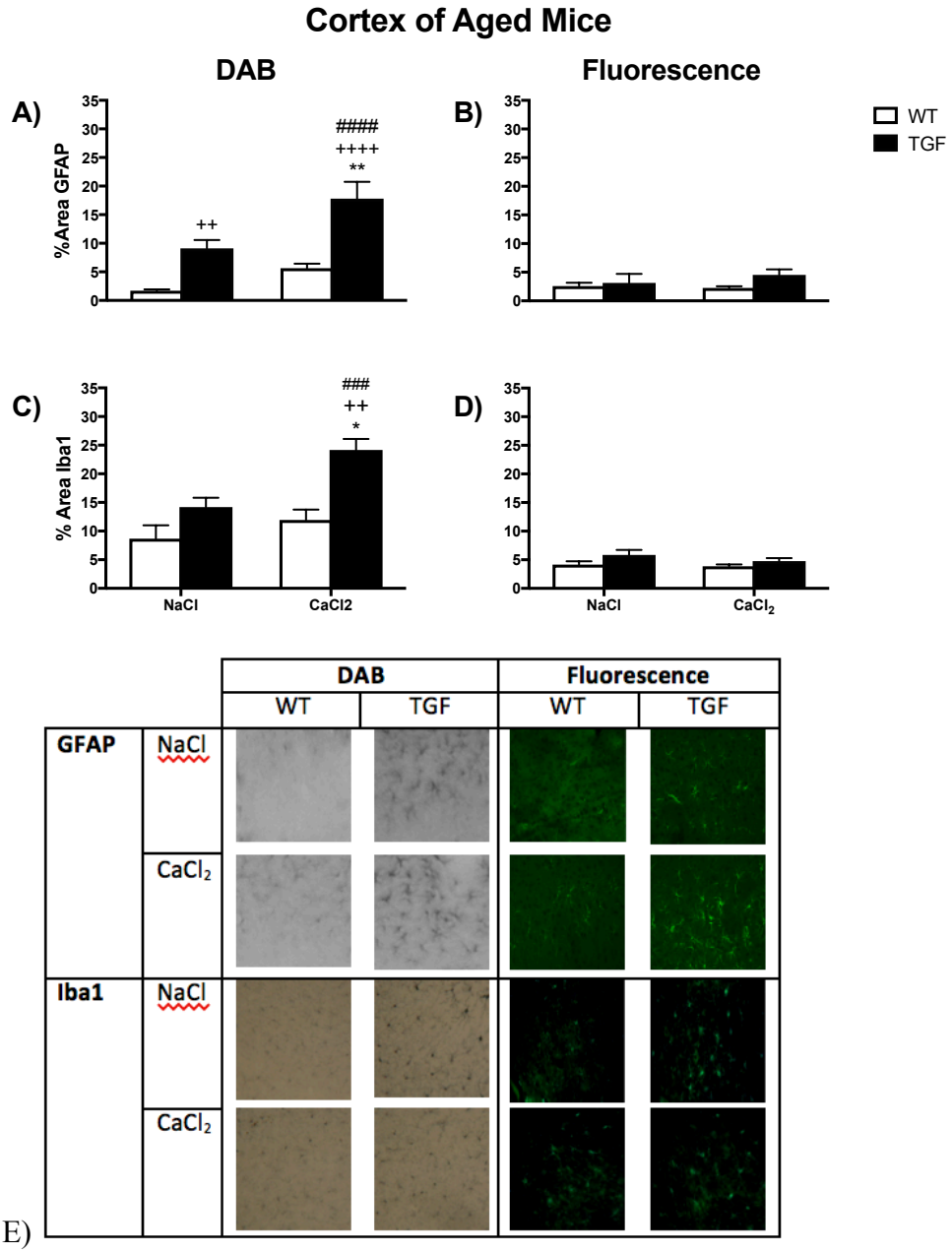

Figure 13 **Cortex of middle age mice, comparing DAB and fluorescent staining.**

Average percent area (±SEM) of DAB (A, C) and fluorescent (B, D) staining for GFAP and Iba1 (n=3 to 7 for DAB staining and n=4 to 7 for fluorescent staining; ++ $P<0.01$, ++++ $P<0.0001$ compared with WT, ### $P<0.001$, #### $P<0.0001$ compared with WT-NaCl, * $P<0.05$, ** $P<0.01$ compared with NaCl). Statistical information was derived using 2-way ANOVA and Tuckey's method for multiple comparisons. Representative images are shown (E).

DAB staining revealed increased astrogliosis and microglial activation in cortex of aged mice. To evaluate changes in astrogliosis and microglial activation in the cortex of aged TGF mice with calcified carotid arteries, percent area of GFAP and Iba1 were studied respectively using DAB and fluorescence. For GFAP viewed by DAB staining techniques (Fig. 13 A), a significant increase was observed from WT-NaCl to TGF-NaCl (81.3%, n=4-5) P=0.0041 as well as TGF-$CaCl_2$ (90.5%, n=3) P<0.0001. Furthermore, a significant increase was observed from TGF-NaCl to TGF-$CaCl_2$ (P=0.003) and WT-$CaCl_2$ to TGF-$CaCl_2$ (68.4%, n=3-7; P<0.0001). Moreover, surgical calcification of the carotid artery as well as the TGF genotype were determined to be significant sources of variation, P=0.0063 and P=0.0006 respectively. However, fluorescent staining of GFAP in the cortex of aged mice (Fig. 13B) failed to reproduce the significance seen in DAB. Indeed, DAB staining of Iba1 in the cortex of aged mice (Fig. 13C) revealed a significant increase from WT-NaCl to TGF- $CaCl_2$ (64.1%, n=4; P=0.0005), as well as from TGF-NaCl and WT- $CaCl_2$ to TGF- $CaCl_2$, (41.3%, n=4; P=0.0036 and 50.6%, n=4-7; P=0.038 respectively). Furthermore, calcification of the carotid artery and the TGF genotype constitutes significant sources of variation causing increases in Iba1 immunoreactivity, P=0.0063 and P=0.0006 respectively. Again, fluorescent staining of Iba1 in the cortex of aged mice (Fig 13D) showed no significant changes between all groups (n=6-7). For fluorescent staining of Iba1, TGF genotype was seen as a significant source of variation causing an increase in microglial activation P=0.030, though calcification of the carotid artery was not (P=0.232).

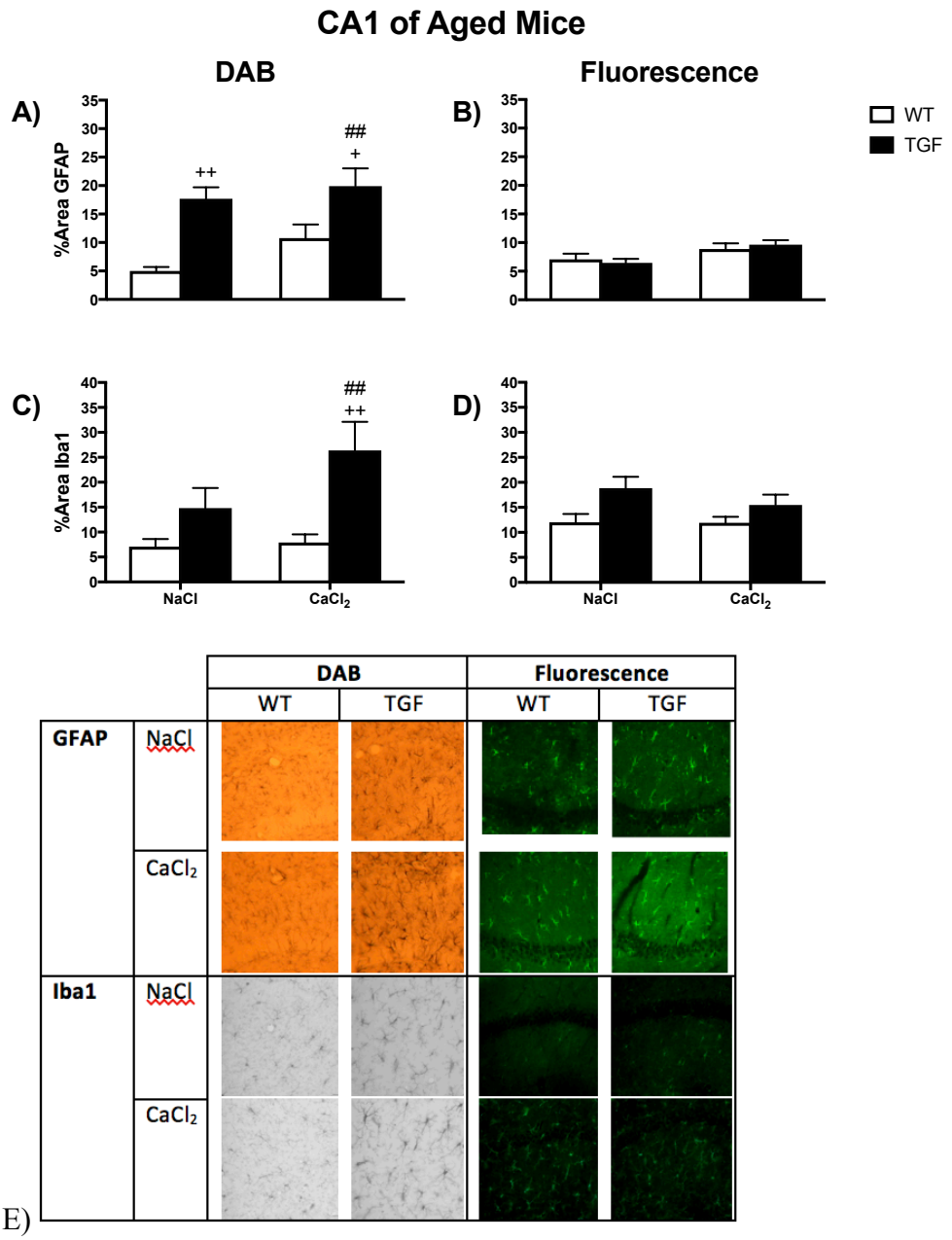

Figure 14 **Hippocampal CA1 region of aged mice, comparing DAB and fluorescent staining.**

Average percent area and SEM of DAB (A, C) and fluorescent (B, D) staining for GFAP and Iba1 respectively (n=4 to 7 for DAB staining and fluorescent staining; + P< 0.05, ++ P<0.01 compared with WT, ## P<0.01 compared with WT-NaCl). Statistical information was derived using 2-way ANOVA and Tuckey's method for multiple comparisons. Representative images are shown (E).

DAB staining revealed increased astrogliosis and microglial activation in hippocampal CA1 region of aged mice. To evaluate changes in astrogliosis and microglial activation in the CA1 of aged TGF mice with calcified carotid arteries, percent area of GFAP and Iba1 were studied respectively using DAB and fluorescence. For GFAP viewed by DAB staining techniques (Fig. 14A), a significant increase was observed from WT-NaCl to TGF-NaCl (71.8%, n=4-6) P=0.0051 as well as TGF- $CaCl_2$ (74.9%, n=4) P=0.0012. Furthermore, a significant increase was observed from WT- $CaCl_2$ to TGF- $CaCl_2$ (27.6%, n=4-7) P=0.0421. The TGF genotype was identified as source of variation causing an increase in astrogliosis in the CA1 by DAB staining, P=0.0001. However, significance between groups failed to manifest in the fluorescent GFAP stain of the CA1 region of aged mice (Fig. 14B): WT-NaCl (7.08%±1.00%, n=6), TGF-NaCl (6.46%±0.71%, n=4), WT-$CaCl_2$ (8.89%±0.97%, n=7) and TGF-$CaCl_2$ (9.64%±0.71%, n=5); with insignificant increases from WT-NaCl to TGF-$CaCl_2$ (P=0.258) and TGF-NaCl to TGF-$CaCl_2$ (P=0.178). Interestingly, although calcification of the carotid artery was seen as a significant source of variation by fluorescence causing an increase in astrogliosis in the CA1 (P=0.0184), the TGF mutation was not a significant one (P=0.9491). In the case of DAB Iba1 staining of the CA1 in aged mice (Fig 14C), a significant increase was observed from WT-NaCl and WT- $CaCl_2$ to TGF- $CaCl_2$ (73.2%, n=4-6; P=0.0019 and 70.0%, n=4-7; P=0.0022 respectively). No significant increase from WT-NaCl to TGF-NaCl and TGF-NaCl to TGF-$CaCl_2$ was observed. The TGF genotype was a significant source of variation causing increase in microglial activation (P=0.0005), though calcification of the carotid artery showed a tendency as a source of variation (P=0.0575). Again, Iba1 fluorescent staining of the CA1 in aged mice (Fig 12 D) showed no significant changes between all groups. As seen in Fig. 8 C, in immunofluorescence, TGF mutation was maintained as a significant source of variation (P=0.0081), though calcification of the carotid artery was not (P=0.332).

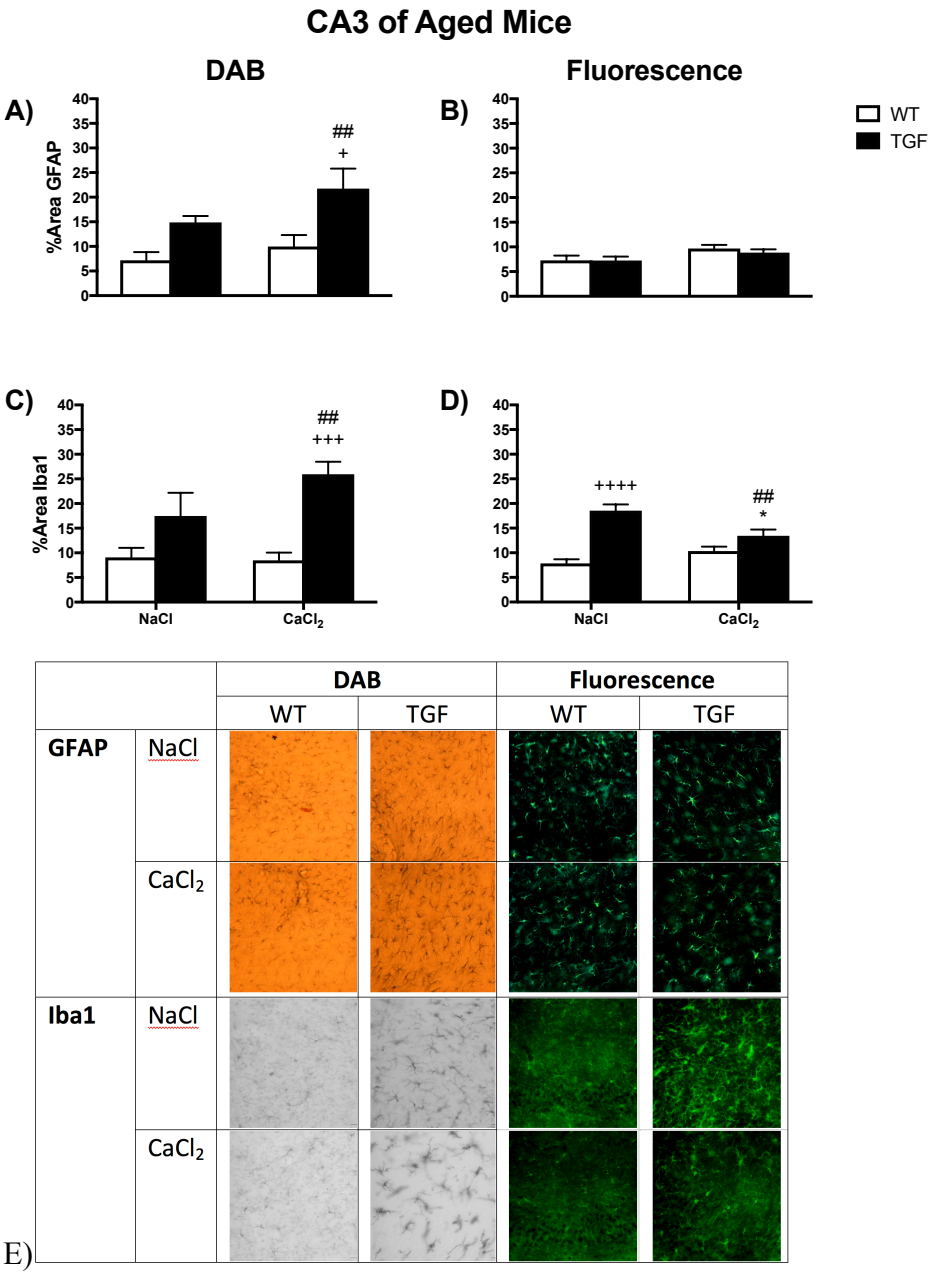

Figure 15 **Hippocampal CA3 region of aged mice, comparing DAB and fluorescent staining.**

Average percent area and SEM of DAB (A, C) and fluorescent (B, D) staining for GFAP and Iba1 respectively (n=4 to 7 for DAB staining and fluorescent staining; + $P<0.05$ WT, +++ $P<0.001$, ++++ $P<0.0001$ compared with WT, ## $P<0.01$ compared with WT-NaCl and * $P<0.05$ compared with NaCl). Statistical information was derived using 2-way ANOVA and Tuckey's method for multiple comparisons. Representative images are shown (E).

DAB staining revealed increased astrogliosis and microglial activation in hippocampal CA3 region of aged mice. To evaluate changes in astrogliosis and microglial activation in the CA3 of aged TGF mice with calcified carotid arteries, percent area of GFAP and Iba1 were studied respectively using DAB and fluorescence. For GFAP viewed by DAB staining techniques (Fig. 15A), a significant increase was detected from WT-NaCl as well as WT-$CaCl_2$ to TGF-$CaCl_2$ (66.9%, n=4-6; P=0.0042 and 54.0%, n=4-7; P=0.0176 respectively). The TGF genotype was a significant source of variation causing increase in astrogliosis in the CA3 of aged mice (P=0.0012). On the other hand, fluorescent GFAP staining of the CA3 region in aged mice (Fig. 15B) showed no significance between all groups (n=4-7). Calcification of the carotid was observed as a significant source of variation causing an increase in the CA3 of aged mice (P=0.0298), though the TGF genotype lost significance as a source of variation when evaluated through fluorescent staining (P=0.631). For DAB Iba1 staining of the CA3 in aged mice (Fig 15C), a significant increase was observed from WT-NaCl and WT-$CaCl_2$ to TGF-$CaCl_2$ (65.0%, n=4-6; P=0.0014 and 67.3%, n=4-7; 0.0007, respectively). Though calcification was not considered as a significant source of variation (P=0.140), TGF genotype was highly significant (P=0.0001) causing an increase in microglial activation in the CA3. For GFAP fluorescent staining within the CA3 region of aged mice (Fig 13 D), significance was revealed for the increase from WT-NaCl to TGF-NaCl (57.7%, n=4-6; P<0.0001) and TGF-$CaCl_2$ (41.6%, n=5; P=0.0067 respectively) and significant decreases were revealed from TGF-NaCl to WT-$CaCl_2$ (44.2%, n=4-7; P=0.0002) and TGF-$CaCl_2$, (27.6%; n=4; P=0.0267). Calcification of the carotid artery was determined as a non-significant source of variation (P=0.234), while the TGF mutation was significant (P<0.0001).

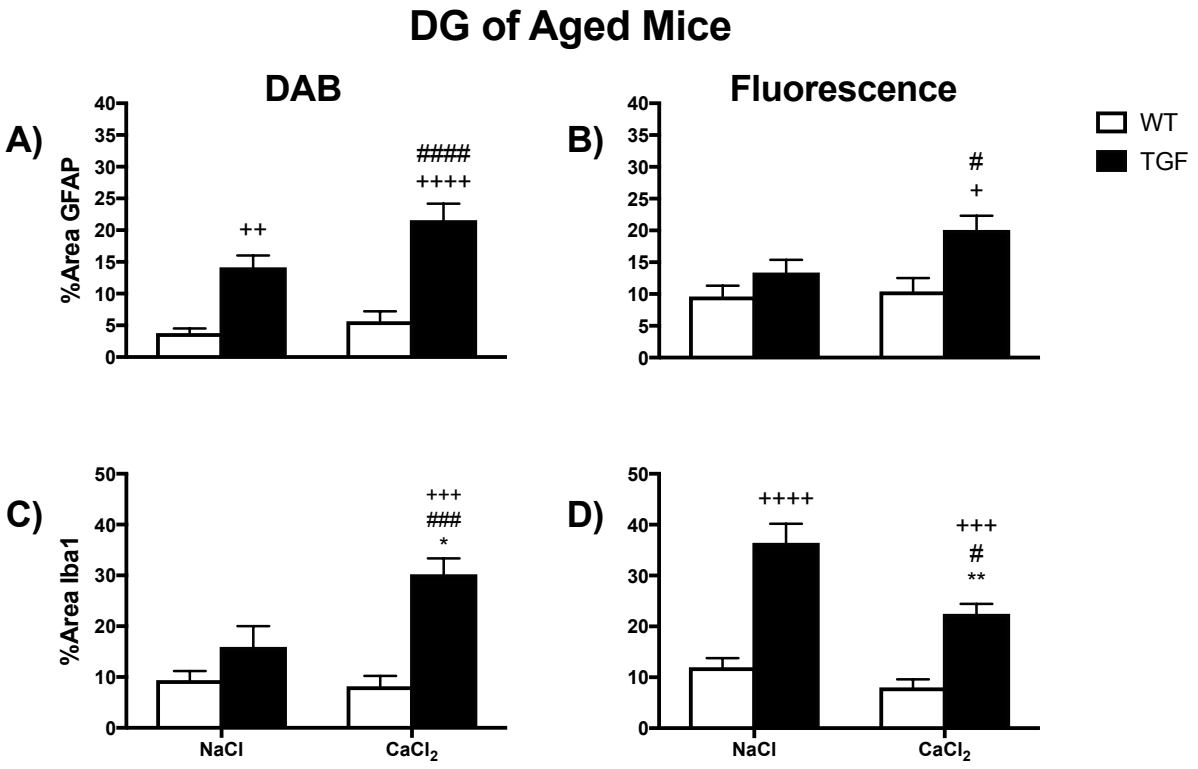

Figure 16 **Hippocampal DG region of aged mice, comparing DAB and fluorescent staining.**

Average percent area and SEM of DAB (A, C) and fluorescent (B, D) staining for GFAP and Iba1 respectively (n=4 to 7 for DAB staining and fluorescent staining; + P<0.05, ++ P<0.01, +++ P<0.001, ++++ P<0.0001 compared with WT, # P<0.05, ### p<0.001 #### P<0.0001 compared with WT-NaCl, * P<0.05, ** P<0.01 compared with NaCl). Statistical information was derived using 2-way ANOVA and use of Tuckey's method for multiple comparisons.

DAB and fluorescent staining revealed increased astrogliosis and microglial activation in hippocampal DG region of aged mice. To evaluate changes in astrogliosis and microglial activation in the DG of aged TGF mice with calcified carotid arteries, percent area of GFAP and Iba1 were studied respectively using DAB and fluorescence. For GFAP viewed by DAB staining techniques (Fig. 16A), a significant increase was detected from WT-NaCl and WT-$CaCl_2$ to TGF-NaCl (73.2%, n=4-6; P=0.0027 and 60.0%; n=4-7; P=0.0107 respectively), as well as TGF-$CaCl_2$ (82.4%, n=4-6 and 73.8%, n=4-7 respectively) with P<0.0001 in both cases. However, no significant increase was determined from WT-NaCl to WT-$CaCl_2$ (P=0.8090), though the ≈34.5% increase from TGF-NaCl to TGF-$CaCl_2$ shows a tendency (P=0.0541). Both calcification of the carotid artery and the TGF genotype were analyzed as significant sources of variation, P=0.0135 and P<0.0001 respectively. Fluorescent GFAP staining in the DG of aged mice (Fig. 16B) revealed similar tendencies. Though the ≈4% increase from WT-NaCl to TGF-NaCl (P=0.6343) and the 28.0% increase from TGF-NaCl to TGF-$CaCl_2$ (P=0.2000) lacked significance, the increases from WT-NaCl and WT-$CaCl_2$ to TGF-$CaCl_2$ were significant (52.1%, n=4-6; P=0.0106 and 48.2%; n=4-7; P=0.0147, respectively). Furthermore, the TGF mutation was a significant source of variation causing an increase in astrogliosis P=0.0051, while calcification of the carotid artery did not show a significant effect. For Iba1 DAB staining in the DG of aged mice (Fig. 16C), significance was determined for the increase from WT-NaCl, TGF-NaCl and WT-$CaCl_2$ (68.9%, n=4-6; P=0.0001, 47.3%, n=4; P=0.0001 and 72.9%, n=4-7; P=0.0143 respectively). However, there was no significant difference from WT-NaCl to TGF-NaCl (P=0.3113). Both calcification of the carotid artery and the TGF mutation were significant sources of variation causing an increase in microglial activation, P=0.0233 and P<0.0001 respectively. For fluorescent Iba-1 staining of the DG in aged mice (Fig. 16D), significant increases were detected from WT-NaCl, WT-$CaCl_2$ and TGF-$CaCl_2$ to TGF-NaCl (67.1%, n=4-6; P<0.0001, 78.0%, n=4-7; P<0.0001 and 38.3%, n=4-5; P=0.0027 respectively). Significant increases were also observed from WT-NaCl and WT-$CaCl_2$ to TGF-$CaCl_2$ (46.7%, n=5-6; P=0.0124 and 64.3%, n=5-7; P=0.0005 respectively). Again, both the TGF genotype (P<0.0001, causing an increase) and the calcification of the carotid artery (P=0.0006, causing a decrease) were observed to be significant sources of variation.

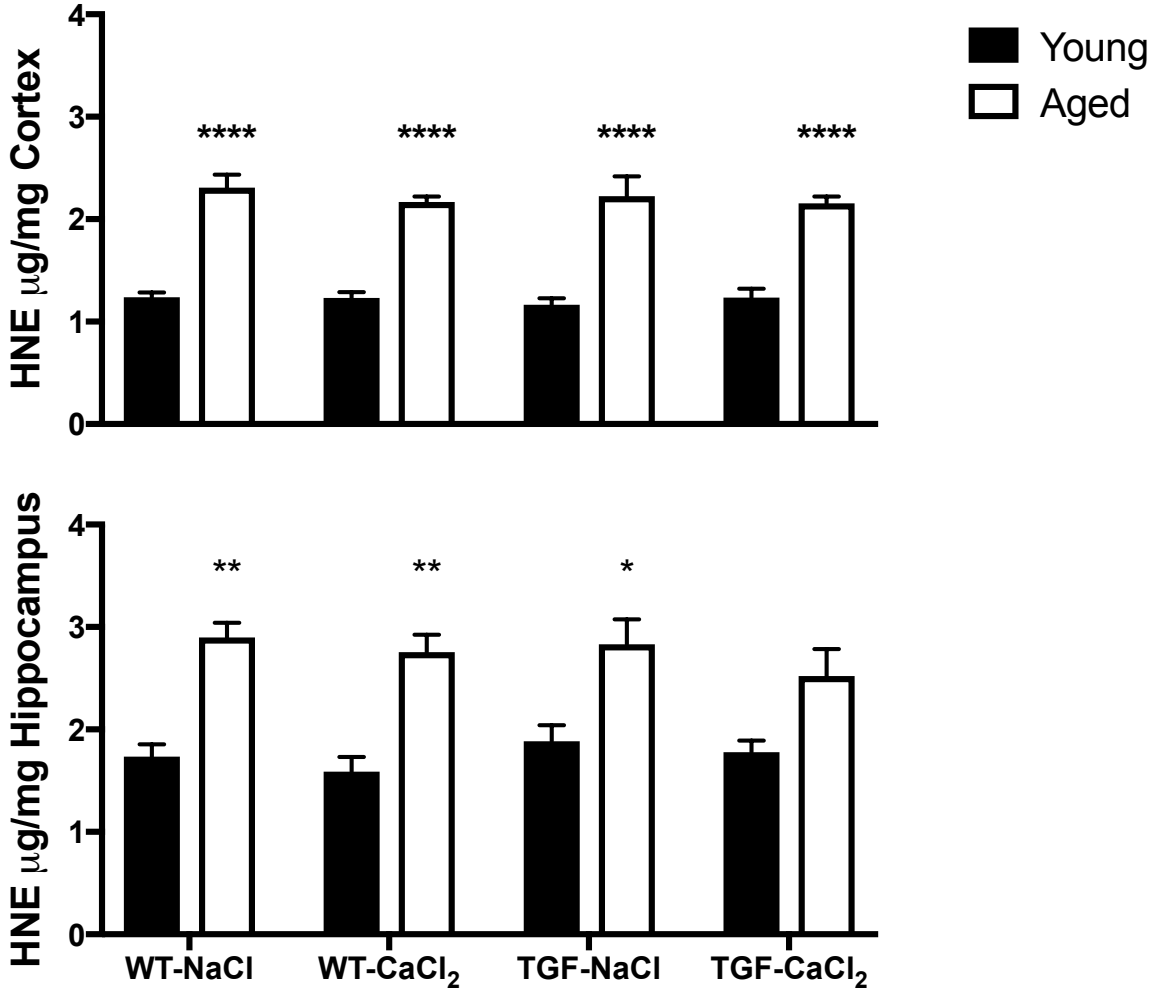

Figure 17 **4-Hydroxynonenal (HNE) ELISA assessing oxidative stress in the cortex and hippocampus of young and aged mice**.

For young and aged mice, HNE concentrations (μg/mg) were evaluated in the cortex and hippocampus (n=4 to 5 for young mice and n=5 for aged mice; *P<0.05, **P<0.01, ****P<0.0001 compared with young mice). Statistical information was derived using 2-way ANOVA and Tuckey's method for multiple comparisons.

Significant increases of 4-Hydroxynonenal (HNE) detected between young and aged mice. (Fig. 17) To evaluate oxidative stress levels in TGF mice with calcified carotid arteries, concentrations of HNE (μg/mg) were detected in the cortex and hippocampus of young and aged mice. For cortex and hippocampus, no significant changes were observed between all groups: WT-NaCl, TGF-NaCl, WT-$CaCl_2$ and TGF-$CaCl_2$. However, significance was observed between young and aged mice of respective groups. In the cortex, HNE levels of aged mice were approximately double for all respective groups ($P<0.0001$ for all groups). For the hippocampus, significant increases in the levels of HNE from young to old were detected for WT-NaCl (1.74±0.121, n=5 for young; 2.90±0.143, n=5 for aged, P=0.0012), WT-$CaCl_2$ (1.59±0.144, n=5 for young; 2.76±0.168, n=5 for aged, P=0.0011) and TGF-NaCl (1.89±0.154, n=5 for young; 2.83±0.244, n=5 for aged, P=0.0127). For TGF-$CaCl_2$ in the hippocampus, there was a 30% increase from young to old mice (1.78±0.144, n=5 for young; 2.52±0.261, n=5 for aged, P=0.0884).

Discussion

The AD pathology is known to be a multifactorial disease with multiple causes for the resulting dementia. Much research has been conducted on the APP mouse which generates the Aβ pathology; however, drugs successfully abolishing the cognitive deficits in APP mice fail to do so in humans. Due to this, other pathologies seen in AD patients began to be researched, one of the possible culprits being the increased production of TGFβ1 cytokine. TGF mice overexpressing the TGFβ1 cytokine demonstrated an increase in profibrotic proteins causing stiffening and damage to the cerebrovasculature. This modification to the vessel wall in brain gives rise to an increased vulnerability to the development of vascular pathologies such as chronic hypoperfusion, cerebral microhemorrages, vascular fibrosis and SVD, most of which were also exhibited in the brains of AD patients. Although TGF mice display multiple vascular pathologies attributed to VaD, cognitive deficits appear much later than in other murine models of AD (8).

The pattern of the TGFβ pathology seen in AD patients and the lack of cognitive deficits exhibited by TGF mice raises the question: could the vascular pathologies of TGFβ work in unison with other pathologies to cause dementia? To this end, we combined the TGFβ vascular pathologies of AD with another pathological pattern demonstrated by aged patients: arterial rigidity. Stiffening of the arterial wall has been identified as an independent risk factor of dementia in aging patients. To better understand the underlying mechanisms, Sadekova *et al*. of the Girouard laboratory (2014) developed a murine model of arterial rigidity by surgically isolating and calcifying the right carotid artery. The changes to the carotid vessel

wall, which is responsible for 40% of vascular resistance to the brain, resulted in an increase in blood pulsatility in smaller cerebral vessels. Examination of the acute effects at 2 weeks post-surgery revealed increased astrogliosis and microglial activation (s100β and Iba1 respectively) as well as increased ROS and neuronal cell death (124). Interestingly, it has since been revealed by Dr. Thorin's laboratory that pulse pressure is affiliated with the mechanical response of EC to shear stress, resulting in the production of NO by eNOS under physiological conditions, and ROS under uncoupled conditions (68). Therefore, here we propose that the increased pulsatility resulting from the calcification of a single carotid artery on the TGF mouse model exhibiting an array of vascular pathologies would result in the demonstration of cognitive deficits as well as increased ROS and gliosis in alternatively young and aged brain.

Discussion

Part I – Bahavioral Testing

To evaluate the cognitive deficiencies activated by coupling TGFβ overexpression and arterial stiffness, responses to two behavioral tests were investigated: the Morris Water Maze (MWM) and Novel Object Recogition (NOR).

Morris Water Maze

The MWM is widely used to validate murine neurocognitive disorders (165). In the observation of AD and VaD, MWM is often used to observe the progression of the disease (165). In order to observe disease progression, MWM has often been performed on the same group of mice with adequate time in between experimentations (172). Conceptually, place cells located in the hippocampus are responsible for quick escape from the MWM (163).

For both young and aged mice, we performed MWM three times (at 1-, 2-, and 4-months post-surgery) to determine whether calcification of the carotid artery might cause delays and cognitive deficiencies over time. In our studies, an effect was seen in the learning curve through 3-way ANOVA for young mice at 5 months of age (2 months post-surgery) for factors of Genetics (TGF or WT) and training days of invisible platform (days 2-6); however,

throughout the experiments, this was an isolated case. For wild type sham groups (WT-NaCl), TGF sham (TGF-NaCl) and wild type mice with calcified ateries (WT-$CaCl_2$), these results correspond with published data. Experiments conducted by Hamel *et al*. have shown no significant differences in the learning curves between WT and TGF mice less than 12 months of age (8, 116). For mice with calcified arteries, MWM learning curve data from a previous study in the Girouard lab (173) showed a significant increase in escape latency on the second day of learning compared to control, indicating a delay in learning. However, WT-$CaCl_2$ latencies coincided with WT in the following days (173). These results were not demonstrated in our mice due to a difference in protocols. While our protocol called for a training period with a visible platform of one to three days, this training period was absent for the mice recorded in past data. Our target group of TGF mice with calcified carotid arteries (WT-$CaCl_2$) did not display any significance on any day. It is possible that with the altered protocol a difference in learning curves may have been detected and so it may be a good idea to repeat the experiments without a training period.

For MWM test probes, our target group showed significance for aged mice at 7 months/ 1 month post-surgery (Fig. 4D, 4F) and young mice at 7 months/ 4 months post-surgery (Fig. 6A, 6C and 6E), thus demonstrating a deficiency in memory consolidation. Past data comparing probes of TGF mice and experiments on WT-$CaCl_2$ and WT mice showed significant changes for probes at three weeks post-surgery (173). Though no significance was detected in our analysis of WT and WT-$CaCl_2$ mice, it is possible that the significance occurs few weeks only after the surgery. Here we investigated probe data after longer periods of time but tendencies are still visible.

Past experiments investigating memory consolidation in the hippocampus demonstrated that drug-induced inactivation of the CA3 subfield caused deficits in memory consolidation of spatial information (164). These experiments demonstrated significances in the probe tests (164). Therefore, it is possible that over the long term, changes occur in the CA3 region of the hippocampus due to TGFβ overexpression and increased pulsatility instigated by arterial rigidity. Furthermore, it has been shown that impaired pre-frontal and frontal-subcortical circuits in Vascular Dementia (VaD) patients result in an inability to perform retrieval strategies (9). Given this information, it is possible that our target group demonstrated symptoms of VaD. Another interesting point is that our probe results in young mice only show significance in the target group (TGF-$CaCl_2$) at 4-months post-surgery and in aged mice at 1-month post-surgery. This difference in results between the young and aged mice suggests an important difference in the way aged TGFβ mice are affected by calcification and increased pulsatility. Collectively, these results suggest that arterial rigidity functions together with vascular pathologies initiated by TGFβ to trigger memory consolidation deficits seen in VaD.

Novel Object Recognition

Testing for the capacity to recognize a familiar stimulus in animals is a fundamental method reflecting human amnesia. The NOR test allows us to analyze the ability of the target group to recognize an object and differentiate it from a new one. Previous experiments of TGFβ mice in NOR demonstrated a significant decrease in the time spent with the novel object related to

the time spent with the familiar one (174, 175). In our experiments, we did not see any significant differences between groups. This may be due to the familiar and novel objects in our protocol being too similar. Another possible issue with the protocol is the 2 hours delay time between the familiarization and novel phase. Past experiments by other groups with longer delay times are usually aimed at sensitivity for retention duration; however a shorter delay time of 1 hour is a popular choice (166). Because NOR identifies neurocognitive disorders relating to the cortex as well as the hippocampus, it would be beneficial to improve the NOR protocol in order to test TGF-$CaCl_2$ mice with more sensitivity (166).

Part II – Vascular Assessments

Circumferential Strain

The lack of effect of a longer exposure to carotid calcification may be due to lost of stiffness with time. To address this possibility, we investigated the circumferential strain of isolated carotid artery. Our data matched those obtained by Sadekova *et al.* for WT-NaCl and WT-$CaCl_2$ (124). Our studies indicate that TGF carotid arteries are significantly less affected by calcification than WT arteries, indicated by a source of variation of P=0.0009. Previous studies investigating the effects of calcification on the carotid artery also detected an increase in macrophage and monocyte infiltration (124). Interestingly, macrophages secrete TGFβ which inhibits nitric oxide synthesis, thus influencing blood flow and blood pressure (176-178). These results may suggest that the increased TGFβ cytokine baseline in TGFβ mice decreases the production of proinflammatory cytokine production which may have been present in WT-$CaCl_2$ mice.

Cerebral Blood Flow

Blood supply to the brain was investigated in our experiments through CBF measurements using laser Doppler flowmetry. Past data of the calcification model exploring differences between the ipsilateral and contralateral sides demonstrated abnormalities in the ipsilateral side. At 2-weeks post-surgery, resting CBF levels were significantly weakened in the

ipsilateral hemisphere, thus corresponding with changes in pulsatility (179). The changes in CBF obtained here do not correspond to past data. Here we examined changes in CBF at 6- to 7-months post-surgery, therefore allowing the possibility for the Circle of Willis and other proximal vessels to acclimate to the change in pulsatility originating from the periphery. However, the results produced were suboptimal. Past results studying CBF of TGF mice detected a significant ≈23% decrease in CBF of TGF mice (52) compared to WT while here we detected a non significant ≈45-50% decrease in both hemispheres. Furthermore, the CBF detected in WT-NaCl mice was much below average in the right hemisphere.

Multiple explanations may account for the suboptimal readings by laser Doppler. Collectively, it may be possible that a significant difference could have been observed between TGF-NaCl and calcified TGF mice given good experimental conditions. These results are important in determining whether hypoperfusion in AD patients with high levels of TGFβ is further affected by arterial rigidity, which is capable of independently contributing to decreased resting CBF and neurovascular coupling.

Part III – Gliosis and Oxidative Stress

Gliosis

Past data examining gliosis obtained with DAB in the TGF mouse showed significant increases in astrogliosis as demonstrated by GFAP immunoreactivity and insignificant increases for microglial activation assessed by Iba1 immunoreactivity (116, 180). However, our results with immunofluorescence often failed to follow the general consensus. Indeed, in the case of fluorescent GFAP in the cortex, CA1, CA3 and DG of aged mice (Fig. 11 B, 12 B, 13 B and 14 B respectively), no significant increase was detected for TGF-NaCl mice compared to WT-NaCl mice. Furthermore, in the CA3 and DG of aged mice (Fig. 13 D and 14 D respectively), Iba1 showed significantly high increases compared to WT-NaCl. These distortions were due to the high fluorescent background as well as fluorescent clouds that hid astroglial fluorescence. We tried to correct for this effect in the analysis, but the results remained similar. In order to better understand the difference between these results and the past ones obtained with DAB staining, we repeated Iba1 and GFAP immunoreactivity assessment using DAB. DAB immunoreactivity functioned without issue, and we were able to detect the expected significances for TGF-NaCl relative to WT-NaCl. DAB staining was performed for aged mice, though not enough samples remained of the young mice to repeat the stains. Therefore, we will continue by only discussing gliosis results of aged mice in the somatosensory/cingulate cortex and CA1, CA3 and DG of the hippocampus.

Past results investigating the acute effects of calcification on WT mice reported significant increases of Iba1 and s100β in the CA1, CA3 and DG of the hippocampus (181) while no differences was observed using GFAP. At 6-7 months post-surgery and using GFAP, no difference was observed either. Interestingly, our DAB results in the cortex show significant increases in microglial activation and astrogliosis for aged TGF-$CaCl_2$ mice in the cingulate/somatosensory cortex compared to the other groups, but no significance was observed in the CA1, CA3 and DG of the hippocampus in relation to TGF-NaCl mice. We investigated the cingulate cortex, which has been shown to display atrophy as well as volume abnormalities in AD patients (182, 183). For the hippocampus, we first studied the CA1 due to its relationship with memory as well as AD patients demonstrating atrophy only in the CA1 subregion (184, 185). Moreover, the CA1 is high in NMDA receptors relative to other areas of the hippocampus, which are particularly vulnerable to the effects of hypoxia and hypoxia symptomatic of vascular disease (186). The CA3 was also studied due to inflammation-inducing triads of astrocytes, microglia and neurons in aged memory-impaired rats (187). Finally, the DG has been shown to be responsible for neurogenesis in the adult brain and serves in multiple important functions such as spatial and sensory output to the CA3 (188, 189).

Human cognitive studies as well as fMRI have suggested that age-related memory loss may originate in the DG (189). Interestingly, the CA3 and DG have been associated with age-related memory loss, while the changes to the CA1 is associated with vascular disease (186). Collectively, our results may suggest that arterial stiffness together with the TGFβ pathology may cause increased neuroinflammation in the cortex. For this reason, it may be worth repeating these tests using s100β for gliosis. Another location which should be examined for

the common effects of arterial rigidity and TGFβ pathology is the white matter, which is highly affected by vascular disease (186).

Oxidative Stress

Oxidative stress was analyzed through ELISA assay of 4-hydroxynonenal (HNE), a primary cytotoxic product of lipid peroxidation (147). Interestingly, aside from being a highly specific test capable of detecting minute amounts, HNE has also been shown to be found at higher levels in AD patients (190). Previous studies of oxidative stress noted that vascular abnormalities of TGF mice were not responsive to antioxidants and concluded that oxidative stress was not a factor in the TGFβ pathology (191). This conclusion correlates with the results found here indicating no significant change in HNE levels in either the hippocampus or the cortex of TGF-NaCl mice compared to WT-NaCl. For calcified mice, past results using dihydroethidium staining to investigate superoxide anion levels in the hippocampus at 2-weeks post-surgery detected a significant 1.2-fold increase in the CA1, CA3 and dentate gyrus (124). However, the present study does not show any increase in HNE concentrations in the $CaCl_2$ group in both hippocampus and cortex. However, reassessment by use of dihydroethidium staining which provides information for localized production of the superoxide anion may be necessary to support our results.

Interestingly, though no significance was determined between all groups, aged mice displayed significantly higher concentrations of HNE in both the cortex and hippocampus ($P<0.0001$ for both cases). Therefore, although the aged mice were only three months older than the young

mice at the time of surgery, all neurological results obtained from the aged group occurred in a milieu of elevated oxidative stress.

Part IV – Limitations

To fully appreciate the link between vascular stiffness represented by the carotid calcification model and AD, an investigation of amyloid β would have been appropriate. However, not enough brain tissue remained for the assay. A previous pilot study by the Girouard laborarory discovered that at 3 weeks post-surgery a significant increase in the Aβ40/Aβ42 ratio was detected in the frontal cortex of mice with a calcified artery compared to their control (179). This increase suggests an altered clearance and compartmentalization of the Aβ species in brain (192). It is possible that this hightened ratio may have been further exacerbated due to the presence of TGFβ protein.

Conclusion

AD patients with high levels of TGFβ cytokines depict multiple vascular pathologies rendering the cerebrovascular system vulnerable to insults yielded by the periphery. One such common insult in the elder is increased pulsatility due to arterial rigidity: an independent predictor of cognitive decline. Here, we isolated the two vascular pathologies to determine whether they work synergistically to cause cognitive disorders. Through the Morris Water Maze we detected deficits relating to memory consolidation and significantly increased neuroinflammation was detected in the cingulate/somatosensory cortex. The effects of the calcification of both carotid arteries are worth exploring to fully validate the hypothesis that arterial stiffness may amplify the existing cerebrovascular abnormalities observed in AD. In

addition different approaches to assess oxidative stress and CBF regulation should be used to fully characterized these models. The next step would be to test different therapies.

Bibliographie

1. Alzheimer's Association Chicago, Illnois2017 [Available from: http://www.alz.org/what-is-dementia.asp.
2. Alzheimer Society of Canada Toronto, Ontario2016 [updated 07/22/16. Available from: http://www.alzheimer.ca/en/About-dementia/What-is-dementia.
3. Helman AM, Murphy MP. Vascular cognitive impairment: Modeling a critical neurologic disease in vitro and in vivo. Biochim Biophys Acta. 2016;1862(5):975-82.
4. Kapasi A, Schneider JA. Vascular contributions to cognitive impairment, clinical Alzheimer's disease, and dementia in older persons. Biochim Biophys Acta. 2016;1862(5):878-86.
5. Cummings JL. Alzheimer's disease. N Engl J Med. 2004;351(1):56-67.
6. Zenaro E, Piacentino G, Constantin G. The blood-brain barrier in Alzheimer's disease. Neurobiol Dis. 2016.
7. Querfurth HW, LaFerla FM. Alzheimer's disease. N Engl J Med. 2010;362(4):329-44.
8. Hamel E. Cerebral circulation: function and dysfunction in Alzheimer's disease. Journal of cardiovascular pharmacology. 2015;65(4):317-24.
9. Cerciello M, Isella V, Proserpi A, Papagno C. Assessment of free and cued recall in Alzheimer's disease and vascular and frontotemporal dementia with 24-item Grober and Buschke test. Neurol Sci. 2016.
10. Knopman DS, Jack CR, Jr., Wiste HJ, Weigand SD, Vemuri P, Lowe VJ, et al. Age and neurodegeneration imaging biomarkers in persons with Alzheimer disease dementia. Neurology. 2016;87(7):691-8.
11. Whitwell JL, Przybelski SA, Weigand SD, Knopman DS, Boeve BF, Petersen RC, et al. 3D maps from multiple MRI illustrate changing atrophy patterns as subjects progress from mild cognitive impairment to Alzheimer's disease. Brain. 2007;130(Pt 7):1777-86.
12. Calabrese V, Giordano J, Signorile A, Laura Ontario M, Castorina S, De Pasquale C, et al. Major pathogenic mechanisms in vascular dementia: Roles of cellular stress response and hormesis in neuroprotection. J Neurosci Res. 2016;94(12):1588-603.
13. Venkat P, Chopp M, Chen J. Models and mechanisms of vascular dementia. Exp Neurol. 2015;272:97-108.
14. Iadecola C. The pathobiology of vascular dementia. Neuron. 2013;80(4):844-66.
15. Song J, Lee WT, Park KA, Lee JE. Association between Risk Factors for Vascular Dementia and Adiponectin. BioMed Research International. 2014;2014:13.
16. Une K, Takei YA, Tomita N, Asamura T, Ohrui T, Furukawa K, et al. Adiponectin in plasma and cerebrospinal fluid in MCI and Alzheimer's disease. European Journal of Neurology. 2011;18(7):1006-9.
17. Rohn TT. Is apolipoprotein E4 an important risk factor for vascular dementia. Int J Clin Exp Pathol. 2014;7(7):3504-11.
18. Chen K-L, Sun Y-M, Zhou Y, Zhao Q-H, Ding D, Guo Q-H. Associations between APOE polymorphisms and seven diseases with cognitive impairment including Alzheimer's disease, frontotemporal dementia, and dementia with Lewy bodies in southeast China. Psychiatric Genetics. 2016;26(3):124-31.

19. Ban Y, Watanabe T, Miyazaki A, Nakano Y, Tobe T, Idei T, et al. Impact of increased plasma serotonin levels and carotid atherosclerosis on vascular dementia. Atherosclerosis. 2007;195(1):153-9.
20. Arntzen K, Mathiesen E. Subclinical carotid atherosclerosis and cognitive function. Acta Neurologica Scandinavica. 2011;124(s191):18-22.
21. Srinivasan V, Braidy N, Chan EKW, Xu Y-H, Chan DKY. Genetic and environmental factors in vascular dementia: an update of blood brain barrier dysfunction. Clinical and Experimental Pharmacology and Physiology. 2016;43(5):515-21.
22. Skoog I, Wallin A, Fredman P, Hesse C, Aevarsson O, Karlsson I, et al. A population study on blood-brain barrier function in 85-year-olds: relation to Alzheimer's disease and vascular dementia. Neurology. 1998;50(4):966-71.
23. Baumgart M, Snyder HM, Carrillo MC, Fazio S, Kim H, Johns H. Summary of the evidence on modifiable risk factors for cognitive decline and dementia: A population-based perspective. Alzheimer's & Dementia. 2015;11(6):718-26.
24. Fillit H, Nash DT, Rundek T, Zuckerman A. Cardiovascular risk factors and dementia. The American journal of geriatric pharmacotherapy. 2008;6(2):100-18.
25. Yates KF, Sweat V, Yau PL, Turchiano MM, Convit A. Impact of metabolic syndrome on cognition and brain. Arteriosclerosis, thrombosis, and vascular biology. 2012;32(9):2060-7.
26. Kokubo Y, Iwashima Y. Higher blood pressure as a risk factor for diseases other than stroke and ischemic heart disease. Hypertension. 2015;66(2):254-9.
27. Rabkin SW. Arterial stiffness: detection and consequences in cognitive impairment and dementia of the elderly. J Alzheimers Dis. 2012;32(3):541-9.
28. Qiu C, Fratiglioni L. A major role for cardiovascular burden in age-related cognitive decline. Nature Reviews Cardiology. 2015;12(5):267-77.
29. Diniz BS, Butters MA, Albert SM, Dew MA, Reynolds CF. Late-life depression and risk of vascular dementia and Alzheimer's disease: systematic review and meta-analysis of community-based cohort studies. The British Journal of Psychiatry. 2013;202(5):329-35.
30. Taylor WD, Aizenstein HJ, Alexopoulos GS. The vascular depression hypothesis: mechanisms linking vascular disease with depression. Molecular psychiatry. 2013;18(9):963-74.
31. Day RJ, Mason MJ, Thomas C, Poon WW, Rohn TT. Caspase-Cleaved Tau Co-Localizes with Early Tangle Markers in the Human Vascular Dementia Brain. PLOS ONE. 2015;10(7):e0132637.
32. Gardener H, Wright CB, Rundek T, Sacco RL. Brain health and shared risk factors for dementia and stroke. Nature Reviews Neurology. 2015.
33. Corriveau RA, Bosetti F, Emr M, Gladman JT, Koenig JI, Moy CS, et al. The science of vascular contributions to cognitive impairment and dementia (VCID): a framework for advancing research priorities in the cerebrovascular biology of cognitive decline. Cellular and molecular neurobiology. 2016;36(2):281-8.
34. Lopez-Valdes HE, Martinez-Coria H. The Role of Neuroinflammation in Age-Related Dementias. Revista de investigacion clinica; organo del Hospital de Enfermedades de la Nutricion. 2016;68(1):40-8.
35. Chui HC, Ramirez-Gomez L. Clinical and imaging features of mixed Alzheimer and vascular pathologies. Alzheimers Res Ther. 2015;7(1):21.

36. Rosenberg GA, Wallin A, Wardlaw JM, Markus HS, Montaner J, Wolfson L, et al. Consensus statement for diagnosis of subcortical small vessel disease. J Cereb Blood Flow Metab. 2016;36(1):6-25.
37. Schneider JA, Arvanitakis Z, Bang W, Bennett DA. Mixed brain pathologies account for most dementia cases in community-dwelling older persons. Neurology. 2007;69(24):2197-204.
38. Neuropathology G. Pathological correlates of late-onset dementia in a multicentre, community-based population in England and Wales. Neuropathology Group of the Medical Research Council Cognitive Function and Ageing Study (MRC CFAS). Lancet (London, England). 2001;357(9251):169.
39. White L. Brain lesions at autopsy in older Japanese-American men as related to cognitive impairment and dementia in the final years of life: a summary report from the Honolulu-Asia aging study. J Alzheimers Dis. 2009;18(3):713-25.
40. Raz L, Knoefel J, Bhaskar K. The neuropathology and cerebrovascular mechanisms of dementia. J Cereb Blood Flow Metab. 2016;36(1):172-86.
41. Kalaria R. Similarities between Alzheimer's disease and vascular dementia. Journal of the Neurological Sciences. 2002;203:29-34.
42. De Reuck J, Deramecourt V, Cordonnier C, Pasquier F, Leys D, Maurage CA, et al. The incidence of post-mortem neurodegenerative and cerebrovascular pathology in mixed dementia. J Neurol Sci. 2016;366:164-6.
43. Brown WR, Thore CR. Review: cerebral microvascular pathology in ageing and neurodegeneration. Neuropathol Appl Neurobiol. 2011;37(1):56-74.
44. De Carolis A, Cipollini V, Donato N, Sepe-Monti M, Orzi F, Giubilei F. Cognitive profiles in degenerative dementia without evidence of small vessel pathology and small vessel vascular dementia. Neurol Sci. 2016.
45. Schwartz RS, Halliday GM, Cordato DJ, Kril JJ. Small-vessel disease in patients with Parkinson's disease: a clinicopathological study. Movement disorders : official journal of the Movement Disorder Society. 2012;27(12):1506-12.
46. Nelson AR, Sweeney MD, Sagare AP, Zlokovic BV. Neurovascular dysfunction and neurodegeneration in dementia and Alzheimer's disease. Biochim Biophys Acta. 2016;1862(5):887-900.
47. Zhao Y, Gong CX. From chronic cerebral hypoperfusion to Alzheimer-like brain pathology and neurodegeneration. Cell Mol Neurobiol. 2015;35(1):101-10.
48. Ueberham U, Ueberham E, Bruckner MK, Seeger G, Gartner U, Gruschka H, et al. Inducible neuronal expression of transgenic TGF-beta1 in vivo: dissection of short-term and long-term effects. The European journal of neuroscience. 2005;22(1):50-64.
49. Ainslie PN, Brassard P. Why is the neural control of cerebral autoregulation so controversial? F1000Prime Rep. 2014;6:14.
50. Venkat P, Chopp M, Chen J. New insights into coupling and uncoupling of cerebral blood flow and metabolism in the brain. Croat Med J. 2016;57(3):223-8.
51. Dormanns K, Brown RG, David T. The role of nitric oxide in neurovascular coupling. J Theor Biol. 2016;394:1-17.
52. Lecrux C, Hamel E. The neurovascular unit in brain function and disease. Acta Physiol (Oxf). 2011;203(1):47-59.

53. Girouard H, Iadecola C. Neurovascular coupling in the normal brain and in hypertension, stroke, and Alzheimer disease. J Appl Physiol (1985). 2006;100(1):328-35.
54. Iulita MF, Girouard H. Treating Hypertension to Prevent Cognitive Decline and Dementia: Re-Opening the Debate. Adv Exp Med Biol. 2016.
55. Toth P, Tarantini S, Csiszar A, Ungvari ZI. Functional Vascular Contributions to Cognitive Impairment and Dementia (VCID): Mechanisms and Consequences of Cerebral Microvascular Dysfunction in Aging. Am J Physiol Heart Circ Physiol. 2016:ajpheart 00581 2016.
56. Farkas E, Luiten PG. Cerebral microvascular pathology in aging and Alzheimer's disease. Prog Neurobiol. 2001;64(6):575-611.
57. Edvinsson L, Krause DN. Cerebral Blood Flow and Metabolism: Lippincott Williams & Wilkins; 2002.
58. Vrselja Z, Brkic H, Mrdenovic S, Radic R, Curic G. Function of circle of Willis. J Cereb Blood Flow Metab. 2014;34(4):578-84.
59. Cooper LL, Mitchell GF. Aortic Stiffness, Cerebrovascular Dysfunction, and Memory. Pulse (Basel). 2016;4(2-3):69-77.
60. Cipolla MJ. The Cerebral Circulation. 2009. San Rafael (CA): Morgan & Claypool Life Sciences. Available from: https://www.ncbi.nlm.nih.gov/books/NBK53082/.
61. Cipolla MJ, Smith J, Kohlmeyer MM, Godfrey JA. SK_{Ca} and IK_{Ca} Channels, Myogenic Tone, and Vasodilator Responses in Middle Cerebral Arteries and Parenchymal Arterioles. Stroke. 2009;40(4):1451.
62. Toth P, Tucsek Z, Tarantini S, Sosnowska D, Gautam T, Mitschelen M, et al. IGF-1 deficiency impairs cerebral myogenic autoregulation in hypertensive mice. J Cereb Blood Flow Metab. 2014;34(12):1887-97.
63. Cai W, Zhang K, Li P, Zhu L, Xu J, Yang B, et al. Dysfunction of the neurovascular unit in ischemic stroke and neurodegenerative diseases: An aging effect. Ageing Res Rev. 2016.
64. Girouard H, Bonev AD, Hannah RM, Meredith A, Aldrich RW, Nelson MT. Astrocytic endfoot Ca2+ and BK channels determine both arteriolar dilation and constriction. Proceedings of the National Academy of Sciences. 2010;107(8):3811-6.
65. Bergers G, Song S. The role of pericytes in blood-vessel formation and maintenance. Neuro Oncol. 2005;7(4):452-64.
66. Cai W, Liu H, Zhao J, Chen LY, Chen J, Lu Z, et al. Pericytes in Brain Injury and Repair After Ischemic Stroke. Transl Stroke Res. 2016.
67. Niwa K, Haensel C, Ross ME, Iadecola C. Cyclooxygenase-1 Participates in Selected Vasodilator Responses of the Cerebral Circulation. Circulation Research. 2001;88(6):600-8.
68. Raignault A, Bolduc V, Lesage F, Thorin E. Pulse pressure-dependent cerebrovascular eNOS regulation in mice. Journal of Cerebral Blood Flow & Metabolism. 2017;37(2):413-24.
69. Drouin A, Thorin-Trescases N, Hamel E, Falck JR, Thorin E. Endothelial nitric oxide synthase activation leads to dilatory H2O2 production in mouse cerebral arteries. Cardiovascular Research. 2007;73(1):73-81.
70. Chaubey S, Jones GE, Shah AM, Cave AC, Wells CM. Nox2 Is Required for Macrophage Chemotaxis towards CSF-1. PLOS ONE. 2013;8(2):e54869.

71. Blackwell KA, Sorenson JP, Richardson DM, Smith LA, Suda O, Nath K, et al. Mechanisms of aging-induced impairment of endothelium-dependent relaxation: role of tetrahydrobiopterin. Am J Physiol Heart Circ Physiol. 2004;287(6):H2448-53.
72. Berkowitz DE, White R, Li D, Minhas KM, Cernetich A, Kim S, et al. Arginase reciprocally regulates nitric oxide synthase activity and contributes to endothelial dysfunction in aging blood vessels. Circulation. 2003;108(16):2000-6.
73. Austin SA, Santhanam AV, Hinton DJ, Choi DS, Katusic ZS. Endothelial nitric oxide deficiency promotes Alzheimer's disease pathology. J Neurochem. 2013;127(5):691-700.
74. Iadecola C, Zhang F, Niwa K, Eckman C, Turner SK, Fischer E, et al. SOD1 rescues cerebral endothelial dysfunction in mice overexpressing amyloid precursor protein. Nat Neurosci. 1999;2(2):157-61.
75. Papetti M, Shujath J, Riley KN, Herman IM. FGF-2 antagonizes the TGF-beta1-mediated induction of pericyte alpha-smooth muscle actin expression: a role for myf-5 and Smad-mediated signaling pathways. Invest Ophthalmol Vis Sci. 2003;44(11):4994-5005.
76. Filosa JA, Nelson MT, Gonzalez Bosc LV. Activity-dependent NFATc3 nuclear accumulation in pericytes from cortical parenchymal microvessels. American Journal of Physiology - Cell Physiology. 2007;293(6):C1797-C805.
77. Kettenmann H, Ransom BR. Neuroglia: Oxford University Press; 2004.
78. Bell RD, Winkler EA, Sagare AP, Singh I, LaRue B, Deane R, et al. Pericytes Control Key Neurovascular Functions and Neuronal Phenotype in the Adult Brain and during Brain Aging. Neuron. 2010;68(3):409-27.
79. Winkler EA, Sengillo JD, Bell RD, Wang J, Zlokovic BV. Blood–spinal cord barrier pericyte reductions contribute to increased capillary permeability. Journal of Cerebral Blood Flow & Metabolism. 2012;32(10):1841-52.
80. Salminen A, Ojala J, Kaarniranta K, Haapasalo A, Hiltunen M, Soininen H. Astrocytes in the aging brain express characteristics of senescence-associated secretory phenotype. Eur J Neurosci. 2011;34(1):3-11.
81. Wevers NR, de Vries HE. Morphogens and blood-brain barrier function in health and disease. Tissue Barriers. 2016;4(1):e1090524.
82. Widmaier EP, Raff H, Strang KT. Vander's Human Physiology: McGraw-Hill Higher Education; 2005.
83. Filosa JA, Morrison HW, Iddings JA, Du W, Kim KJ. Beyond neurovascular coupling, role of astrocytes in the regulation of vascular tone. Neuroscience. 2016;323:96-109.
84. Capani F, Quarracino C, Caccuri R, Sica RE. Astrocytes As the Main Players in Primary Degenerative Disorders of the Human Central Nervous System. Front Aging Neurosci. 2016;8:45.
85. Giaume C, Liu X. From a glial syncytium to a more restricted and specific glial networking. J Physiol Paris. 2012;106(1-2):34-9.
86. Abbott NJ, Ronnback L, Hansson E. Astrocyte-endothelial interactions at the blood-brain barrier. Nat Rev Neurosci. 2006;7(1):41-53.
87. Cardoso FL, Brites D, Brito MA. Looking at the blood-brain barrier: molecular anatomy and possible investigation approaches. Brain Res Rev. 2010;64(2):328-63.
88. Simpson JE, Ince PG, Haynes LJ, Theaker R, Gelsthorpe C, Baxter L, et al. Population variation in oxidative stress and astrocyte DNA damage in relation to Alzheimer-type pathology in the ageing brain. Neuropathology and Applied Neurobiology. 2010;36(1):25-40.

89. Menet V, Gimenez YRM, Sandillon F, Privat A. GFAP null astrocytes are a favorable substrate for neuronal survival and neurite growth. Glia. 2000;31(3):267-72.
90. Garwood CJ, Ratcliffe LE, Simpson JE, Heath PR, Ince PG, Wharton SB. Review: Astrocytes in Alzheimer's disease and other age-associated dementias; a supporting player with a central role. Neuropathol Appl Neurobiol. 2016.
91. Hu X, Liou AKF, Leak RK, Xu M, An C, Suenaga J, et al. Neurobiology of microglial action in CNS injuries: Receptor-mediated signaling mechanisms and functional roles. Progress in Neurobiology. 2014;119–120:60-84.
92. Harry GJ. Microglia during development and aging. Pharmacology & Therapeutics. 2013;139(3):313-26.
93. Paolicelli RC, Bolasco G, Pagani F, Maggi L, Scianni M, Panzanelli P, et al. Synaptic Pruning by Microglia Is Necessary for Normal Brain Development. Science. 2011;333(6048):1456-8.
94. Wake H, Moorhouse AJ, Jinno S, Kohsaka S, Nabekura J. Resting Microglia Directly Monitor the Functional State of Synapses In Vivo and Determine the Fate of Ischemic Terminals. The Journal of Neuroscience. 2009;29(13):3974-80.
95. Sierra A, Encinas JM, Deudero JJP, Chancey JH, Enikolopov G, Overstreet-Wadiche LS, et al. Microglia Shape Adult Hippocampal Neurogenesis through Apoptosis-Coupled Phagocytosis. Cell Stem Cell. 2010;7(4):483-95.
96. Nagamoto-Combs K, Morecraft RJ, Darling WG, Combs CK. Long-Term Gliosis and Molecular Changes in the Cervical Spinal Cord of the Rhesus Monkey after Traumatic Brain Injury. Journal of Neurotrauma. 2010;27(3):565-85.
97. Olah M, Amor S, Brouwer N, Vinet J, Eggen B, Biber K, et al. Identification of a microglia phenotype supportive of remyelination. Glia. 2012;60(2):306-21.
98. Lourbopoulos A, Ertürk A, Hellal F. Microglia in action: how aging and injury can change the brain's guardians. Mechanisms of Neuroinflammation and Inflammatory Neurodegeneration in Acute Brain Injury. 2015:24.
99. Lee S, Wu Y, Shi XQ, Zhang J. Characteristics of spinal microglia in aged and obese mice: potential contributions to impaired sensory behavior. Immunity & Ageing. 2015;12(1):22.
100. Schütze S, Ribes S, Kaufmann A, Manig A, Scheffel J, Redlich S, et al. Higher mortality and impaired elimination of bacteria in aged mice after intracerebral infection with E. coli are associated with an age-related decline of microglia and macrophage functions. Oncotarget. 2014;5(24):12573-92.
101. Babcock AA, Ilkjær L, Clausen BH, Villadsen B, Dissing-Olesen L, Bendixen ATM, et al. Cytokine-producing microglia have an altered beta-amyloid load in aged APP/PS1 Tg mice. Brain, Behavior, and Immunity. 2015;48:86-101.
102. Gosselin D, Link V, Romanoski CE, Fonseca GJ, Eichenfield DZ, Spann NJ, et al. Environment drives selection and function of enhancers controlling tissue-specific macrophage identities. Cell. 2014;159(6):1327-40.
103. Butovsky O, Jedrychowski MP, Moore CS, Cialic R, Lanser AJ, Gabriely G, et al. Identification of a unique TGF-[beta]-dependent molecular and functional signature in microglia. Nat Neurosci. 2014;17(1):131-43.
104. Strang KT, Raff H, Widmaier EP. Vander's Human Physiology: The Mechanisms of Body Function. Tenth Edition ed: McGraw Hill; 2006.

105. Sim FJ, Zhao C, Penderis J, Franklin RJM. The Age-Related Decrease in CNS Remyelination Efficiency Is Attributable to an Impairment of Both Oligodendrocyte Progenitor Recruitment and Differentiation. Journal of Neuroscience. 2002;22(7):2451-9.
106. Peters A. The effects of normal aging on myelinated nerve fibers in monkey central nervous system. Front Neuroanat. 2009;3(11).
107. Wyss-Coray T, Masliah E, Mallory M, McConlogue L. Amyloidogenic role of cytokine TGF-beta-1 in transgenic mice and in Alzheimer's disease. Nature. 1997;389(6651):603.
108. Tesseur I, Zou K, Esposito L, Bard F, Berber E, Can JV, et al. Deficiency in neuronal TGF-β signaling promotes neurodegeneration and Alzheimer's pathology. Journal of Clinical Investigation. 2006;116(11):3060-9.
109. Wyss-Coray T, Lin C, Sanan DA, Mucke L, Masliah E. Chronic overproduction of transforming growth factor-beta1 by astrocytes promotes Alzheimer's disease-like microvascular degeneration in transgenic mice. The American journal of pathology. 2000;156(1):139-50.
110. LEASK A, ABRAHAM DJ. TGF-β signaling and the fibrotic response. The FASEB Journal. 2004;18(7):816-27.
111. Laskowitz D, Grant G. Translational Research in Traumatic Brain Injury: CRC Press; 2016.
112. Finch CE, Laping NJ, Morgan TE, Nichols NR, Pasinetti GM. TGF-β1 is an organizer of responses to neurodgeneration. Journal of Cellular Biochemistry. 1993;53(4):314-22.
113. Nicolakakis N, Hamel E. Neurovascular function in Alzheimer's disease patients and experimental models. J Cereb Blood Flow Metab. 2011;31(6):1354-70.
114. Tong XK, Nicolakakis N, Kocharyan A, Hamel E. Vascular remodeling versus amyloid beta-induced oxidative stress in the cerebrovascular dysfunctions associated with Alzheimer's disease. J Neurosci. 2005;25(48):11165-74.
115. Gaertner RF, Wyss-Coray T, Von Euw D, Lesne S, Vivien D, Lacombe P. Reduced brain tissue perfusion in TGF-beta 1 transgenic mice showing Alzheimer's disease-like cerebrovascular abnormalities. Neurobiol Dis. 2005;19(1-2):38-46.
116. Nicolakakis N, Aboulkassim T, Aliaga A, Tong XK, Rosa-Neto P, Hamel E. Intact memory in TGF-beta1 transgenic mice featuring chronic cerebrovascular deficit: recovery with pioglitazone. J Cereb Blood Flow Metab. 2011;31(1):200-11.
117. Galea E, Feinstein DL, Lacombe P. Pioglitazone does not increase cerebral glucose utilisation in a murine model of Alzheimer's disease and decreases it in wild-type mice. Diabetologia. 2006;49(9):2153-61.
118. Papadopoulos P, Rosa-Neto P, Rochford J, Hamel E. Pioglitazone Improves Reversal Learning and Exerts Mixed Cerebrovascular Effects in a Mouse Model of Alzheimer's Disease with Combined Amyloid-β and Cerebrovascular Pathology. PLoS ONE. 2013;8(7):e68612.
119. Papadopoulos P, Tong X-K, Hamel E. Selective benefits of simvastatin in bitransgenic APP_{Swe,Ind}/TGF-β1 mice. Neurobiology of Aging.35(1):203-12.
120. Pase MP, Herbert A, Grima NA, Pipingas A, O'Rourke MF. Arterial stiffness as a cause of cognitive decline and dementia: a systematic review and meta-analysis. Internal medicine journal. 2012;42(7):808-15.

121. Cooper LL, Woodard T, Sigurdsson S, van Buchem MA, Torjesen AA, Inker LA, et al. Cerebrovascular Damage Mediates Relations Between Aortic Stiffness and Memory. Hypertension. 2016;67(1):176-82.
122. Scuteri A, Tesauro M, Appolloni S, Preziosi F, Brancati AM, Volpe M. Arterial stiffness as an independent predictor of longitudinal changes in cognitive function in the older individual. Journal of hypertension. 2007;25(5):1035-40.
123. Waldstein SR, Rice SC, Thayer JF, Najjar SS, Scuteri A, Zonderman AB. Pulse pressure and pulse wave velocity are related to cognitive decline in the Baltimore Longitudinal Study of Aging. Hypertension. 2008;51(1):99-104.
124. Sadekova N, Vallerand D, Guevara E, Lesage F, Girouard H. Carotid calcification in mice: a new model to study the effects of arterial stiffness on the brain. J Am Heart Assoc. 2013;2(3):e000224.
125. van Sloten TT, Stehouwer CD. Carotid Stiffness: A Novel Cerebrovascular Disease Risk Factor. Pulse (Basel). 2016;4(1):24-7.
126. Matsumoto T, Sugita S, Yaguchi T. Biomechanics of Blood Vessels: Structure, Mechanics, and Adaptation. In: Niinomi M, Narushima T, Nakai M, editors. Advances in Metallic Biomaterials: Tissues, Materials and Biological Reactions. Berlin, Heidelberg: Springer Berlin Heidelberg; 2015. p. 71-98.
127. Witter K, Tonar Z, Schopper H. How many Layers has the Adventitia? - Structure of the Arterial Tunica Externa Revisited. Anat Histol Embryol. 2016.
128. Michiels C. Endothelial cell functions. J Cell Physiol. 2003;196(3):430-43.
129. Hall JE. Guyton and Hall Textbook of Medical Physiology: Enhanced E-book. Philadelphia, PA: Elsevier Health Sciences; 2010.
130. Adji A, O'Rourke MF, Namasivayam M. Arterial stiffness, its assessment, prognostic value, and implications for treatment. American journal of hypertension. 2011;24(1):5-17.
131. Laurent S, Cockcroft J, Van Bortel L, Boutouyrie P, Giannattasio C, Hayoz D, et al. Expert consensus document on arterial stiffness: methodological issues and clinical applications. Eur Heart J. 2006;27(21):2588-605.
132. Lee H-Y, Oh B-H. Aging and Arterial Stiffness. Circulation Journal. 2010;74(11):2257-62.
133. Sehgel NL, Vatner SF, Meininger GA. "Smooth Muscle Cell Stiffness Syndrome"—Revisiting the Structural Basis of Arterial Stiffness. Frontiers in Physiology. 2015;6:335.
134. Atkinson J. Age-related medial elastocalcinosis in arteries: mechanisms, animal models, and physiological consequences. J Appl Physiol (1985). 2008;105(5):1643-51.
135. Niederhoffer N, Lartaud-Idjouadiene I, Giummelly P, Duvivier C, Peslin R, Atkinson J. Calcification of medial elastic fibers and aortic elasticity. Hypertension. 1997;29(4):999-1006.
136. Nichols WW, Denardo SJ, Johnson BD, Sharaf BL, Bairey Merz CN, Pepine CJ. Increased wave reflection and ejection duration in women with chest pain and nonobstructive coronary artery disease: ancillary study from the Women's Ischemia Syndrome Evaluation. Journal of hypertension. 2013;31(7):1447-54; discussion 54-5.
137. Mitchell GF, Wang N, Palmisano JN, Larson MG, Hamburg NM, Vita JA, et al. Hemodynamic correlates of blood pressure across the adult age spectrum: noninvasive evaluation in the Framingham Heart Study. Circulation. 2010;122(14):1379-86.

138. Gepner AD, Korcarz CE, Colangelo LA, Hom EK, Tattersall MC, Astor BC, et al. Longitudinal effects of a decade of aging on carotid artery stiffness: the multiethnic study of atherosclerosis. Stroke. 2014;45(1):48-53.
139. Baumann M, Wassertheurer S, Suttmann Y, Burkhardt K, Heemann U. Aortic pulse wave velocity predicts mortality in chronic kidney disease stages 2-4. Journal of hypertension. 2014;32(4):899-903.
140. Scuteri A, Cunha PG, Rosei EA, Badariere J, Bekaert S, Cockcroft JR, et al. Arterial stiffness and influences of the metabolic syndrome: a cross-countries study. Atherosclerosis. 2014;233(2):654-60.
141. Mitchell GF, van Buchem MA, Sigurdsson S, Gotal JD, Jonsdottir MK, Kjartansson Ó, et al. Arterial stiffness, pressure and flow pulsatility and brain structure and function: the Age, Gene/Environment Susceptibility – Reykjavik Study. Brain. 2011;134(11):3398-407.
142. Tzourio C, Laurent S, Debette S. Is Hypertension Associated With an Accelerated Aging of the Brain? Hypertension. 2014;63(5):894.
143. Capogna M. Neurogliaform cells and other interneurons of stratum lacunosum-moleculare gate entorhinal–hippocampal dialogue. The Journal of Physiology. 2011;589(Pt 8):1875-83.
144. Braak H, Braak E. Entorhinal-hippocampal interaction in mnestic disorders. Hippocampus. 1993;3 Spec No:239-46.
145. Betteridge DJ. What is oxidative stress? Metabolism: clinical and experimental. 2000;49(2 Suppl 1):3-8.
146. Salminen A, Haapasalo A, Kauppinen A, Kaarniranta K, Soininen H, Hiltunen M. Impaired mitochondrial energy metabolism in Alzheimer's disease: Impact on pathogenesis via disturbed epigenetic regulation of chromatin landscape. Progress in Neurobiology. 2015;131:1-20.
147. Cobb CA, Cole MP. Oxidative and nitrative stress in neurodegeneration. Neurobiol Dis. 2015;84:4-21.
148. Quillinan N, Herson PS, Traystman RJ. Neuropathophysiology of Brain Injury. Anesthesiol Clin. 2016;34(3):453-64.
149. Fang YZ, Yang S, Wu G. Free radicals, antioxidants, and nutrition. Nutrition (Burbank, Los Angeles County, Calif). 2002;18(10):872-9.
150. Abdul-Muneer PM, Chandra N, Haorah J. Interactions of oxidative stress and neurovascular inflammation in the pathogenesis of traumatic brain injury. Mol Neurobiol. 2015;51(3):966-79.
151. Lardenoije R, Iatrou A, Kenis G, Kompotis K, Steinbusch HW, Mastroeni D, et al. The epigenetics of aging and neurodegeneration. Progress in neurobiology. 2015;131:21-64.
152. Daiber A, Münzel T. Increased Circulating Levels of 3-Nitrotyrosine Autoantibodies. Am Heart Assoc; 2012.
153. Sofroniew MV, Vinters HV. Astrocytes: biology and pathology. Acta neuropathologica. 2010;119(1):7-35.
154. Kettenmann H, Hanisch U-K, Noda M, Verkhratsky A. Physiology of microglia. Physiological reviews. 2011;91(2):461-553.
155. Ito D, Imai Y, Ohsawa K, Nakajima K, Fukuuchi Y, Kohsaka S. Microglia-specific localisation of a novel calcium binding protein, Iba1. Molecular brain research. 1998;57(1):1-9.

156. Imai Y, Kohsaka S. Intracellular signaling in M-CSF-induced microglia activation: Role of Iba1. Glia. 2002;40(2):164-74.
157. Sofroniew MV. Molecular dissection of reactive astrogliosis and glial scar formation. Trends in neurosciences. 2009;32(12):638-47.
158. Silver J, Miller JH. Regeneration beyond the glial scar. Nature Reviews Neuroscience. 2004;5(2):146-56.
159. Gonçalves C-A, Concli Leite M, Nardin P. Biological and methodological features of the measurement of S100B, a putative marker of brain injury. Clinical Biochemistry. 2008;41(10–11):755-63.
160. Wahlsten D. Chapter 11 - Motivating Mice. Mouse Behavioral Testing. London: Academic Press; 2011. p. 177-201.
161. Vorhees CV, Williams MT. Morris water maze: procedures for assessing spatial and related forms of learning and memory. Nature protocols. 2006;1(2):848-58.
162. Morris R. Morris water maze. Scholarpedia. 2008;3(8):6315.
163. O'keefe J, Conway D. Hippocampal place units in the freely moving rat: why they fire where they fire. Experimental brain research. 1978;31(4):573-90.
164. Florian C, Roullet P. Hippocampal CA3-region is crucial for acquisition and memory consolidation in Morris water maze task in mice. Behavioural brain research. 2004;154(2):365-74.
165. D'Hooge R, De Deyn PP. Applications of the Morris water maze in the study of learning and memory. Brain research reviews. 2001;36(1):60-90.
166. Antunes M, Biala G. The novel object recognition memory: neurobiology, test procedure, and its modifications. Cognitive Processing. 2012;13(2):93-110.
167. Bevins RA, Besheer J. Object recognition in rats and mice: a one-trial non-matching-to-sample learning task to study 'recognition memory'. Nat Protocols. 2006;1(3):1306-11.
168. Buckmaster CA, Eichenbaum H, Amaral DG, Suzuki WA, Rapp PR. Entorhinal Cortex Lesions Disrupt the Relational Organization of Memory in Monkeys. The Journal of Neuroscience. 2004;24(44):9811.
169. Clark RE, Zola SM, Squire LR. Impaired recognition memory in rats after damage to the hippocampus. J Neurosci. 2000;20(23):8853-60.
170. Hale G, Good M. Impaired visuospatial recognition memory but normal object novelty detection and relative familiarity judgments in adult mice expressing the APPswe Alzheimer's disease mutation. Behavioral neuroscience. 2005;119(4):884-91.
171. Tong X-K, Hamel E. Simvastatin Restored Vascular Reactivity, Endothelial Function and Reduced String Vessel Pathology in a Mouse Model of Cerebrovascular Disease. Journal of Cerebral Blood Flow & Metabolism. 2015;35(3):512-20.
172. Royea J, Zhang L, Tong X-K, Hamel E. Angiotensin IV receptors mediate the cognitive and cerebrovascular benefits of losartan in a mouse model of Alzheimer's disease. Journal of Neuroscience. 2017;37(22):5562-73.
173. Muhire G, Oualias B, Girouard H, Ferland G. Vitamin K prevents cognitive impairment associated with the arterial stiffness in a murine model of arterial calcification. GRSNC. 2017;Dementia and cognition: a vascular perspective(22).
174. Caraci F, Gulisano W, Guida CA, Impellizzeri AAR, Drago F, Puzzo D, et al. A key role for TGF-β1 in hippocampal synaptic plasticity and memory. 2015;5:11252.

175. Lifshitz V, Weiss R, Benromano T, Kfir E, Blumenfeld-Katzir T, Tempel-Brami C, et al. Immunotherapy of cerebrovascular amyloidosis in a transgenic mouse model. Neurobiology of Aging. 2012;33(2):432.e1-.e13.
176. Ding A, Nathan CF, Graycar J, Derynck R, Stuehr DJ, Srimal S. Macrophage deactivating factor and transforming growth factors-beta 1 -beta 2 and -beta 3 inhibit induction of macrophage nitrogen oxide synthesis by IFN-gamma. The Journal of Immunology. 1990;145(3):940-4.
177. Fadok VA, Bratton DL, Konowal A, Freed PW, Westcott JY, Henson PM. Macrophages that have ingested apoptotic cells in vitro inhibit proinflammatory cytokine production through autocrine/paracrine mechanisms involving TGF-beta, PGE2, and PAF. Journal of Clinical Investigation. 1998;101(4):890-8.
178. Vodovotz Y, Bogdan C, Paik J, Xie QW, Nathan C. Mechanisms of suppression of macrophage nitric oxide release by transforming growth factor beta. The Journal of Experimental Medicine. 1993;178(2):605-13.
179. Iulita MF, Muhire G, Vallerand D, Youwakim J, Petry FR, Gratuze M, et al. Arterial stiffness due to carotid calcification disrupts cerebral blood flow regulation before cognitive deficits manifest. Berlin BRAIN & BRAIN PET. 2017;28th Symposium on Cerebral Blood Flow, Metabolism and Function(A-847-0028-00453).
180. Endo F, Komine O, Fujimori-Tonou N, Katsuno M, Jin S, Watanabe S, et al. Astrocyte-Derived TGF-β1 Accelerates Disease Progression in ALS Mice by Interfering with the Neuroprotective Functions of Microglia and T Cells. Cell Reports. 2015;11(4):592-604.
181. Sadekova N. La rigidité artérielle, induite par une calcification des carotides, altère l'homéostasie cérébrale chez la souris: [Montréal]: Université de Montréal; 2013.
182. Landin-Romero R, Kumfor F, Leyton CE, Irish M, Hodges JR, Piguet O. Disease-specific patterns of cortical and subcortical degeneration in a longitudinal study of Alzheimer's disease and behavioural-variant frontotemporal dementia. NeuroImage. 2017;151:72-80.
183. Tascone LdS, Payne ME, MacFall J, Azevedo D, de Castro CC, Steffens DC, et al. Cortical brain volume abnormalities associated with few or multiple neuropsychiatric symptoms in Alzheimer's disease. PLOS ONE. 2017;12(5):e0177169.
184. Zola-Morgan S, Squire L, Amaral D. Human amnesia and the medial temporal region: enduring memory impairment following a bilateral lesion limited to field CA1 of the hippocampus. The Journal of Neuroscience. 1986;6(10):2950-67.
185. Mak E, Gabel S, Su L, Williams GB, Arnold R, Passamonti L, et al. HIPPOCAMPAL CA1 INVOLVEMENT IN DEMENTIA WITH LEWY BODIES, ALZHEIMER'S DISEASE AND MILD COGNITIVE IMPAIRMENT: THE NIMROD STUDY. Alzheimer's & Dementia: The Journal of the Alzheimer's Association. 2016;12(7):P120-P1.
186. Small SA, Schobel SA, Buxton RB, Witter MP, Barnes CA. A pathophysiological framework of hippocampal dysfunction in ageing and disease. Nat Rev Neurosci. 2011;12(10):585-601.
187. Lana D, Iovino L, Nosi D, Wenk GL, Giovannini MG. The neuron-astrocyte-microglia triad involvement in neuroinflammaging mechanisms in the CA3 hippocampus of memory-impaired aged rats. Experimental Gerontology. 2016;83:71-88.
188. Spalding KL, Bergmann O, Alkass K, Bernard S, Salehpour M, Huttner HB, et al. Dynamics of hippocampal neurogenesis in adult humans. Cell. 2013;153(6):1219-27.

189. Hollands C, Bartolotti N, Lazarov O. Alzheimer's Disease and Hippocampal Adult Neurogenesis; Exploring Shared Mechanisms. Frontiers in Neuroscience. 2016;10:178.
190. Sayre LM, Zelasko DA, Harris PL, Perry G, Salomon RG, Smith MA. 4-Hydroxynonenal-Derived Advanced Lipid Peroxidation End Products Are Increased in Alzheimer's Disease. Journal of neurochemistry. 1997;68(5):2092-7.
191. Hamel E, Nicolakakis N, Aboulkassim T, Ongali B, Tong XK. Oxidative stress and cerebrovascular dysfunction in mouse models of Alzheimer's disease. Experimental Physiology. 2008;93(1):116-20.
192. Fryer JD, Simmons K, Parsadanian M, Bales KR, Paul SM, Sullivan PM, et al. Human apolipoprotein E4 alters the amyloid-β 40: 42 ratio and promotes the formation of cerebral amyloid angiopathy in an amyloid precursor protein transgenic model. Journal of Neuroscience. 2005;25(11):2803-10.